Regulation and conservation of caspase-activated autophagy

by

Courtney Paige Choutka

B.Sc., Simon Fraser University, 2010

Thesis Submitted in Partial Fulfillment of the
Requirements for the Degree of
Doctor of Philosophy

in the
Department of Molecular Biology and Biochemistry
Faculty of Science

SIMON FRASER UNIVERSITY

Summer 2017

Approval

Name:	**Courtney Paige Choutka**
Degree:	**Doctor of Philosophy (Molecular Biology and Biochemistry)**
Title:	**Regulation and conservation of caspase-activated autophagy**

Examining Committee:

Chair: Edgar Young
Associate Professor

Dr. Sharon Gorski
Senior Supervisor
Professor

Dr. Nicholas Harden
Supervisor
Professor

Dr. Jonathan Choy
Supervisor
Associate Professor

Dr. Michel Leroux
Internal Examiner
Professor
Molecular Biology and Biochemistry

Dr. Lynne Megeney
External Examiner
Professor
Department of Cellular and Molecular Medicine, Department of Medicine
University of Ottawa

Date Defended/Approved: June 27, 2017

Abstract

Autophagy is an evolutionarily conserved cellular process that recycles proteins and organelles to maintain cellular homeostasis or provide an alternative source of energy in times of stress. While autophagy promotes cell survival, it can also be regulated by proteins associated traditionally with apoptosis. In an effort to better understand the complex intersections of these disparate cell fates, previous studies in *Drosophila* identified an apoptotic effector caspase, Dcp-1, as a positive regulator of starvation-induced autophagy. Further, the *Drosophila* heat-shock protein, Hsp83, was identified as a Dcp-1 interacting protein and a putative negative regulator of autophagy. The aims of my thesis were to investigate the relationship between Dcp-1 and Hsp83 in the context of autophagy, and to determine if caspase-regulated autophagy was functionally conserved in humans. *In vivo* analyses of *Hsp83* loss-of-function mutants in fed conditions showed increases in both autophagic flux and cell death. Hsp83 mutants also had elevated levels of pro-Dcp-1, which was attributed to reduced proteasomal activity. Analyses of an *Hsp83*/*Dcp-1* double mutant revealed that the caspase was not required for cell death in this context but was essential for the ensuing compensatory autophagy, female fertility, and organism viability. These studies not only demonstrated unappreciated roles for Hsp83 in proteasomal activity and new forms of Dcp-1 regulation, but also identified an effector caspase as a key regulatory factor for sustaining adaptation to cell stress *in vivo* by inducing compensatory autophagy. To address whether effector caspases also regulate starvation-induced autophagy in human cells, caspase-3 (CASP3), a human homolog of Dcp-1, was examined in several human cell lines. These studies showed that CASP3 was required for the upregulation of starvation-induced autophagy in most cell lines examined, but was not required for maintaining basal levels of autophagy. In human cells, another heat-shock family member, HSP60, was identified as a CASP3-interacting protein. HSP60 was shown to negatively regulate autophagy by controlling the subcellular localization of CASP3 in response to nutritional status. Epistasis analyses suggest that the increase in autophagy observed from loss of HSP60 was dependent on the accumulation of cleaved CASP3 in the cytosol. This work highlights a novel function for CASP3 in starvation-induced autophagy in human cells and illustrates how its response is regulated by HSP60-controlled subcellular localization. Altogether, my studies provide novel insights into stress adaptive relationships between heat-shock proteins and caspases in *Drosophila* and human cells.

Keywords: caspase; autophagy; heat-shock proteins; regulation; proteostasis; stress

To my mother,

whose passing led me to discover my passion for research

To my husband,

whose enduring support sustained that passion

Acknowledgements

First and foremost, I would like to express my sincerest gratitude to my senior supervisor Dr. Sharon Gorski for her continuous support throughout graduate school. I am eternally grateful for her optimism, passion for research, belief in me, and all the long hours she spent reading my written works. I cannot imagine succeeding and growing as I have without her superb mentorship. Additionally, I would like to thank my supervisory committee, Dr. Nicholas Harden and Dr. Jonathan Choy for their encouragement, enthusiasm and constructive feedback over the years.

I would like to thank my colleagues in the Gorski lab, past and present, for all of their support since I joined “PCD”. In particular, I would like to thank Nancy Erro Go for her instrumental experimental support, Dr. Suganthi Chittaranjan for her mentorship, Svetlana Bortnik for great collaborations, Helen Chen for her administrative support and Dr. Lindsay DeVorkin for my introduction into *Drosophila* laboratory work. I am also indebted to Dr. Lynne Quarmby for fostering me as a green scientist and introducing me to academic research when I was an undergrad. I grew exponentially there and it is also where I met a group of lifelong scientist friends who kept me laughing even through difficult times: Julie Rodriguez, Adam Staniscia and particularly Dr. Laura Hilton for being both a supportive friend and mentor. Furthermore, I’m appreciative of all the confocal assistance from collaborators Tim Heslip, Charles Soong and especially Dr. Dan Luciani for support and access to his microscope. I’m grateful to Amy Tien for her help with the cleaved caspase-3 assays, Govinda Sharma for flow support, Mimi Fourie for her graduate assistance and Dr. Gregg Morin for his contributions to my manuscript.

Thank you to my non-research friends who didn’t understand what I was doing but accepted at times I would be very busy, in particular my best friend Anna Bazarjani. I would not be here if it weren’t for all the members of my family who have loved and believed in me throughout my entire educational journey, especially my dad, mom, brother, and three auxiliary parents: Auntie, Marisa and Charmaine. Last but certainly not least, I would like to thank my greatest collaborator, Erik Nielson. He has worked hard behind the scenes throughout my PhD and I owe at least a part of my successes to him being such a loving, insightful, and patient spouse.

Table of Contents

List of Tables

List of Figures

List of Acronyms

AMPK	adenosine monophospate-activated protein kinase
ANOVA	analysis of variance
ANT2	adenine nucleotide translocator 2
Atg	autophagy-related
ATP	adenosine triphosphate
ATP5A	ATP synthase alpha-subunit
BafA1	bafilomycin A1
BIR	baculovirus inhibitior of apoptosis protein repeat
BSA	bovine serum albumin
CARD	caspase activation and recruitment domain
caspase	cysteine-dependent aspartate specific protease
cg	combgap gene
CL1-GFP	fusion protein with a degradation signal in GFP
clDcp-1	cleaved Dcp-1
CMA	chaperone-mediated autophagy
DAPI	4’6-diamidino-2-phenylindole
Dcp-1	death caspase-1
Dcr	dicer-2
DED	death-effector domain
Diap1	death-associated inhibitor of apoptosis 1
DMEM	Dulbecco's modified Eagle's medium
DMSO	dimethylsulfoxide
Drice	death related ICE-like caspase
Dronc	death Nedd-2-like caspase
dsRNA	double-stranded ribonucleic acid
EDTA	ethylenediaminetetraacetic acid
FBS	fetal bovine serum
G418	Geneticin®
GAL4	galactose-responsive transcription factor
GFP	green fluorescent protein
HEK293	human embryonic kidney cells 293

HEPES	4-(2-hydroxyethyl)-1-piperazineethanesulfonic acid
HER2	human epidermal growth factor receptor 2
Hsp	heat shock protein
HSP90	human heat shock protein 90
IAP	inhibitor of apoptosis proteins
IF	immunofluorescence
IgG	immunoglobulin G
IP	immuno-affinity purification
l(2)mbn	lethal (2) malignant blood neoplasm
LAMP	lysosome-associated membrane glycoprotein
LC	liquid chromatography
LC3	light-chain 3
LTG	LysoTracker® Green
LTR	LysoTracker® Red
mCherry	monomeric red fluorescent construct
MDA-MB-231	HER2- human breast adenocarcinoma line
MES	2-(N-morpholino)ethanesulfonic acid
MG132	proteasome inhibitor
MKRS	stubble bristles balancer chromosome
MOPS	3-(N-morpholino)propanesulfonic acid
MS	mass spectrometry
MSDEC	mid-stage degenerating egg chamber
MSEC	mid-stage egg chamber
NCI-H2170	lung squamous cell carcinoma cell line
nos	nanos gene
PAGE	polyacrylamide gel electrophoresis
PANC1	pancreatic ductal epitheliod carcinoma cell line
PBS	phosphate buffered saline
PE	Phosphatidylethanolamine
PI	propidium iodide
PI3K	class III phosphatidylinositol-3-kinase
PINK1	PTEN-induced putative kinase 1
PMSF	phenylmethylsulfonyl fluoride

Prosα1	proteasome α1 subunit
PVDF	polyvinylidene fluoride
qRT-PCR	quantitative reverse transcription polymerase chain reaction
RFP	red fluorescent protein
Rheb	ras homolog enriched in brain
RIPA	radioimmunoprecipitation assay
RNAi	ribonucleic acid interference
RPMI	Roswell Park Memorial Institute medium
Rpn	regulatory particle non-ATPase
S.E.M.	standard error of the mean
S2	Schneider 2 cells
S6K	ribosomal protein S6 kinase
SDS	sodium dodecyl sulfate
SEM	sucrose-EDTA-MOPS
sesB	stress sensitive B
siRNA	small interfering RNA
SKBR3	$HER2^+$ breast adenocarcinoma line
TNF	tumour necrosis factor
TOMM20	translocase of outer mitochondrial membrane 20
TOR	target of rapamycin protein
transhet	transheterozygote
TUNEL	terminal deoxynucelotidyl transferase dUTP nick end labelling
UAS	upstream activation sequence
ULK	unc-51-like kinase
UPS	ubiquitin-proteasome system
VPS	vacuolar protein sorting

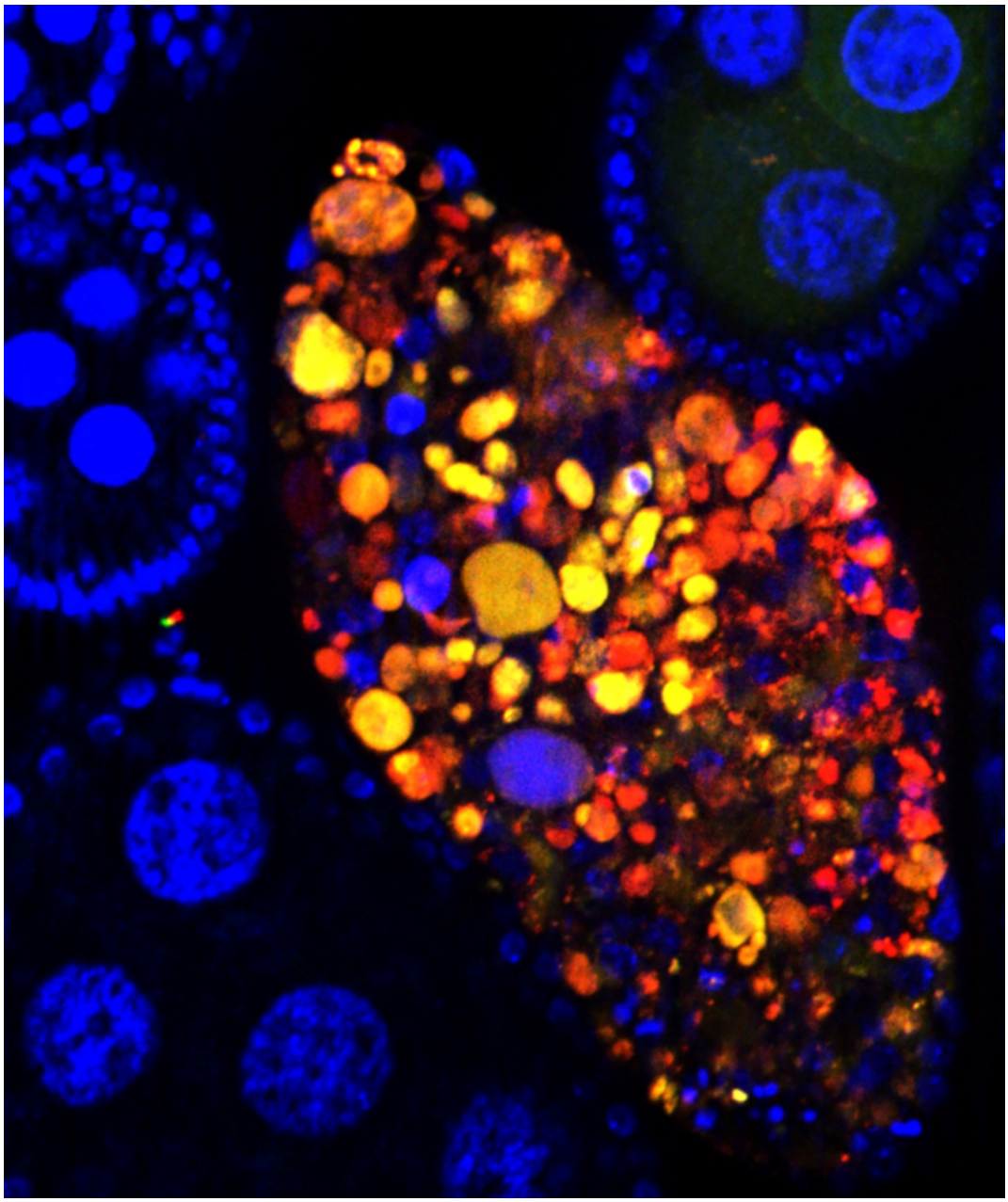

Chapter 1. General Introduction

1.1. Autophagy

1.1.1. Types of autophagy

Autophagy is a conserved eukaryotic cellular recycling process that relies on the lysosome. There are three main forms of autophagy: macroautophagy, microautophagy, and chaperone-mediated autophagy (Figure 1-1). Microautophagy is a non-selective degradative process where the lysosome, or vacuole in plants and fungi, directly engulfs cytosolic components by using autophagic tubes and invagination (Figure 1-1B) (Ahlberg and Glaumann, 1985; Marzella et al., 1980). Comparatively, less is known about this process than the other forms of autophagy but it appears to function in the maintenance of organellar size, cell survival under nitrogen deprivation and membrane homeostasis (Li et al., 2012). Chaperone-mediated autophagy (CMA) is another discovered form of autophagy that functions to target only single proteins (Figure 1-1C) (Neff et al., 1981). Targeting occurs through the recognition of a five amino acid KFERQ or KFERQ-like motif by heat-shock cognate 70 (Hsc70) (Dice et al., 1990). This complex then binds to lysosome-associated membrane protein type 2a, LAMP-2A, which mediates its transfer inside the lysosome for lysosomal degradation (Cuervo and Dice, 1996; Cuervo et al., 1997). Macroautophagy, hereafter referred to as autophagy, is the best studied mechanism of autophagy and is the pathway that is the focus in this thesis (Figure 1-1A). The process begins by the formation of a double-membraned autophagophore or isolation membrane that expands and sequesters bulk cytoplasm containing organelles and proteins. This double-membrane structure containing selective and non-selective cytosolic components eventually closes to form the autophagosome. The autophagosome then fuses with lysosomes to form a single-membraned structure known as the autolysosome. The process is completed when the lysosomal hydrolases degrade the inner membrane and contents of the autolysosome back to basic building blocks, such as amino acids and

metabolites, which are then returned to the cell via lysosomal permeases (Yang and Klionsky, 2010). Macroautophagy is dynamic and often completion of the entire process is distinguished as autophagic flux. There are several specific forms of macroautophagy that are studied which focus on the nature of the targeted degradative product such as mitophagy (mitochondria), xenophagy (foreign microbes), and pexophagy (peroxisomes) to name a few (Klionsky et al., 2007).

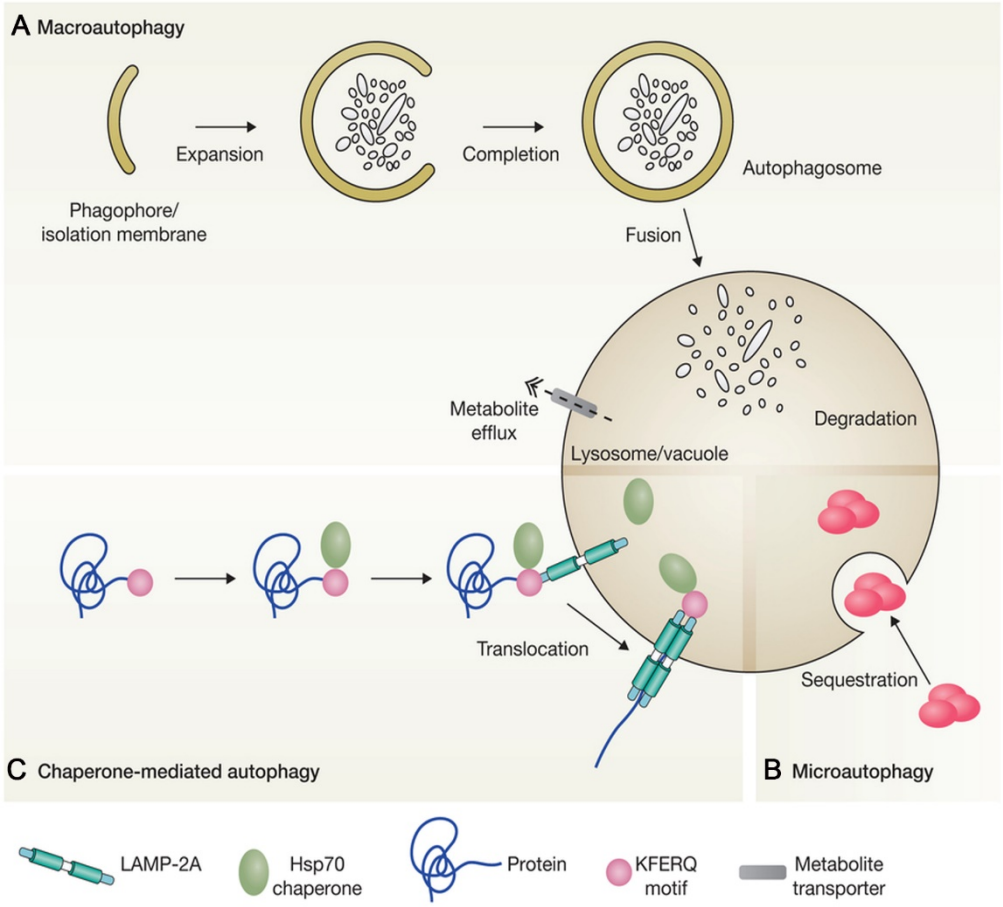

Figure 1-1 Types of autophagy

All forms of autophagy are dependent on the lysosomes/vacuole. (**A**) Macroautophagy begins by the formation of the double-membraned phagophore which expands and sequesters cytosolic components. This encloses to form the autophagosome which then directly fuses with the lysosomes. (**B**) Microautophagy occurs when the lysosome invaginates and degrades small proteins or protein complexes directly into the lysosomes where the substrates are degraded. (**C**) Chaperone-mediated autophagy involves first the Hsp70 recognition of a single protein by its KFERQ motif. This complex then binds to lysosomes receptor, LAMP2A, to translocate the protein and Hsp70 complex inside of the lysosomes for it to be degraded. Adapted from Boya et al., 2013.

1.1.2. Functions of autophagy

Autophagy occurs at basal levels in most cell types to play a housekeeping role by recycling unnecessary and potentially harmful cellular components such as damaged organelles or aggregated proteins (Hara et al., 2006; Komatsu et al., 2005). Additionally, autophagy was shown to play roles in development, differentiation and immunology (Mintern and Harris, 2015; Mizushima and Levine, 2010). However, autophagy arguably is best known for its ability to function as an adaptation process that is upregulated in response to several kinds of cellular stresses to aid in cell survival. One of the most common and well-characterized stresses that induces autophagy is nutrient deprivation from the depletion of amino acids, glucose or oxygen (Yorimitsu and Klionsky, 2005). The primary function of autophagy under this condition is to recycle macromolecules into basic metabolites and building blocks to assist in providing an alternative source of energy (Kaur and Debnath, 2015). To maintain genomic and cellular integrity, autophagy also responds to cellular assaults from reactive oxygen species, chemicals or radiation by clearing proteins or organelles which have been damaged (Zhang, 2013). The selective autophagy process, xenophagy, can be upregulated in response to the recognition of foreign properties from extracellular microbes and serves to promote clearance of these foreign entities (Bauckman et al., 2015). These examples of key roles that autophagy plays in cellular homeostasis help explain why dysfunction or dysregulation of autophagy has been associated with a plethora of diseases such as neurodegeneration and cancer (Levine and Kroemer, 2008).

1.1.3. Brief history of autophagy discoveries

The origins of the discovery of autophagy began first with Christian de Duve's identification of the lysosome in the 1950's (de Duve et al., 1955). Christian de Duve later went on to coin the term "autophagy" from the Greek "auto" meaning "self" and "phagy" meaning "eating" from his observations of cellular structures in mammalian tissues in 1966 (De Duve and Wattiaux, 1966). The cellular structures he observed, using electron microscopy, were the signature double-membraned or single-membraned structures, known as autophagosomes and autolysosomes respectively, containing cytosolic proteins and organelles at various stages of disintegration (De Duve and Wattiaux, 1966).

Autophagic structures were then demonstrated to also occur in yeast and fuse with the vacuole, a lysosome-like organelle in yeast cells, several decades later by Yoshinori Ohsumi's laboratory in 1992 (Takeshige et al., 1992). This discovery was key as further studies in yeast identified many of the core conserved autophagy-related (*Atg*) genes through mutagenesis experiments identifying autophagy-defective yeast strains (Thumm et al., 1994; Tsukada and Ohsumi, 1993). Yoshinori Ohsumi's pioneering work in the autophagy field through discovery of key proteins and mechanisms was recently recognized when the Nobel Prize for Physiology and Medicine was awarded to him in 2016. The first human autophagy genes showing conservation between yeast and mammals were then identified as *ATG5* and *ATG12* in 1998 (Mizushima et al., 1998). Two years later, the most commonly used marker for autophagy and the basis of several autophagy-related assays was identified as the mammalian protein light-chain 3 (LC3) (Kabeya et al., 2000). The field of autophagy has since then exploded with research being performed in diverse organisms such as fungi, *Drosophila*, mice, and humans, leading to elucidation of the autophagy molecular machinery and many of its regulators as well as the roles of autophagy in development, aging and disease (Feng et al., 2014). Although there have been great lengths accomplished in the autophagy field, there are still many remaining questions such as the origin of the double-membrane, the importance and role of autophagy in diverse tissues and development states, substrate selection and recognition and the complex regulatory pathways that can activate or inhibit autophagy.

1.2. Molecular machinery of autophagy

To date there are more than 35 autophagy-related (*atg*) genes identified in yeast; many of which are conserved among higher eukaryotes (Klionsky, 2014). *Atg* genes have specific roles in the dynamic stages of autophagy that can be mechanistically divided into autophagy induction, autophagosome nucleation, autophagosome expansion and completion. The proteins involved in the mammalian autophagic machinery are summarized in Figure 1-2.

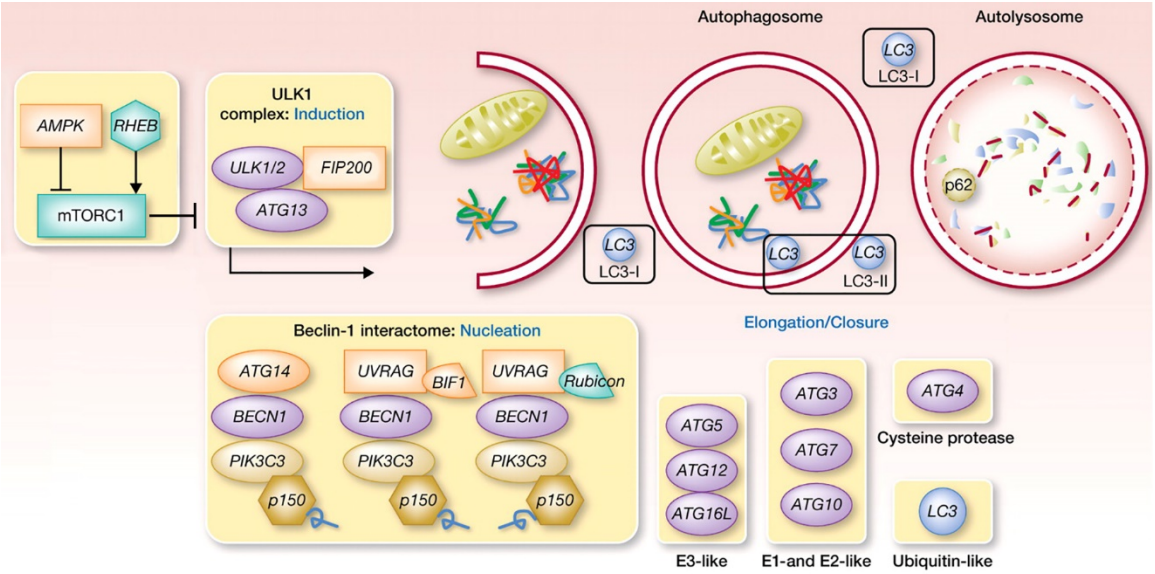

Figure 1-2 Molecular machinery of autophagy in mammals

Autophagy induction, autophagosome nucleation and vesicle elongation are required for autophagosome formation. Autophagy induction is initiated by inhibition of the TOR kinase, mTORC1, which can be performed by the energy sensor AMPK. Once mTORC1 is inhibited, the formation of the ULK1/2 complex with ATG12 and FIP200 localizes to the phagphore to induce autophagosome formation. Nucleation is dependent on the formation of the PI3K complex which consists of PI3KC3, BECN1, p150 and ATG14 in order to produce PI3K and attract the ATG proteins needed for elongation. Two well conserved ubiquitin-like conjugation systems are required for autophagosome elongation. The ATG12-ATG5-ATG16 complex forms to act like an E3 protein at the autophagosome. ATG4 cleaves LC3 where it is then transferred amongst E1 and E2-like enzymes ATG7 and ATG3, respectively. The two pathways come together when the ATG12-ATG5-ATG16 complex inserts LC3 into the autophagosomal membrane for elongation. Lastly, ATG4 recycles LC3 off of the outer membrane to assist with maturation and eventual fusion with the lysosomes. Adapted from Lebovitz et al., 2012.

1.2.1. Autophagy induction

While autophagy occurs at low levels in basal conditions, the cell has specific signaling pathways to induce autophagy in response to stress. One recognized control point is through the serine/threonine kinase target-of-rapamycin, TOR (dTOR in *Drosophila*, mTOR in mammals) which is a metabolic sensor that negatively regulates autophagy but positively regulates several other processes including protein synthesis, transcription and ribosome biogenesis (Díaz-Troya et al., 2008). TOR suppresses autophagy in nutrient-rich conditions by preventing the association of the key autophagy inducer serine/threonine kinase Atg1 with other autophagy substrates (Chang and Neufeld, 2009). TOR can phosphorylate and interact with Atg1 and Atg13 to prevent the

interaction and formation of the autophagy-inducing complex Atg1-Atg13-Atg17 (Kamada et al., 2000, 2010). Signals from energy sensor AMP-activated protein kinase (AMPK) and amino acid signaling can inactivate TOR in low nutrient conditions (Jewell et al., 2013). When TOR is inactivated, Atg13 becomes dephosphorylated and the Atg1 complex can be assembled and activated by phosphorylation to induce autophagy (Kijanska et al., 2010; Yeh et al., 2010). In mammals, there are two homologs of Atg1, Unc-51-like kinase-1 (ULK1) and -2 (ULK2) as well as a homolog of Atg17 called focal adhesion kinase family-interacting protein of 200kDa (FIP200) (Hara et al., 2008; Jung et al., 2009). Once the Atg-1/ULK complex is assembled and activated it localizes to the phagophore to initiate autophagosome formation (Cheong et al., 2008).

1.2.2. Autophagosome nucleation

There are still several theories of the origin of the phagophore membrane with groups postulating it originates from various organelles such as the endoplasmic reticulum (ER), mitochondria, the plasma membrane and the golgi apparatus (Axe et al., 2008; Hamasaki et al., 2013; Hayashi-Nishino et al., 2009; Ravikumar et al., 2010). Induction of autophagy causes the phagophore to be expanded into the double-membraned structure, the autophagosome, through an Atg-specific pathway. In order to recruit the Atg proteins to the phagophore, the class III phosphatidylinositol-3-kinase (PI3K) complex must produce phosphatidyl-inositol 3-phospate (PI3P) (Nice et al., 2002; Obara et al., 2008). The PI3K complex is composed of Vps34 (PI3KC3 in mammals), Vps15 (p150 in mammalian cells), Atg14 and Atg6/Vps30 (BECLIN1 in mammalian cells) (Itakura et al., 2008; Kihara et al., 2001; Sun et al., 2008). Dissociation of Beclin1 from the anti-apoptotic protein Bcl-2 is required and triggered under nutrient poor conditions to induce autophagy (Liang et al., 1999). AMBRA1 interacts with BECLIN1 and is phosphorylated by the ULK1 protein upon autophagy induction which allows translocation of the BECLIN1 complex to the ER to promote autophagosome formation (Di Bartolomeo et al., 2010). The PI3K complex then recruits several Atg proteins and ubiquitin-like (Ubl) conjugation systems to the phagophore to enable expansion (Suzuki et al., 2001a).

1.2.3. Autophagosome expansion and completion

There are two main Ubl conjugation systems for autophagosome expansion: the Atg12-Atg5-Atg-16 system and the Atg8-Atg4-Atg3 system. The systems are described as ubiquitin-like because Atg12 and Atg8 undergo a similar E1/E2/E3 conjugation process. Atg12 is first activated by the E1-like activating enzyme Atg7, transferred to the E2 conjugating enzyme Atg10 and finally attached to a lysine on Atg5 (Geng and Klionsky, 2008). This Atg12-Atg5 conjugate interacts with E3-like enzyme Atg16 forming the Atg12-Atg-5-Atg16 complex which is tetramerized and attached to the phagophore (Mizushima et al., 1999, 2003). In the other system, Atg8/LC3 is first cleaved by the cysteine protease Atg4 to create Atg8/LC3-I which allows a now exposed C-terminal glycine to be lipidated. Atg8/LC3-I is then further activated by the same E1-like enzyme Atg7 before being transferred to the E2 enzyme Atg3 (Taherbhoy et al., 2011). These two Ubl systems then meet when the Atg12-Atg5-Atg16 acts like an E3 enzyme by conjugating Atg8/LC3-I to the target lipid phosphatidylethanolamine (PE),becoming LC3-II, and assisting with its insertion into the autophagosomal membrane (Fujita et al., 2008b; Hanada et al., 2007; Thukral et al., 2015). The lipid-conjugated LC3-II form is present on the inner and outer membrane of the autophagosome and is involved in controlling the size of the autophagosome, and the curvature and closure of the membrane (Knorr et al., 2014; Xie et al., 2008). The Atg8/LC3-II on the outside of the completed autophagosome is then recycled back to the unlipidated form through cleavage by Atg4 (Kirisako et al., 2000), a step that has been shown necessary for maturation and eventual lysosomal fusion in yeast (Yu et al., 2012). Once lysosomes fuse with the autophagosome, the acidic hydrolases degrade its contents (including the inner lipidated Atg8/LC3) into small molecules, such as amino acids, lipids and carbohydrates, which are returned to the cytoplasm by lysosomal permeases completing autophagic flux (Mizushima, 2007; Yang et al., 2006).

1.3. Autophagy assays

Autophagic flux is dynamic and therefore can be a challenging process to evaluate. The recommended way to determine if autophagic flux is affected in a particular model system is to utilize several different assays to come to a consensus, especially since many of the assays have their own caveats or limitations. The autophagy community has a

frequently updated manual called “Guidelines for the use and interpretation of assays for monitoring autophagy” where specific assays for organisms from yeast to humans have been extensively evaluated for their utility and practicality (Klionsky et al., 2016). Described below are the three autophagy assays that are used in this thesis.

1.3.1. RFP/mCherry-GFP-LC3B (Atg8a)

Atg8 (Atg8a in *Drosophila*) and its mammalian homologue LC3 are central to several autophagy assays. There are three human LC3 isoforms, LC3A, LC3B and LC3C, that are all modified in a ubiquitin-like manner (He et al., 2003). LC3B has been the most commonly studied LC3 family member to date and thus most assays have been designed to focus autophagic flux analysis on this isoform (Figure 1-3). As described above, Atg8a/LC3B is lipidated and then inserted into the autophagosomal membrane and thus essentially can act as a marker for autophagosomes or autolysosomes (Kabeya et al., 2000; Thukral et al., 2015). A common method to monitor autophagy is through visualization of Atg8a/LC3B, as the lipidated form lines the autophagosomes and consequently appears in punctate structures (Kabeya et al., 2000). Atg8a/LC3B can be monitored directly by immunofluorescence (Tanida et al., 2005) but more commonly it is fused to a fluorescent protein, such as GFP, using an overexpression reporter construct. One of the best ways to accurately monitor autophagic flux is by tagging Atg8a/LC3B with two different fluorescent markers, RFP/mCherry and GFP, which takes advantage of GFP’s sensitivity to acidity and makes it possible to differentiate the autophagosomal stage from the autolysosomal stage (Kimura et al., 2007). Both fluorescent markers are detected at autophagosomes using microscopy where overlap of the RFP and GFP signals can be displayed as yellow puncta in the cell (Figure 1-3A). However, if lysosomal fusion has occurred and the pH has been lowered in the autolysosome, the GFP signal becomes quenched, resulting in the appearance of red puncta. The RFP/mCherry-GFP-Atg8a/LC3B (also referred to as tandem-Atg8a/LC3B) is a construct that can be expressed *in vivo* in fly stocks or can be stably transfected in *Drosophila* or human cell lines making it a very useful tool to monitor induction and completion of autophagic flux (DeVorkin and Gorski, 2014a; Kimura et al., 2007).

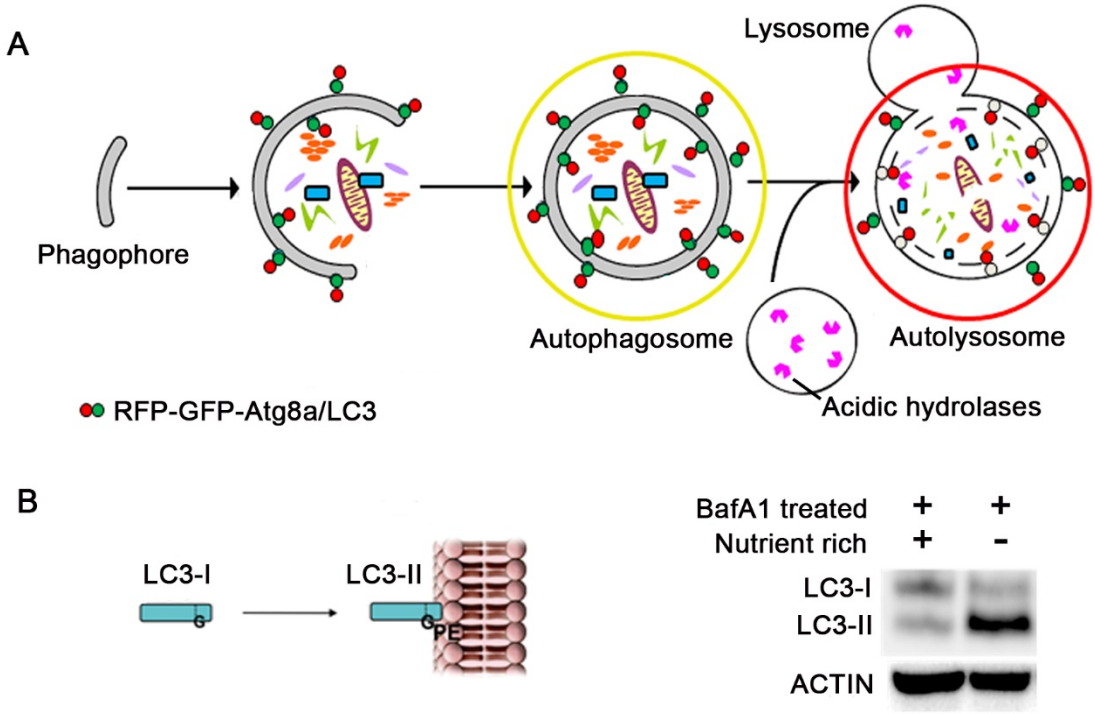

Figure 1-3 Autophagy LC3B assays

(**A**) Exogenous expression of the tandem reporter, RFP-GFP-Atg8a/LC3B, lines the inner and outer membranes of the autophagosome when autophagic flux is initiated. Using microscopy, the signals from GFP and RFP overlap giving the appearance of yellow puncta. When autophagic flux is completed by lysosomal fusion, the autolysosome only expresses signal from the RFP because the acidity from the lysosomes quenches the GFP signal giving the appearance of red puncta. Adapted from Hannigan and Gorski, 2009. (**B**) The membrane bound LC3-II with its covalently attached PE has a different mobility on immunoblots than LC3-I. Cells treated with Bafilomycin A1, to block the lysosomal fusion step of autophagy, leads to an accumulation of LC3-II when autophagic induction is upregulated.

1.3.2. Bafilomycin LC3B-I/LC3B-II immunoblot

Another method that relies on LC3B monitors the conversion of LC3B from the delipidated form (LC3B-I) to the lipidated form (LC3B-II) (Kadowaki and Karim, 2009). If there is an increase in autophagy induction, LC3B-I is rapidly converted to LC3B-II to enable the formation of autophagosomes (Tanida et al., 2005). However, autophagy is a dynamic process and the LC3B-II can be recycled back through completion of autophagic flux. Thus, to compare levels of pools of both LC3B-I and LC3B-II proteins, it is important to block the final steps of autophagy (Tanida et al., 2005). There are several late stage autophagy inhibitors that affect the acidity of the lysosomes or the lysosomal fusion step; one commonly used inhibitor is Bafilomycin A1 that works to inhibit vacuolar H-ATPases

of the lysosomes, causing an increase in the intralysosomal pH (Ashoor et al., 2013; Klionsky et al., 2008). Treatment with Bafilomycin A1 prevents lysosomal fusion leading to a distinct accumulation of LC3B-II-decorated autophagosomes if autophagy has been induced (Figure 1-3B). LC3B-I and LC3B-II have distinct mobilities on SDS-PAGE gels which makes it possible to compare the relative amounts of autophagy induction between controls and treatments by immunoblot densitometry analysis.

1.3.3. Acidotropic dyes

A supportive autophagy assay is quantitation of the cellular level of lysosomal activity, represented by lysosomes and autolysosomes, which typically correlates with the level of autophagic activity (Zhou et al., 2013). The lysosomes can be marked by specific antibodies, for example LAMP1, or lysosomes/autolysosomes can be visualized using acidotropic dyes such as LysoTracker® Red or LysoTracker® Green (Chikte et al., 2014; DeVorkin and Gorski, 2014b). These live cell dyes are weak bases linked to a fluorophore that accumulate in acidic organelles where they become protonated and trapped. The intensity of the staining can be assessed using flow cytometry or quantitative fluorescent microscopy to compare levels of lysosomal activity in cells following different treatments (Chikte et al., 2014; DeVorkin and Gorski, 2014b). These assays are useful as supporting evidence to determine whether autophagic flux is increased or decreased, but always require complementation by an autophagy-specific assay.

1.4. *Drosophila* as a model organism for studying autophagy

Drosophila melanogaster has become a powerful organism in which to monitor autophagy because of the development of *in vivo* tools to analyze differences in autophagy regulation and flux between tissues and developmental stages (Nagy et al., 2015). Autophagy contributes to developmental processes in several tissues through the steroid hormone ecdysone or various signaling pathways (Calamita and Fanto, 2011; Lee and Baehrecke, 2001; Lee et al., 2002; Rusten et al., 2004). During *Drosophila* development, the availability of nutrients critical for growth signaling needs to be sustained so tissues such as the larval fat body, the midgut, and the ovary are sensitive to nutrient deprivation

and readily induce autophagy (Barth et al., 2011; DeVorkin et al., 2014; Hou et al., 2008; Scott et al., 2004; Wu et al., 2009). In my thesis I analyzed autophagy in the mid-stage egg chambers of the ovary as well as larval fat bodies since they are established models of autophagy (Figure 1-4).

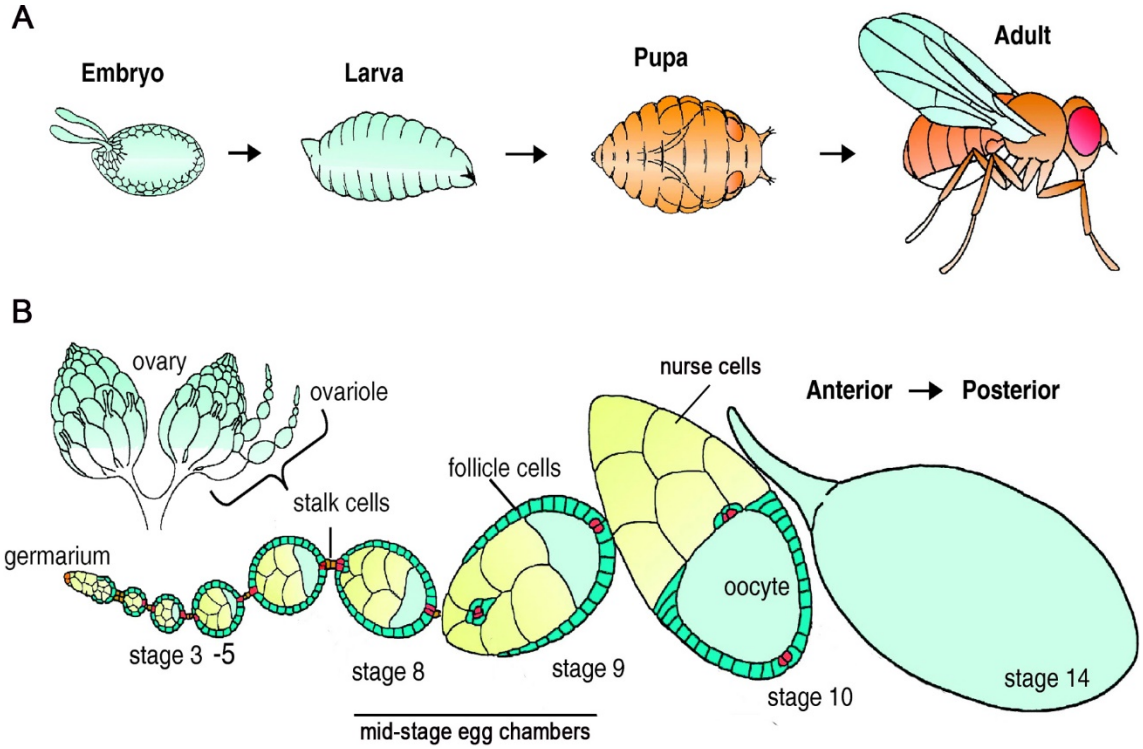

Figure 1-4 Drosophila life stages and oogenesis development

(**A**) The life cycle of Drosophila consists of four main stages: embryo, larva, pupa and adult. In my thesis, I focus on the fat bodies of larva and oogenesis in adult Drosophila. (**B**) Drosophila ovaries consist of 15 to 20 ovarioles that contain 14 well-defined stages of developing egg chambers beginning at the germarium. The mid-stage egg chambers consist of somatic follicle cells surrounding the germline nurse cells and oocyte, and mark beginning of yolk formation. Adapted from He et al., 2011.

1.4.1. *Drosophila* oogenesis and autophagy

Each female *Drosophila* has two ovaries, each containing 15 to 20 ovarioles (Figure 1-4B). Ovarioles are composed of a series of developing egg chambers that arise from the germarium and progress posteriorly through 14 well-defined stages (King, 1970). Stem cells give rise to two types of cells within the germarium: the somatic cells and the germline cells (Kirilly and Xie, 2007). Beginning in stage one, each egg chamber is made up of 15 germline nurse cells and one developing oocyte connected by ring canals and

surrounded by the somatic-derived follicle cells (Spradling, 1993). The nurse cells function to support growth of the oocyte by providing a source of nutrients through the ring canals. At stage eight of development, vitellogenesis begins to produce the yolk, and the oocyte nucleus begins to increase in size. By stage eleven, the contents of the nurse cells are distributed into the oocyte and the nurse cells begin to shrink. At stage twelve, the nurse cells begin apoptosis once depleted of their cytoplasm and the remnants are engulfed by surrounding follicle cells (Cavaliere et al., 1998; Nezis et al., 2000). The final stage of oogenesis allows the fully developed ooctyte to be encased by the completed chorion secreted from the apoptotic follicle cells (Nezis et al., 2002). Autophagy occurs in both the germline and follicle cells under basal conditions and is an important form of communication between the follicle cells and the germline cells (Barth et al., 2011). Autophagy is notably upregulated in the germarium and mid-stage egg chambers in response to nutritional cues (Barth et al., 2011; Hou et al., 2008; Nezis et al., 2009). For my thesis I chose to focus on stage 7-9 egg chambers, or mid-stage egg chambers, as they represent a key nutritionally-sensitive checkpoint that is associated with autophagy and determines if the oocyte will undergo the energy-demanding process of vitellogenesis (Drummond-Barbosa and Spradling, 2001).

1.4.2. *Drosophila* larval fat body and autophagy

The *Drosophila* larval fat body is a nutrient storage organ analogous to the mammalian liver and adipose tissue, serving as a major storage site for glycogen, lipids and proteins (Azeez et al., 2014). Autophagy is enhanced in the larval fat body in the late larval stages and during metamorphosis to provide nutrients to developing imaginal tissues (Juhász et al., 2003). Larval development is divided into three larval instars that are distinguished by larval spiracles and mouthparts, and signify the different stages of moulting. During development in the late larval stages, or the third larval instar, there is an upregulation of autophagy in response to an increase in the steroidal hormone ecdysone which also alters the behavior of the larva to include foraging activities (Rusten et al., 2004). Autophagy is also readily induced in the larval fat body in response to amino acid starvation (Scott et al., 2004). Without autophagy, larva do not survive starvation due to defects associated with lipid accumulation (Britton et al., 2002; Hou et al., 2008; Wang et al., 2012). For my thesis I included studies of the fat body from first instar larva because

they are sensitive to starvation-induced autophagy but do not undergo hormone-related autophagy during this stage(Scott et al., 2004).

1.5. Apoptosis

Apoptosis, meaning “falling off” in Greek, was coined after Kerr et al. noticed a type of cell death characterized by cell shrinkage as opposed to the cell rupture that is characteristic of necrosis (Kerr et al., 1972). Also commonly known as Type I programmed cell death, apoptosis is characterized by distinct morphologies including nuclear fragmentation, chromatin condensation, and membrane blebbing (Hengartner, 2000). The cell shrinks and blebs to form smaller cellular fragments which are engulfed and digested by surrounding phagocytic cells to prevent an inflammatory response (Kerr et al., 1972). Apoptosis is a common event in development to clear superfluous cells but can also be triggered in response to cell death stimuli such as DNA damage, hypoxia, and heat (Rich et al., 2000). Apoptosis can be activated through two separate pathways that differentiate between internal and external signals: the intrinsic apoptotic pathway and the extrinsic apoptotic pathway (Figure 1-5). Mitochondria are central to instrinsic pathway activation. Cell death stimuli trigger mitochondrial permeability transition (MPT) pores to form as well as the loss of mitochondrial transmembrane potential which results in the release of pro-apoptotic proteins to the cytosol where they can become activated (Saelens et al., 2004). External signals can also stimulate activation of apoptosis through transmembrane receptor recognition in the extrinsic pathway. The two best characterized ligand/receptor interactions identified in the extrinsic pathway are FasL/FasR and TNF-α/TNFR1 (Bang et al., 2000). After ligand recognition, a signal transduction pathway is induced where adaptor proteins with death domains (DED) are recruited to the cytoplasmic side of the receptors to form the death-inducing signaling complex (DISC) (Ouyang et al., 2012). Both pathways eventually converge to the final phase of apoptosis, the execution phase, which requires the activation of cysteine-aspartic proteases (caspases) to cleave a variety of downstream targets.

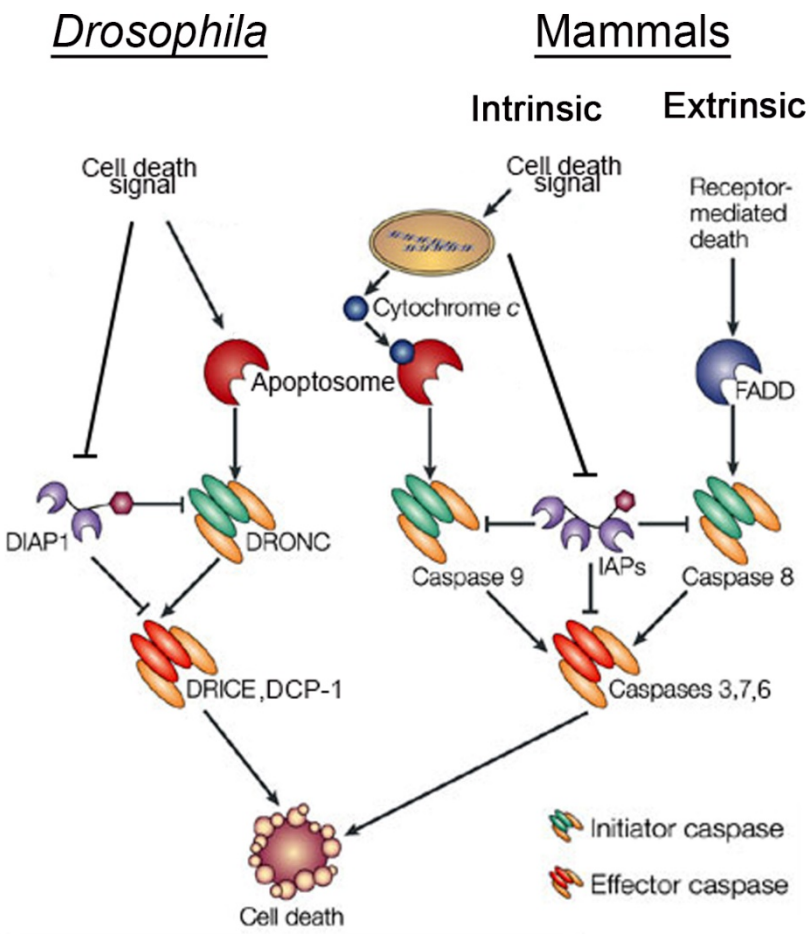

Figure 1-5 Apoptotic cascades in *Drosophila* and mammals

Drosophila and mammalian cascades have similar structured hierarchies of proteins. In Drosophila, a cell signal triggers activation of initiator caspase Dronc through Diap1 inhibition or through activation of the apoptosome. Dronc then goes on to activate the effector caspases, Drice and Dcp-1, which cleave a variety of substrates to effect apoptosis. In mammals, the intrinsic pathway is induced through mitochondrial perturbation which leads to apoptosome formation from cytochrome c release or blockage of inhibitor of apoptosis proteins (IAPs). This subsequently leads to activation of the initiator caspase, caspase-9. The extrinsic pathway begins when a ligand binds a death receptor to start a signal cascade that causes activation of Caspase-8. Active caspase-8 and active caspase-9 cleave effector caspases, caspase-3, caspase-6, and caspase-7, to induce the final cleavage steps of apoptosis. Adapted from Hay et al., 2004.

1.5.1. Caspases

Caspases are cysteine-aspartic proteases that are traditionally associated with roles in programmed cell death and inflammation. Their name reflects their mechanism of action: cleavage of proteins by nucleophilic attack of a target aspartic acid using a cysteine in the active site of the caspase (McIlwain et al., 2013). Caspases exist in the cell as

inactive zymogens (pro-caspases) so that they only become active with the proper stimulus. Caspases are tightly regulated by subcellular localization and inhibitor of apoptosis proteins (IAPs). The inactive pro-caspase consists of a pro-domain of variable lengths, a large p20 subunit, a small p10 subunit, and a linker between the p20 and p10 subunit (Figure 1-6A). Activation leads to proteolytic processing of the linker between the subunits which allows the protein to assemble into an active tetramer consisting of two p20 and two p10 subunits (Figure 1-6B) (Chang and Yang, 2000). Each tetramer has two cavity-shaped active sites formed from both large and small subunits (Chang and Yang, 2000). A final step involves removal of the pro-domain, allowing the caspase to mature and be stabilized but does not affect the catalytic activity (Pop and Salvesen, 2009). The catalytic activity of caspases is localized to the p20 subunit which contains the catalytic dyad residues Cys and His, while the p10 subunit contributes to formation of the substrate binding groove (Pop and Salvesen, 2009). Caspases recognize the substrate peptide sequence P_4-P_3-P_2-P_1-P_1' where P_1-P_1' is the scissile bond and the P_1 peptide is invariably an aspartic acid (D) (Talanian et al., 1997). However, in *Drosophila*, the P_1 peptide can be another small uncharged residue (Hawkins et al., 2000). The different caspases have variable affinities for certain combinations of amino acids to form the catalytic groove. The most common peptide recognition sequences in mammals are YVAD, DVDAD, DEVD, LEVD, WEHD, VEID, IETD, LEHD and AEVD for caspase-1, caspase-2, caspase-3/ -7, caspase-4, caspase-5, caspase-6, caspase-8, caspase-9, and caspase-10 respectively (Talanian et al., 1997). However, cross-reactivity is a common occurrence and fidelity is low for the specific sequences (McStay et al., 2008).

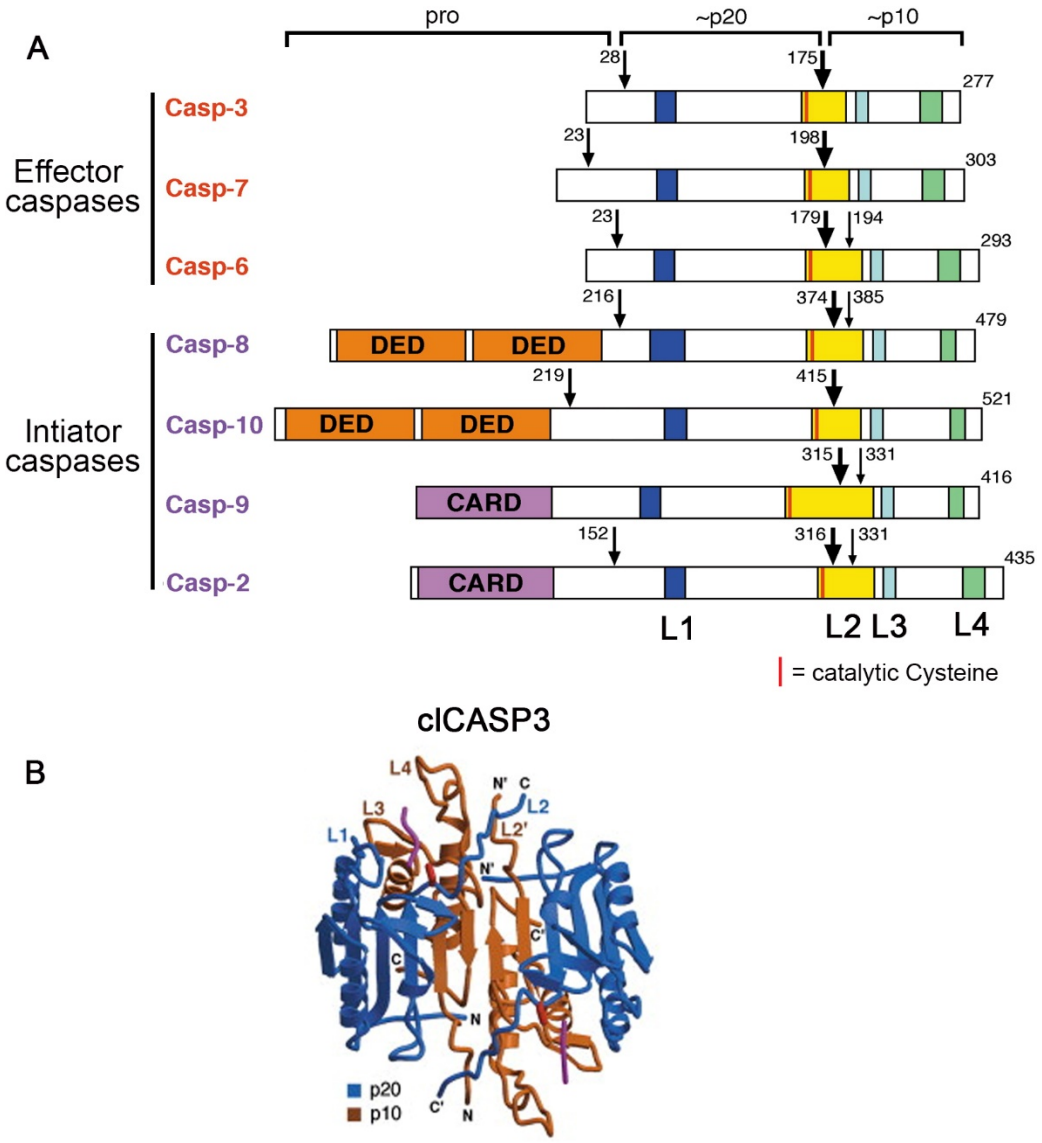

Figure 1-6 Structures of zymogens and active apoptotic caspases

(**A**) All apoptotic caspase zymogens can be divided into three sections: the prodomain, the p20 subunit and the p10 subunit. The initiator caspases have longer pro-domains that contain caspase recruitment domains (CARD) or death effector domains (DED). Effector caspases have very short pro-domains as their activation only requires cleavage between the p20 and p10 subunit as opposed to the recruiting domains on the initiator caspases. The main cleavage site for caspase activity is indicated by a large arrow, while the smaller arrows represent further processing steps that aren't required for activation. The four loops which compose the catalytic groove are shown from L1-L4. The catalytic Cysteine residue is indicated by a red line in L2. (**B**) Cleavage between the p20 and p10 domain allows the formation of active caspase-3 heterotetramer. The catalytic binding groove is between the p20 and p10 subunit. Adapted from Shi, 2002.

1.5.2. Classification of caspases

Caspases are classified by their role in apoptosis or inflammation with the exception of caspase-14 which plays a role in epithelial cell differentiation (Denecker et al., 2008). In humans, the group of inflammatory caspases includes caspase-1, caspase-4, caspase-5, and caspase-12. Caspase-11 is an inflammatory caspase but has been shown to only exist in mice (Broz and Monack, 2013) while caspase-13 is an inflammatory caspase only found in bovine species (Koenig et al., 2001). The apoptotic pathway in humans includes caspases-2,-3,-6, -7, -8, -9 and -10. In *Drosophila* there are seven identified caspases: Dronc, Dredd, Strica, Dcp-1, Drice, Damm, and Decay. The caspases can then be further subdivided into initiator or effector caspases based on their hierarchal position in the apoptotic cascade.

1.5.3. Initiator caspases

Initiator caspases are upstream of effector (executioner) caspases in the apoptotic cascade and have longer pro-domains containing protein-protein interaction domains such as the caspase recruitment domain (CARD) and the death effector domain (DED) (Figure 1-6A) (Degterev et al., 2003). Initiator caspases exist as stable monomers that are recruited to activation platforms where the concentration of caspases cause proximity-induced dimerization (Boatright and Salvesen, 2003). The dimerization facilitates autocatalytic activity allowing proteolytic processing of the p20 and p10 subunits. Once the initiator caspase is activated, it subsequently targets effector caspases to propagate the apoptotic cascade. In humans, initatior caspases are identified as caspase-2, caspase-8, caspase-9 and caspase-10. Currently, there is little known about the mechanism of action for caspase-10 other than it appears to behave like an initiator caspase in the apoptotic pathway (Wachmann et al., 2010). In Drosophila, Dronc, Dredd and Strica contain long pro-domains and thus are classified as initatior caspases. Dronc is recognized as the main initiator caspase as it is required for all apoptotic cell death (Kumar and Doumanis, 2000).

1.5.4. Effector caspases

In comparison to the initiator caspases, effector caspases have a relatively short pro-domain and already exist as inactive homodimers (Figure 1-6A) (Parrish et al., 2013). Effector caspases become activated due to a conformational change when the linker between the p20 and p10 subunits is proteolyzed predominantly by initiator caspases (Chai et al., 2001; Riedl et al., 2001). Once activated, the effector caspases cleave a variety of targets such as important structural proteins, kinases, cell cycle proteins and other effector caspases, to complete the cascade through dismantling of the cell (Degterev et al., 2003). In humans, the effector caspases are identified as caspase-3, caspase-6 and caspase-7, with caspase-3 being recognized as the most prolific effector caspase. In *Drosophila*, Dcp-1, Drice, and the lesser studied Damm and Decay are all effector caspases. Drice is recognized as the main effector caspase due to its abundance, similarity to caspase-3, and more prevalent cell death defects observed in genetic experiments (Fraser and Evan, 1997). In this thesis, my focus is on *Drosophila* Dcp-1 and human caspase-3.

1.5.5. Dcp-1 and caspase-3 in cell death

Dcp-1 is theorized to fine-tune the apoptotic process as it can induce apoptosis on its own but generally has weaker cell death phenotypes than Drice (Florentin and Arama, 2012; Xu et al., 2006). Dcp-1 null flies (*Dcp-1*^{Prev1}) are viable (Laundrie et al., 2003), as opposed to Drice mutants (Xu et al., 2006), and display several neuronal (Keller et al., 2011; Schoenmann et al., 2010) and oogenesis defects (Laundrie et al., 2003). Caspase-3 cleaves the majority of the caspase substrates that are essential to induce apoptosis and cause nuclear collapse, such as DNase inhibitors, topoisomerase and signal transducers of transcription, whereas caspase-6 and caspase-7 have minimal impacts in human cells when they are solely expressed (Abraham and Shaham, 2004; Slee et al., 2001). Caspase-3 knock-out mice have detrimental phenotypes with variable effects on survival throughout development depending on their genetic background with severity ranging from perinatal death to fully developed adults with few neuronal abnormalities (Leonard et al., 2002). These mice are shown to have defects in DNA and nuclear fragmentation which ultimately cause neuronal defects (Leonard et al., 2002). The

difference between developmental outcomes in different strains of mice was discovered to be due to a difference in the levels of compensatory activation from caspase-7, which is equally efficient as caspase-3 in mice (Houde et al., 2004).

1.5.6. Non-apoptotic roles of "apoptotic" caspases

There is a growing appreciation that the classically defined "apoptotic" caspases have many important roles other than the execution of cell death. Apoptotic caspases in *Drosophila* and mammals have been identified as having apoptosis-independent functions in proliferation, tissue regeneration, differentiation, neural development, immune responses and autophagy.

Proliferation and tissue regeneration

Compensatory proliferation in response to cell damage or injury is a phenomenon that occurs in *Drosophila* and highlights *Drosophila*'s regenerative capacity. When apoptosis is blocked by the caspase inhibitor p35 after exposure to cell death stimuli, Dronc is still required to induce compensatory proliferation through the Wingless (Wg) and Decapentaplegic (Dpp) pathways for the growth of neighbouring cells (Huh et al., 2004; Kondo et al., 2006; Wells et al., 2006). In a second mechanism, effector caspases Drice and Dcp-1 can also induce compensatory proliferation through the Hedgehog (Hh) signaling pathway in differentiating eye tissues (Fan and Bergmann, 2008). Caspase-3 and caspase-7 support liver regeneration through cleavage and subsequent activation of a phospholipase which promotes secretion of factors that interact with the Wnt pathway (Goessling et al., 2009; Li et al., 2010a). Conversely, caspase-8 appears to hinder liver regeneration as knockout mice no longer cleave receptor-interacting protein 1 (RIP-1) which accelerated the regenerative pathways controlled by NFκB signaling (Freimuth et al., 2013). Key bone-forming genes underwent reduced expression in caspase-7 knockout mice, resulting in a decrease in bone density and volume indicating that caspase-7 is important for osteogenesis (Svandova et al., 2014). Additionally, caspase-8 and caspase-6 have been implicated in lymphocyte proliferation and homeostasis in mice and humans, respectively (Beisner et al., 2005; Olson et al., 2003). Caspase-3 deficient mice show hyperproliferation of B-cells which can be mitigated with the deletion of the common

apoptotic caspase target, the cell cycle activating cyclin-dependent kinase, *Cdnk1a* (Woo et al., 2003).

Differentiation

An important role for a caspase in cell differentiation has been identified in *Drosophila.* The *Drosophila* initiator caspase Dronc cleaves Shaggy46, a protein that negatively regulates Wnt-signalling, to activate it for the formation of neural precursor cells (Kanuka et al., 2005). Mammalian apoptotic caspases have been implicated in the differentiation of several different types of progenitor cells including erythroid cells (Zermati et al., 2001), keratinocytes (Okuyama et al., 2004), lens cells (Ishizaki et al., 1998), muscle progenitor cells (Fernando et al., 2002; Murray et al., 2008), bone marrow stromal stem cells (Miura et al., 2004), osteoblasts (Mogi and Togari, 2003), odontoblasts (Matalova et al., 2013), monocytes (Sordet et al., 2002), neurons (Yan et al., 2001), embryonic stem cells (Fujita et al., 2008a) and hematopoietic stem cells (Janzen et al., 2008). Of the above listed progenitor cells, caspase-3 is the dominant force in differentiation as it has been implicated in all with the exception of odontoblasts which require caspase-7.

Neural development

While caspases were shown to be important for apoptosis during *Drosophila* neural development, they can also have apoptosis-independent effects in the nervous system (Hyman and Yuan, 2012). Dronc was shown to be required for dendritic pruning during larval development. Dendritic pruning requires cleavage of substrates similar to those in apoptosis that affect the cytoskeleton and phagocytic clearance, but without the presence of cell death (Kuo et al., 2006). Similarly, caspase-3 and-6 were shown to affect dendrite pruning in mice . Caspase-9 is needed to cleave the protein Semaphorin 7A for proper axonal projection and, without it, mice experience improper axonal guidance and synaptogenesis (Ohsawa et al., 2009). The synaptic modification known as long-term depression (LTD) through AMPA receptor internalization requires caspase-3 activity as loss of caspase-3 or overexpression of caspase-3 inhibitors prevent LTD (Li et al., 2010b).

Immune response

Apoptotic caspases have exhibited a role in the regulation of the immune response. In *Drosophila*, initiator caspase Dredd was shown to be a regulator of the immune response by activating the key innate immune response transcription factor, Relish, through endoproteolytic cleavage (Stoven et al., 2003; Tanji and Ip, 2005). Caspase-8 in humans was shown to regulate inflammasome activation independently of apoptosis through priming of a cytokine interleukin (Maelfait et al., 2008). Additionally, caspase-8 can suppress inflammation and its loss can lead to inflammation-related skin diseases and cancer (Ben Moshe et al., 2007; Kovalenko et al., 2009; Liedtke et al., 2011).

Autophagy

In *Drosophila,* the effector caspase Dcp-1 was identified as a positive regulator of autophagy; Dcp-1 overexpression induces autophagy whereas loss of Dcp-1 results in the inhibition of autophagy induction in response to starvation conditions (DeVorkin et al., 2014; Hou et al., 2008; Kim et al., 2010). In mammals, caspases were found to both promote and inhibit autophagic flux. The initiator caspases in the apoptotic cascade, caspase-2, caspase-8 and caspase-9, were identified as suppressors of autophagy in certain contexts through control of reactive oxygen species (ROS) levels or by cleaving substrates involved in the regulation of autophagy or the autophagic process itself (Bell et al., 2008; Cho et al., 2009; Oral et al., 2012; Tiwari et al., 2011, 2014; You et al., 2013). Conversely, caspase-9 was shown to promote autophagy by enhancing the priming and lipidation of LC3B through complexing with autophagy protein Atg7 (Han et al., 2014; Jeong et al., 2011). The effector caspases, caspase-3, caspase-6, and caspase-7, were linked to suppression of autophagy through promoting extrusion of autophagic vesicles or through cleavage of proteins involved in autophagic flux (Cho et al., 2009; Norman et al., 2010; Pagliarini et al., 2012; Sirois et al., 2012; Wirawan et al., 2010; You et al., 2013). In contrast, it was suggested, though not demonstrated directly, that caspase-3 could upregulate autophagy by cleavage and subsequent activation of ATG4D (Betin and Lane, 2009). While *in vitro* cleavage of autophagy proteins by effector caspases was shown in human cells in response to cell death stimuli, there is very little known about caspase regulation of autophagy in other cellular contexts.

1.6. Ubiquitin-proteasome system (UPS)

In addition to autophagy, the other main degradative process in eukaryotic cells is the ubiquitin-proteasome system (UPS). The UPS functions to control the half-lives of regulatory proteins and to eliminate misfolded or damaged proteins. Protein degradation was originally solely attributed to lysosomes until the Goldberg group reported in 1977 that ATP-dependent proteolysis occurs in lysosome-free reticulocytes (Etlinger and Goldberg, 1977). This discovery was followed up by the finding that proteins could be conjugated to a small protein called ubiquitin and that these conjugated proteins were degraded through ATP-dependent proteolysis (Ciehanover et al., 1978; Hershko et al., 1980).

1.6.1. The ubiquitin-conjugation system

The ubiquitin-conjugation system was further elucidated to identify the groups of E1, E2 and E3 enzymes – proteins with their own sequential role in conjugating ubiquitin to target proteins (Hershko et al., 1983, 2000). E1 enzymes, or ubiquitin-activating enzymes, activate ubiquitin through an ATP-dependent process where the ubiquitin protein is covalently attached to a cysteine on the E1 enzyme through its C-terminus. Activated ubiquitin is then transferred to a specific cysteine residue on an E2 enzyme, or ubiquitin-conjugating enzyme. The E2 enzyme then conjugates the C-terminal glycine residue of ubiquitin via an isopeptide bond to an internal lysine residue of a target substrate. E3 enzymes, or ubiquitin-ligase enzymes, are required in certain conjugation reactions for substration recognition. After a single ubiquitin is attached, ubiquitin can itself be targeted for further ubiquitination, differentiating monoubiquitination and polyubiquitination which can lead to different cell fates: monoubiquitination generally regulates DNA repair, viral budding and gene expression whereas polyubiquitination targets proteasomal degradation through lysine48 (K48), and signaling and endocytosis through lysine63 (K63) (Sadowski and Sarcevic, 2010). While the UPS is known to traditionally process ubiquitin-tagged proteins, there are examples of ubiquitin-free proteasomal degradation (Hoyt and Coffino, 2004).

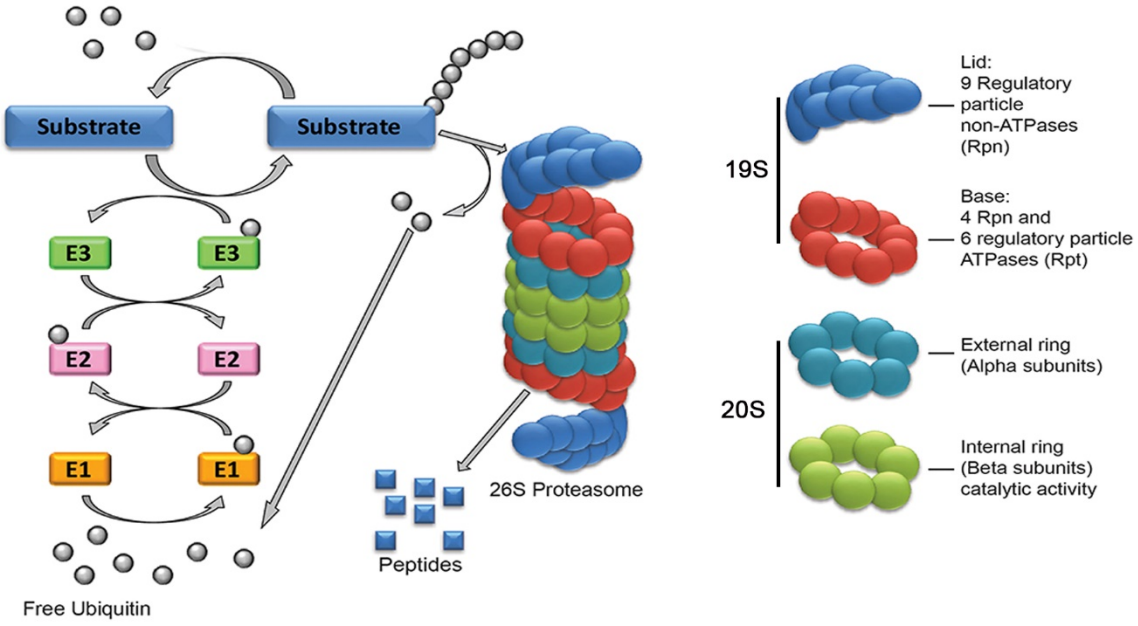

Figure 1-7 The ubiquitin-proteasome system

The ubiquitin-proteasome system consists of the targeting of a substrate through the ubiquitin-conjugation system and subsequent degradation through the 26S proteasome. Free ubiquitin is activated through an E1 enzyme and then transferred to an E2 enzyme. The ubiquitin from the E2 enzyme is transferred to the substrate of interest by an E3 enzyme. This can happen in multiple rounds in order for a protein to become polyubiquitinated for recognition by the proteasome. The 26S proteasome consists of one core 20S particle structure with two 19S regulatory particles. The 20S core particle is a hollow chamber consisting of four stacked heptameric rings that are made up of α and β subunits. Seven α subunits compose each outer ring of the 20S core particle and function as a docking platform for the regulatory particles and also sterically control the entry of subsrates. The 19S particles are composed of 19 individual proteins which can be divided into a nine subunit base that binds directly to the 20S particle, and a ten subunit lid. Adapted from Massaly et al., 2015.

1.6.2. The proteasome

The machinery to degrade ubiquitinated proteins was discovered as a multimeric complex called the 26S proteasome, with “S” referring to the Svedberg sedimentation coefficient (S) (Hough et al., 1987). The 26S proteasome consists of one core 20S particle structure with two 19S regulatory particles (Figure 1-7). The 20S core particle is a hollow chamber consisting of four stacked heptameric rings that are made up of α and β subunits. Seven α subunits compose each outer ring of the 20S core particle and function as a docking platform for the regulatory particles and also sterically control the entry of subsrates. On the inside, the inner β subunits are stacked on top of each other and contain the catalytic activity. In mammals, there are three types of β subunits with distinct catalytic

recognition and cleavage: caspase-like subunits (β1) which cleave after glutamate, trypsin-like subunits (β2) which cleave after the basic amino acids lysine and arginine, and chymotrypsin-like subunits (β5) which cleave after hydrophobic amino acids (Heinemeyer et al., 1997). The 19S regulatory particles contain multiple ATPase active sites and ubiquitin binding sites to recognize and transfer substrates into the catalytic core. The 19S particles are composed of 19 individual proteins which can be divided into a nine subunit base that binds directly to the 20S particle, and a ten subunit lid. The 19S particle contains ATPase subunits which, through ATP hydrolysis, are able to unfold proteins. Additionally, ATP binding is required for all of the other steps of proteasomal degradation including complex assembly, gate opening, translocation and proteolysis (Liu et al., 2006). Once the unfolded target protein is within the 20S particle, it is proteolyzed into polypeptides 7-9 amino acids in length. Heat-shock proteins can act as molecular chaperones to assist with unfolding targeted proteins and delivery of substrates to the proteasome.

1.7. Heat-shock proteins

Heat-shock proteins (HSPs) are a family of proteins that were first discovered when chromosomal puffs exposed several genes that are transcriptionally upregulated in response to heat stress in *Drosophila* (Ritossa, 1996). Currently, heat-shock protein could be considered a misnomer as these proteins can be upregulated in response to a variety of stresses and also have crucial roles at basal expression levels in unstressed conditions. HSPs act regularly as molecular chaperones and play critical roles in maintaining protein homeostasis (proteostasis). Chaperones have a variety of functions such as assisting native proteins with folding/unfolding, assembly/disassembly, and transport or sorting of proteins within subcellular compartments (Richter et al., 2010). Due to their vast clientele and general role in protein folding, HSPs control many essential processes and pathways such as cell division, cell signaling, and cytoprotective responses to stress (Li and Srivastava, 2004). HSP proteins are typically classified into one of five families according to their relative molecular sizes (kilodalton): HSP100, HSP90, HSP70, HSP60/chaperonins, and the small HSPs (Richter et al., 2010). Each family has distinct

functions, structures, clientele and characteristics. In this thesis I focus on *Drosophila* Hsp83 from the HSP90 family and human HSP60 (Figure 1-8).

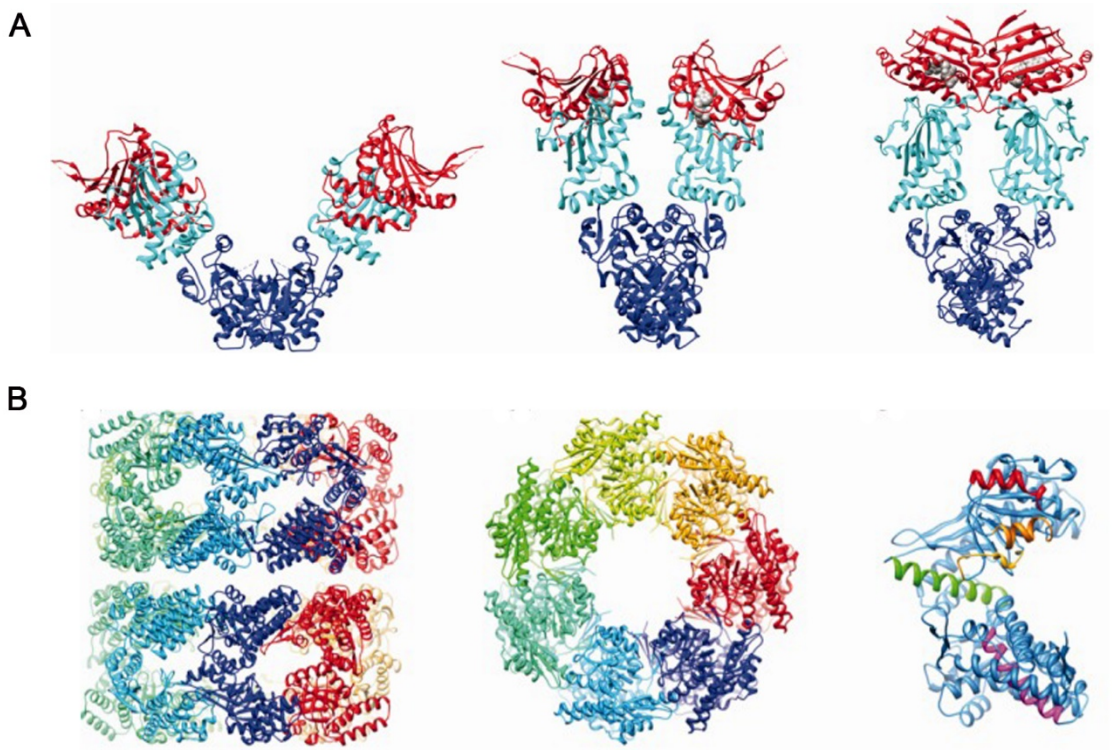

Figure 1-8 Structures of HSP90 and HSP60

(**A**) The 3D structure of HSP90 in open and closed states with variable ATP-binding. HSP90 exists and functions as a homodimer. Each HSP90 molecule consists of three domains: the ATP-binding amino-terminal domain (red), the clientele-recognizing middle domain (cyan) and the dimerizing carboxy-terminal domain (blue). (**B**) 3-D structures of HSP60 from a side view (left), top view (middle) and of a single subunit (right). HSP60 consists of one or two stacked heptameric rings. The centre of the protein provides a chamber of hydrophobic interactions for unfolded proteins. HSP molecules have three domains: the substrate-binding apical domain, the ATP-binding equatorial domain and the intermediate domain that hinges the other two domains. Adapted from Clare and Saibil, 2013.

1.7.1. HSP90

The HSP90 family functions to help stabilize, regulate and activate a growing clientele of over 200 recognized interacting proteins (Echeverría et al., 2011). Of the clientele, there is an enhanced number of signal transducers such as kinases, transcription factors and receptors (Taipale et al., 2010). HSP90 is one of the most abundant proteins in the cell constituting 1-2% of the proteins in the cytoplasm during basal conditions, and HSP90 expression can be even further increased to manage cellular

stress (Borkovich et al., 1989). HSP90 can be found in several compartments of the cell and many eukaryotes encode a compartment-specific HSP90. Cytosolic HSP90 is essential for life in all eukaryotes as null mutants are lethal (Young et al., 2001). The mitochondrial HSP90 (TRAP1) and endoplasmic reticulum HSP90 (GRP94) isoforms are found in most higher eukaryotes and they participate in stress adaptation and development, respectively (Altieri et al., 2012; Marzec et al., 2012). HSP90 is a large dimeric protein that can be divided into three domains: the ATP-binding amino-terminal domain, the clientele recognizing middle domain and the dimerizing carboxy-terminal domain (Figure 1-8A) (Pearl and Prodromou, 2006). HSP90 uses its ATPase activity to hydrolyze ATP to achieve several dynamic structural conformations which vary depending on its state in the ATPase cycle. HSP90 interacts with its specific clientele with the assistance of several co-chaperones, including CDC37 and HSP70, and generally acts in a late stage of protein folding and not nascent protein folding (Jakob et al., 1995; Prodromou, 2012).

1.7.2. HSP60

HSP60, also referred to as a type I chaperonin, is a highly conserved essential mitochondrial chaperone. Type I chaperonins are proteins that require a second oligomer, HSP10 or chaperonin10, to function as a lid, and also require ATP hydrolysis to power activity. The type I chaperonin in *Escherichia coli,* the groEL/groES complex, was discovered before mammalian HSP60 and gave key insights into HSP60's structure and function (Hemmingsen et al., 1988). HSP60 consists of one or two stacked heptameric rings where the centre provides a chamber of hydrophobic interactions for unfolded proteins (Figure 1-8B) (Fenton et al., 1994). Subunits of HSP60 have three domains: the substrate-binding apical domain, the ATP-binding equatorial domain and the intermediate domain that hinges the other two domains. Binding of ATP allows the intermediate domain to undergo a conformational change that results in its hydrophobic residues being exposed to promote association with unfolded proteins (Ranford et al., 2000). While HSP60 has a mitochondrial localization signal, it can also be found in the cytoplasm. HSP60 not only assists with protein folding in the mitochondria, it assists with a number of other processes such as mitochondrial transport, transmission and replication of mitochondrial DNA, and control of apoptosis (Henderson et al., 2013; Koll et al., 1992).

1.8. Rationale

The intersections between the cell survival pathway of autophagy and the cell death process of apoptosis are complex and our current understanding is limited. It is important to clarify how enzymes in these processes can regulate both pathways to better appreciate the potential consequences of modulating or targeting components of one or the other pathway. Such pathway modulation and its downstream effects could be especially important in the context of development or disease. In the model organism *Drosophila melanogaster*, it was discovered that an effector caspase, Dcp-1, was required to activate starvation-induced autophagy (DeVorkin et al., 2014; Hou et al., 2008). What remained unknown is how Dcp-1 was able to activate autophagy and, additionally, if this represented an evolutionarily conserved relationship between caspases and autophagy activation. I hypothesized that Dcp-1 is either being suppressed by a negative regulator of autophagy under basal conditions to prevent autophagy activation and/or that Dcp-1 cleaves a negative regulator of autophagy in starvation conditions to induce autophagy. In a previous effort to identify Dcp-1 interacting proteins, an immunoprecipitation and mass spectrometry experiment was performed that identified 24 candidate interactors (Table 1.1). These candidate interactors were screened for their potential to regulate autophagy, yielding several putative negative regulators of autophagy (Figure 3-1). This screen became the foundation for the continued investigation of Dcp-1 and its relationship to one of the putative negative regulators, the chaperone Hsp83. Furthermore, I hypothesized that the Dcp-1-mediated autophagy regulation observed in *Drosophila* was a function conserved in higher eukaryotes, such as humans. In order to address this hypothesis, I utilized previous results from the Dcp-1 interaction screen (Table 1.1), the short list of candidate negative regulators of autophagy from the RNAi screen (Figure 3-1) and the published literature describing the role of Dcp-1 in autophagy regulation (DeVorkin et al., 2014; Hou et al., 2008).

Table 1.1 Candidate Dcp-1 interactors and substrates identified by mass spectrometry

Symbols, CG numbers and molecular functions are from Flybase. The mean number of unique peptides that corresponded to each gene and the mean X!Tandem log (e) score for the peptides identified are listed. The human gene names were determined from a BLAST analysis of the *Drosophila* genes against the human UniProt database. The list is ordered by number of observations made from four independent immunoprecipitations of the Dcp-1 protein (Expts) (taken from Choutka et. al, "Hsp83 loss suppresses proteasomal activity resulting in an upregulation of caspase-dependent compensatory autophagy", in press, *Autophagy* June 2017).

Flybase Symbol	CG Number	Gene Ontology molecular function	Mean log(e)	Mean unique peps	UniProt human gene	# of Expts
14-3-3ζ	CG17870	Protein binding, protein heterodimerization activity, protein homodimerization activity	-9.6	1.75	14-3-3ζ	4
Ef1α48D	CG8280	Translation elongation factor activity	-27	3.75	EEF1A1	4
Hsc70-4	CG4264	Chaperone binding	-70	8.50	HSPA8	4
Hsp83	CG1242	ATPase activity, coupled	-32	4.75	HSP90 AA1	4
Jafrac1	CG1633	Thioredoxin peroxidase activity	-30	4.00	PRDX1	4
14-3-3ε	CG31196	Protein binding; protein heterodimerization activity	-23	3.33	14-3-3ε	3
blw	CG3612	Hydrogen exporting ATPase activity; phosphorylative mechanism	-16	2.67	ATP5A1	3
CCT2	CG7033	Unfolded protein binding; ATP binding	-6.5	1.67	CCT2	3
Clic	CG10997	Calcium ion binding; chloride channel activity; lipid binding	-7.2	1.67	CLIC2	3
Ef1-β	CG6341	Translation elongation factor activity	-10	2.00	EEF1B2	3
Rack1	CG7111	Protein kinase c binding	-3.8	1.33	GNB2L 1	3
SesBa	CG16944	ATP:ADP antiporter activity	-27	4.00	ANT2	3
Sgl	CG10072	UDP-glucose 6-dehydrogenase activity	-8.1	1.67	UGDH	3
Ter94	CG2331	ATPase activity; golgi & ER organization	-16	2.67	VCP	3
Uba1	CG1782	Ubiquitin activating enzyme activity	-43	5.67	UBA1	3
ATPsyn-β	CG11154	Hydrogen exporting ATPase activity; phosphorylative mechanism	-3.1	1.00	ATP5B	2
Ef1-β	CG11901	Translation elongation factor activity	-5.6	1.50	EEF1G	2

eIF-4a	CG9075	Translation initiation factor activity; RNA helicase activity	-17	3.00	EIF4A1/ EIF4A2	2
Hsc70Cb	CG6603	Chaperone binding	-19	3.00	HSPA4	2
Hsp60	CG12101	Unfolded protein binding	-4.7	1.50	HSPD1	2
Hsp70Aa	CG31366	ATP binding, response to hypoxia	-19	1.00	HSPA1A/1B	2
Mi-2	CG8103	Protein binding; nucleosome-dependent ATPase activity; chromatin binding	-6.1	1.50	CHD4	2
REG	CG1591	Endopeptidase inhibitor activity; endopeptidase activator activity	-3.4	1.00	PSME3	2
Sta	CG14792	Structural constituent of ribosome	-5.8	1.50	RPSA	2

1.9. Hypotheses and specific aims

The hypotheses and specific aims of this thesis are:

Hypothesis 1: A regulatory relationship exists between effector caspase Dcp-1 and the molecular chaperone Hsp83 to modulate autophagy.
Specifc Aim 1 - To validate the role of Hsp83 and its relationship with Dcp-1 in the context of autophagy regulation in *Drosophila.*

Hypothesis 2: A human caspase functions to regulate starvation-induced autophagy.
Specific Aim 2 - To determine if there is a caspase that regulates starvation-induced autophagy in human cell lines and characterize its regulation.

Chapter 2. Materials and Methods

2.1. Fly strains

w^{1118} was used as the wild-type control strain in this thesis. A complete list of strains can be found in Table 2.1. All flies were collected in nutrient-rich conditions at room temperature unless otherwise stated.

2.2. Tissue harvesting and fluorescence microscopy

Flies were conditioned on wet yeast paste for two days before dissection. Ovaries were dissected in PBS and fixed with 4% paraformaldehyde for twenty minutes. Flies expressing fluorescent reporters were mounted with Slowfade Gold Antifade Reagent with DAPI (ThermoFisher Scientific). Fluorescent intensity for the CL1-GFP reporter (Pandey et al., 2007) was measured by outlining the fat body observed in the DAPI channel and measuring the mean gray value from the unadjusted images in the GFP channel and subtracting the mean background using Image J 1.45s (https://imagej.nih.gov/ij/).

For immunofluorescence, ovaries were washed with PBS-T (PBS+0.3% TritonX-100), permeabilized with 0.5% TritonX-100 and blocked with 2% BSA in PBS-T after fixation. The cleaved Dcp-1 antibody (Cell signaling) was diluted in 0.5% BSA+ PBS-T and incubated overnight at 4°C. Secondary antibodies anti-rabbit Alexa 546 or Alexa 488 (ThermoFisher Scientific) were incubated at room temperature for two hours and subsequently washed with PBS-T. Slides were then mounted as described above.

Table 2.1. *Drosophila* stock list

Genotype	Description	Source
Hsp83^{e6A}/TM6B	point mutation in *Hsp83* gene causing amino acid replacement: S592F	Bloomington Stock Centre (Stock number 36576)
Hsp83^{e6D}/TM6B	point mutation in *Hsp83* gene causing amino acid replacement: E317K	Bloomington Stock Centre (Stock number 5696)
Hsp83$^{6-55}$/TM6B	point mutation in *Hsp83* gene causing amino acid replacement: P380S	B. Edgar (Heidelberg University, Heidelberg, Germany).(Bandura et al., 2013)
Dcp-1^{Prev1}	contains a 40-bp partial P element insertion in the coding region of *Dcp-1*, resulting in an in-frame stop	K. McCall (Boston University, Boston, MA)(Laundrie et al., 2003)
UASp-GFP-mCherry-DrAtg8a	Expression of GFP-mCherry-DrAtg8a under the UASp promoter	T.E. Rusten (Centre for Cancer Biomedicine, Oslo University Hospital, Montebello, Oslo, Norway)(Nezis et al., 2010)
UAS-Dcr-2; nosGAL4	female germline driver and construct of Dicer-2 driven under the UAS promoter	Bloomington Stock Centre (Stock number 25751)
20ProtS-GD	RNAi strain targeted against proteasomal subunit Prosα1	Vienna Drosophila Resource Center (transformant ID 49681)
Rpn2-KK	RNAi strain targeted against regulatory proteasomal subunit Rpn2	Vienna Drosophila Resource Center (transformant ID 106457)
MTD-Gal-4	Maternal triple driver used for crosses	Bloomington Stock Centre (Stock number 31777)
sco/CyO;TM6B/MKRS	Balancer stock used for crosses	Bloomington Stock Centre (Stock number 3703)
UASt-CL1-GFP	Expression of CL1-GFP under the UASt promoter	U. Pandey (University of Pittsburgh Medical Center, Pittsburgh, PA)(Pandey et al., 2007)
Cg-GAL4	GAL4 driver in hemocytes, fat body and lymph gland used for larval fat body experiments	Bloomington Stock Centre (Stock number 7011)
UASp-Diap1.P	Expression of Diap1 under the UASp promoter	Bloomington Stock Centre (Stock number 63820)

2.3. LysoTracker® Red and TUNEL analysis

Ovaries were dissected in PBS three or four days after eclosion. Larval fat bodies were dissected in PBS from first instar larva. Both tissues were then incubated with 50μM Lysotracker® Red (LTR) DND-99 (ThermoFisher) in PBS for three minutes in the dark. Tissues were washed three times with PBS and then fixed for twenty minutes with 4% paraformaldehyde in PBS. For TUNEL staining, fixed tissues were washed three times with PBS + 0.1% Triton-X-100. TUNEL reaction was carried out by the DeadEnd Fluorimetric Tunel System (Promega). Samples were mounted and analyzed as indicated above in the microscopy section.

2.4. Confocal imaging

All microscopic images were acquired at room temperature using one of three confocal apparatuses: Nikon Confocal C1 microscope equipped with a Plan APO 60X/1.45 oil immersion objective (Nikon) with EZ-C1 Ver 3.00 software (Nikon), Nikon A1R Eclipse Ti inverted Laser Scanning Confocal Microscope with a Plan APO 60X/1.40 oil immersion objective (Nikon) with acquisition software NIS Elements AR 4.2 (Nikon), and Leica TCS SP8 inverted confocal microscope with a Leica HC PL APO 63x/1.40 oil objective and LAS AF software (Leica). The pinhole and laser brightness settings were kept constant by applying the same properties between comparable experiments. Brightness and contrast were adjusted using Photoshop (CC 2014, Adobe) and applied to the whole image.

2.5. *Drosophila* cell culture conditions

Drosophila l(2)mbn cells were grown in Schneider's medium (ThermoFisher Scientific) supplemented with 10% FBS in 25cm^2 suspension cell flasks (Sarstedt) at 25°C. *Drosophila S2-RFP-GFP-Atg8a* cells were grown in ESF921 medium (Expression Systems) in 25cm^2 suspension cell flasks (Sarstedt) at 25°C and treated with 50μg/mL of selection agent Zeocin. All experiments were carried out three to four days after the last passage of cells.

2.6. *In vitro Drosophila* RNAi

l(2)mbn cells and *S2-RFP-GFP-Atg8a* were washed and resuspended in ESF921 medium (Expression Systems) to a concentration of $2x10^6$ cells/mL. Cells were aliquoted with volumes of 333µL (24-well plate) or 1mL (6-well plate). dsRNAs were added at 5-10µg (24-well) or 15-30µg (6-well) per well and incubated at 25°C for one hour. Following incubation, 667µL (24-well) or 2mL (6-well) of Schneider's + 10% FBS was added back to each well and incubated for an additional 72 hours at 25°C. S2-RFP-GFP-Atg8a cells were transferred to an 8-well Chamber Slide (EMS) overnight and the next day treated with a second dose of dsRNAs in E2F921 for seven hours before fixation.

2.7. Primer design and dsRNA synthesis

Each PCR primer for RT-PCR was designed to contain a 5' T7 RNA polymerase-binding site (TAATACGACTCACTATAGG) followed by sequences specific for the target gene. The ampicillin resistance gene was used as a control target for dsRNA. The PCR products were generated by RT-PCR using Superscript one-step RT-PCR with Platinum Taq (ThermoFisher Scientific). RT-PCR products were ethanol precipitated and used as a template for *in vitro* transcription reactions using T7 RiboMax Express RNAi systems (Promega). Quality of the RNA was analyzed by gel electrophoresis. dsRNA was quantified using PicoGreen and adjusted to 200-400ng/µL with nuclease-free water. PCR primers for dsRNA synthesis can be found in Table 2.2.

Table 2.2. DNA sequences of PCR primers designed for dsRNA synthesis

Gene	Forward Primer Sequence (5'-3')	Reverse Primer Sequence (5'-3')
Amp	TAATACGACTCACTATAGGATTGGACTA CGATACGGGAGGGCTT	TAATACGACTCACTATAGGATTGGGCTA TGTGGCGCGGTATTAT
Atg1	TAATACGACTCACTATAGGTGCGGCTC TCCCATGTATATG	TAATACGACTCACTATAGGTGATTTTGTT GCTGCTGTGGAC
ATPsyn-β	TAATACGACTCACTATAGGCTCCTGGC TCCATACGC	TAATACGACTCACTATAGGATATGGCCT GAACAGAAGTAAT
Blw	TAATACGACTCACTATAGGGTACTGCAT CTACGTCGCCA	TAATACGACTCACTATAGG ACGTTGGTTGGAATGTAGGC
Clic	TAATACGACTCACTATAGGATCAGCCT GAAGGTGACGAC	TAATACGACTCACTATAGGACAGGTTCT CGATCAGGGTG

Dcp-1	TAATACGACTCACTATAGGACAAAAGCTGGCTGAGAAGC	TAATACGACTCACTATAGGCAGCCATTATAAAGCTGCCC-
eIF4A	TAATACGACTCACTATAGGTCGATTGCTATCCTTCAGCA	TAATACGACTCACTATAGGGATCTGATCCTTGAAACCGC
Hsc70-4	TAATACGACTCACTATAGGGGCTGACAAGGAGGAGTACG	TAATACGACTCACTATAGGTGTCGTTTGACCCGTTTGTA
Hsp60	TAATACGACTCACTATAGGGGGAGGGAGATGTGATGAGA	TAATACGACTCACTATAGGGCGAAGCAAAACAAAGTTCC
Hsp70Aa	TAATACGACTCACTATAGGCCCACTTTCATTGGGAATTG	TAATACGACTCACTATAGGAATGCATTGTTGTCCTTCGTC
Hsp83(2)	TAATACGACTCACTATAGGATTGCTCAGCTGATGTCCCT	TAATACGACTCACTATAGGGGAGTAGAAACCCACACCGA
Hsp83A	TAATACGACTCACTATAGGAAATCCCTGACCAACGACTG	TAATACGACTCACTATAGGTTGCGGATCACCTTTAGGAC
Hsp83B	TAATACGACTCACTATAGGGAGCTGAACAAGACCAAGCC	TAATACGACTCACTATAGGGAGTCGACCACACCCTTCAT
Mi-2	TAATACGACTCACTATAGGATTTGCGTGGTAAATCGGAG	TAATACGACTCACTATAGGGTTCTTGCTTCACCTCGCTC
REG	TAATACGACTCACTATAGGGTTGATCCTCAAGGCAGAGC	TAATACGACTCACTATAGGTCCTCCACAAGCTTCCTGAT
Rheb	TAATACGACTCACTATAGGTGACCCCACCATTGAGAACA	TAATACGACTCACTATAGGTATTTCCAACAGTTCGGC
Rpn11	TAATACGACTCACTATAGGCTGCTACGTCTTGGAGGTGCTATGCCACAGG	TAATACGACTCACTATAGGACAGTGCTCATTGTAGTCGGACAACGTGAGGC
SesB	TAATACGACTCACTATAGGGCAAGAACCCTTCCTTCCTC	TAATACGACTCACTATAGGTTCGGAGGCGAAAGAATCTA
Sta	TAATACGACTCACTATAGGTTTCCACGTTAACATGTCGG	TAATACGACTCACTATAGGCCCAGGTTGAGGATGTTGAC
Ter94	TAATACGACTCACTATAGGGCATGATGATGTTGACCTGG	TAATACGACTCACTATAGGCTGCATGCCAAACTTCAAGA

2.8. LysoTracker® analysis by flow cytometry

For flow cytometry experiments with LysoTracker® Green (LTG) (ThermoFisher Scientific), 66µL of2 x 10^6 cells/mL were plated in triplicate in a 96 well plate. After plating, 10µg of dsRNA was added per well and incubated for one hour at room temperature. Wells were subsequently supplemented with 134µL of Schneider's + 10% FBS and incubated for 72 hours at 25°C. Cells were treated with a second dose of dsRNAs in ESF921 for seven hours before analysis. RNAi-treated cells were centrifuged at 850 rpm for five

minutes at room temperature and resuspended in 50nM LTG (ThermoFisher Scientific) to detect acidic compartments, and 2µg/mL propidium iodide (PI) (ThermoFisher Scientific) to detect dead cells for twenty minutes in the dark. Following centrifugation, cell pellets were washed with ice cold 1XPBS, resuspended in ice cold 1XPBS and aliquoted into flow cytometry tubes on ice. Cells were then analyzed by flow cytometry (FACSCalibur, Becton Dickinson). A minimum of 10,000 cells per sample was acquired in triplicate for each experiment. Fluorescence intensities were obtained using the FL1 channel to measure LTG, and the FL3 channel to measure PI. PI positive cells were excluded and LTG fluorescence was analyzed using FlowJo Software version 5.7.2.

2.9. Proteasomal activity assay

Flies were collected three to four days after eclosion and flash frozen on dry ice. Microcentrifuge tubes were weighed before and after 5-8 flies were collected on an analytical balance to determine the mass per sample. Whole bodies were ground and incubated for thirty minutes on ice in 0.5mL of lysis buffer (50mM HEPES (pH 7.5), 5 mM EDTA, 150 mM NaCl, 1% Triton X-100). Lysates were then separated by centrifugation at 15,000rpm for fifteen minutes at 4°C. In a 96-well black plate, 50µL of lysate was added to 50µL of a combination of chymotrypsin-like, caspase-like, trypsin-like peptide substrates from the Proteasome-Glo kit (Promega). The substrates were incubated with the lysates for ten minutes before luminescence was measured on a Synergy H4 Hybrid (BioTek). Relative luminescence was then determined proportionally to total mass per sample.

2.10. MG132 Treatment

Flies were fed a mixture of 50µM of MG132 (ApexBio) resuspended in 0.2% DMSO with 5% sucrose and green food coloring. This solution was aliquoted on top of wet yeast paste and fed to flies for four days. The control solution had the same percentages of DMSO, sucrose and food coloring but was without MG132. Ingestion of the drug was indicated by green food coloring visible in the abdomen.

2.11. Protein extraction

All cell pellets were resuspended and lysed mechanically via pipette and by using RIPA lysis buffer (Santa-Cruz) plus complete protease inhibitors (Roche). Resuspended cells were incubated in RIPA for one hour at 4°C before being spun down at 12,000rpm for ten minutes at 4°C to obtain a lysate free of cell debris. Protein levels were quantified using the Pierce BCA Protein Assay Kit (Thermo Fisher Scientific) and then adjusted using dH_2O and 4x SDS Loading buffer.

Drosophila cells were centrifuged at 3000rpm for five minutes at 4°C and the pellets were washed with PBS. Mammalian cells were washed in PBS and then trypsinized for 5-10 minutes in the CO_2 incubator. Pellets were collected by adding Pink media and then centrifugation at 3000rpm for five minutes followed by a PBS rinse. Ovary and whole body lysates were mechanically ground using a pestle in RIPA. After the incubation they were spun down twice at 3000rpm at 4°C for five minutes and transferred to new tubes to get rid of tissue debris before isolating lysates.

2.12. Western blot analysis

Proteins were separated on 4-12% or 10% NuPAGE Bis-Tris gels (ThermoFisher Scientific) and transferred to PVDF membranes (with the exception of blots analyzing cleaved caspase-3 whose specific details are mentioned below). Membranes were blocked in milk or Odyssey blocking buffer and incubated in primary antibodies overnight at 4°C. Primary antibodies included anti-β-ACTIN (1:500, Abcam), mouse anti-actin (1:500, JLA20 Developmental Studies Hybridoma Bank), mouse anti-tubulin (1:1000, E7 Developmental Studies Hybridoma Bank), rabbit anti-Dcp-1 (1:1000, a gift from K. McCall; Boston University, Boston, MA), rabbit anti-HSP90 (1:1000, Cell Signalling), rabbit anti-CASP3 (1:1000, Cell Signalling), mouse anti-HSP60 (1:1000, Abcam), rabbit anti-cleaved CASP3 (1:1000, Cell Signalling), rabbit anti-PINK1 (1:1000, Abcam), mouse anti-TOMM20 (1:1000, Abcam), rabbit anti-SLC25A5 (ANT2) (1:1000, Abnova) and rabbit anti-LC3B (1:500, Abcam). Membranes were incubated with HRP-conjugated secondary antibodies or IR-labelled secondary antibodies and were detected using the Amersham ECL™ Enhanced Western Blotting System (GE Healthcare) or the Odyssey System (LI-

COR Biosciences). Densitometry was performed using Image Quant 5.1 software (GE Healthcare) or Image Lab 5.1 software (BioRad).

2.12.1. Cleaved caspase-3 blots

For blots analyzing cleaved CASP3, 50µg samples were resolved on a 15% Tris-Tricine SDS-PAGE resolving gel on a BioRad apparatus using separate anode and cathode buffers. Proteins were then transferred to 0.2µm nitrocellulose membranes (Bio-Rad) for one hour at 50V. Membranes were blocked and probed as above.

2.13. Human tissue cell culture conditions

HER2+ breast adenocarcinoma line SKBR3, human embryonic kidney HEK293, pancreatic ductal epithelioid carcinoma PANC-1 and HER2- human breast adenocarcinoma line MDA-MB-231 (American Type Culture Collection) were maintained in Gibco DMEM (Life Technologies) supplemented with 10% fetal bovine serum (FBS), 20mM HEPES and 1X non-essential amino acids (Pink). Lung adenocarcinoma line NCI-H2170 (American Type Culture Collection) was maintained in RPMI-1640 medium (Life Technologies) supplemented with 10% FBS. All five cell lines were stably transfected with a plasmid expressing mRFP-eGFP-LC3B and selection was maintained using Geneticin at 1µg/mL (G418). All cells were maintained at 37°C with 5% CO_2 and 95% humidity. For starvation experiments, SKBR3 cells were exposed to complete starvation for two hours by incubation in PBS while more starvation-sensitive cell lines were starved for four hours in Earle's Balanced Salt Solution. Well-fed cells were given fresh Pink or RPMI media. For Bafilomycin A (Baf) treatment cells were incubated in 50nM of Baf for two hours in starvation (starved) or nutrient rich conditions (fed).

2.14. Endogenous immunoprecipitation

Cells were trypsinized and collected from four T75 flasks before being pooled and lysed by incubation in 1mL of whole cell lysate buffer (10mM Tris-HCl pH 7.2, 10mM NaCl, 1mM EDTA, 1% NP-40). Cells were sheared using a 22-gauge syringe and then nutated

for thirty minutes at 4°C. The quantified lysate containing 6mg of protein (3mg/reaction) was then added to 62.5µL of Sepharose 4B beads (Sigma-Aldrich) that were previously washed and spun twice before being resuspended in 50µL of IP Wash Buffer (1X Tris-buffered Saline pH7.5, 1mM EDTA, 1% NP-40). The lysate and Sepharose 4B Beads were nutated for one hour at 4°C before the resin was spun down at 2000rpm for one minute at 4°C and then the pre-cleared lysate was transferred to a new tube. The pre-cleared lysate was then divided and incubated in either Caspase3 Rabbit antibody (1:50, Cell Signalling) or IgG Rabbit antibody (1:50, Millipore) overnight nutating at 4°C. The reverse IP used Hsp60 Mouse Antibody (1:50, Abcam) and IgG Mouse Antibody (1:50, Millipore).

Protein G Sepharose beads (GE Healthcare) were aliquoted to 70µL per reaction, washed and centrifuged twice with 500µL of PBS before being blocked with 500µL of 2% BSA overnight. Protein G Sepharose beads were then washed in IP Wash Buffer without NP-40 and added to the pre-cleared lysate-antibody mixture and nutated for four hours at 4°C. The mixture was then spun down at 2000rpm for two minutes at 4°C and resin washed and spun twice with IP Wash Buffer. Samples were eluted with 30µL of 2X SDS sample loading buffer and boiled at 98°C for ten minutes. The eluted product was isolated by centrifugation at 15000rpm for one minute at 4°C and then directly loaded onto an SDS-PAGE gel for western analysis.

2.15. Mitochondrial enrichment and Proteinase K protection assay

Cell pellets harvested from two T75 flasks were ground using a douncer 50-60 times in 1mL of cold SEM-P (320mM sucrose, 1mM EDTA, 10mM MOPS, 5X complete protease inhibitor cocktail (Roche), pH7.5) and then incubated on ice for thirty minutes. Lysates were centrifuged twice at 3000 rpm at 4°C for five minutes to remove cell debris. Cells were then fractionated into membrane (pellet) and cytosolic (supernatant) fractions by centrifugation at 12,000 rpm, 4°C for ten minutes. The supernatant was removed and the pellet was washed, spun and resuspended in 50µL of SEM-P. The mitochondrial fraction was then quantitated to allow for 50µg of protein per reaction. The sample was concentrated by adding 4X its volume of acetone and centrifuging at 15,000rpm for thirty minutes at 4°C to obtain a protein pellet. The pellet was resuspended in SEM without the

protease inhibitor cocktail and divided into three aliquots containing 50µg of proteins. Mitochondria were incubated with 0, 1, and 5 or 10 µg of Proteinase K for fifteen minutes and then 500µL of SEM-P and 1µL of PMSF were added. Samples were spun down at 12,000 rpm for twelve minutes. The pellet was directly resuspended in 4X SDS sample loading buffer to be analyzed directly by western blot.

2.16. siRNA transfections

For western blots, cells were plated at 2×10^5 cells per well in a 6-well plate in Pink media. They were then transfected at twenty-four and forty-eight hours after plating with 150pmol of Caspase3 siRNA constructs, Hsp60 siRNA contructs or a medium GC scramble control siRNA construct (Thermofisher Stealth siRNAs) using Lipofectamine RNAiMAX™ (ThermoFisher Scientific) as per manufacturer's recommendations. Media was replenished every day after initial plating with Pink media. Cells were collected on the fourth day after plating following well-fed or starved treatment with or without Baf for protein analysis.

For microscopic analysis, cells stably transfected with mRFP-eGFP-LC3B were plated at a density of 1,600 cells per well in 200uL of DMEM with G418 in 8-well chamber slides. Similar to above, cells were treated at twenty-four and seventy-two hour intervals with 15pmol of the same siRNA constructs. Cells were fixed and prepared for microscopy on the fourth day after plating following well-fed or starved treatment with or without Baf for protein analysis.

2.17. RFP-GFP-LC3B microscopy assay

After treatment, *in vitro* cell lines expressing the autophagy reporter were washed with PBS and then fixed with 4% paraformaldehyde for twenty minutes in their incubator in the dark. Chambers were removed and cells mounted with Slowfade Gold Antifade Reagent with DAPI (ThermoFisher Scientific). Puncta were either counted manually from stored digital images or automatically by using the OpenCV Python package; a contours discovery algorithm (Suzuki and be, 1985) was applied to images pre-processed by

filtering colors and applying a Gaussian filter and adaptive threshold as performed in Bortnik et al., 2016.

2.18. Statistics

In each graph, error bars represent SEM of *n* independent experiments. As indicated in the legends, statistical significance was calculated by analysis of variance (ANOVA) plus a Dunnett or Bonferroni post test, or a two-tailed Student's *t* test between the indicated samples was used. p-values are shown in the legends and anything less than 0.05% was determined as significant.

Chapter 3. Hsp83 loss suppresses proteasomal activity resulting in an upregulation of caspase-dependent compensatory autophagy.

Adapted and expanded from: Courtney Choutka, Lindsay DeVorkin, Nancy Erro Go, Ying-Chen Claire Hou, Annie Moradian, Gregg B. Morin and Sharon M. Gorski. “Hsp83 loss suppresses proteasomal activity resulting in an upregulation of caspase-dependent compensatory autophagy” (Manuscript in press, *Autophagy* June 2017).

In the original manuscript, the immunoprecipitation and mass spectrometry analysis was performed by YCH, AM and GBM. Creation of the stable cell line, qRT-PCR and the *in vitro* cleavage assay were conducted by NEG. The Dcp-1/Hsp83 IP western blots and the majority of the flow cytometry LTG and initial *in vitro* RFP-GFP-Atg8 RNAi screening were performed by L. DeVorkin. I conceived, designed, and conducted all other experiments as well as prepared the manuscript in collaboration with SMG.

3.1. Abstract

The two main degradative pathways that contribute to proteostasis are the ubiquitin-proteasome system and autophagy but how they are molecularly coordinated is not well understood. Here, I demonstrate an essential role for an effector caspase in the activation of compensatory autophagy when proteasomal activity is compromised. Functional loss of Hsp83, the *Drosophila* homolog of human HSP90/Heat-shock protein 90, resulted in reduced proteasomal activity and elevated levels of the effector caspase Dcp-1. Surprisingly, genetic analyses showed that the caspase was not required for cell death in this context, but instead was essential for the ensuing compensatory autophagy, female fertility, and organism viability. The zymogen pro-Dcp-1 was found to interact with Hsp83 and undergo proteasomal regulation in an Hsp83-dependent manner. Our work not only reveals unappreciated roles for Hsp83 in proteasomal activity and regulation of Dcp-1, but identifies an effector caspase as a key regulatory factor for sustaining adaptation to cell stress *in vivo.*

3.2. Introduction

Proteostasis, or protein homeostasis, is a term that describes how the proteome is regulated and maintained in order to protect cellular integrity. Loss of proteostasis is a common feature of aging and diseases such as cancer and neurogenerative disorders as it causes inappropriate protein aggregate formation in various tissues (Labbadia and Morimoto, 2015). This aggregation is routinely managed by the proteostasis network, a network defined by macromolecular machines that contribute to maintenance of proteome integrity by coordinating protein synthesis, folding, disaggregation, and degradation (Labbadia and Morimoto, 2015). The two main degradative pathways that contribute to proteostasis are the ubiquitin-proteasome system (UPS) and autophagy. In instances when the UPS is dysfunctional it was shown in multiple systems that compensatory autophagy contributes to protein degradation in an effort to maintain healthy cellular proteostasis (Ding et al., 2007; Iwata et al., 2005; Lőw et al., 2013; Pandey et al., 2007). However, the molecular mechanisms that regulate compensatory autophagy are not well understood.

Heat-shock proteins play a central role in proteostasis by controlling protein expression, acting as chaperones, and assisting with protein disaggregation and degradation (Hartl et al., 2011). One of the most conserved, ubiquitous and highly-expressed heat-shock proteins is HSP90. The wide associations of HSP90 play a pivotal role in cell signaling and regulation of diverse cellular processes in normal biology and its dysregulation can have a marked effect on disease. HSP90 has emerged as a molecule of interest for cancer therapeutics as its upregulation, mislocalization and stabilization of proteins involved in metastasis, evasion of apoptosis and proliferation make it a prime target (Kang et al., 2007; Pick et al., 2007; Whitesell and Lindquist, 2005). While HSP90 is known to be an important hub for signaling and proteostasis, there are many HSP90 relationships and related pathways yet to be discovered.

Investigations into the regulation of autophagy led to the discovery of a *Drosophila* effector caspase, Dcp-1, that promotes starvation-induced autophagy in *Drosophila* oogenesis (DeVorkin et al., 2014; Hou et al., 2008). In an effort to elucidate the molecular mechanisms underlying Dcp-1-mediated autophagy regulation, an immune-affinity

purification (IP) and tandem mass spectrometry (MS/MS) assay was performed that identified SesB, an adenine nucleotide translocase, as a downstream regulator of autophagy (DeVorkin et al., 2014). SesB was discovered to negatively suppress autophagic flux through maintenance of ATP levels and its levels were negatively affected by a direct interaction with Dcp-1 (DeVorkin et al., 2014). Upstream factors and other downstream pathway components and their relationship to Dcp-1-mediated autophagy still remain largely unknown.

Here I report the *in vitro* screening of 24 candidate Dcp-1-interacting proteins identified in the IP-MS/MS screen, 13 of which were found to negatively regulate autophagic flux *in vitro*. I focused further on one of the identified interactors, Hsp83, since its human homolog HSP90 has links to disease, proteostasis and a current ambiguous role in autophagy (Bandyopadhyay et al., 2008; Mori et al., 2015; Xu et al., 2011). *In vivo* analyses revealed that loss-of-function *Hsp83* mutants induced autophagy and cell death during *Drosophila* mid-oogenesis. Biochemical analyses showed that Hsp83 binds to the zymogen pro-Dcp-1 and that the loss of Hsp83 led to elevated levels of cleaved and pro-Dcp-1 that were not due to transcriptional regulation. As an explanation for elevated levels of Dcp-1, I investigated the functionality of the UPS, and found that Hsp83 mutants had decreased proteasomal activity. The levels of Dcp-1 were increased in flies with suppressed proteasomal activity supporting that Dcp-1 itself is affected by the proteasome. Analysis of *Dcp-1;Hsp83* double mutants indicated that Dcp-1 was responsible for autophagy induced in mid-stage egg chambers (MSECs) and larval fat bodies, female fertility and organism viability when Hsp83 function is compromised. Additionally, *in vitro* double RNAi experiments revealed that Dcp-1 is needed to induce autophagy when Hsp83 or the proteasomal subunit Rpn11 is knocked down. These findings indicate that Hsp83 is important for basal proteasomal activity and that loss of it causes an induction of Dcp-1-mediated compensatory autophagy.

3.3. An RNAi screen identified candidate Dcp-1-interacting proteins that modulate autophagy

All 24 candidates identified in the Dcp-1 IP/MS screen (Table 1.1) were further investigated by autophagy analyses, initially employing a RNAi and LysoTracker® Green

(LTG) flow cytometry strategy conducted by L. DeVorkin. Of the 24 candidates, 13 showed a statistically significant increase in LTG fluorescence following RNAi and starvation treatment, indicating that these candidates act as potential negative regulators of autophagy (Figure 3-1A). The 24 candidates were compared to control RNAi treated cells: RheB, a negative regulator of autophagy that significantly increased LTG fluorescence following starvation, and S6K, a positive regulator of autophagy that significantly reduced LTG fluorescence (Figure 3-1A). These findings were validated with a second set of non-overlapping dsRNAs. The 13 validated hits included the heat shock proteins Hsc70-4, Hsp70Aa, Hsp60 and Hsp83, translation initiation factor eIF-4a, the chromatin remodeler Mi-2, the ribosomal constituent Sta, the AAA+ ATPase Ter94, the chloride intracellular channel protein Clic, the proteasome activator REG, and the mitochondrial proteins ATPsynthase-β, Blw and SesB.

To investigate the role of candidate Dcp-1 substrates and interacting partners in autophagic flux *in vitro*, autolysosome formation was monitored using a *Drosophila S2* cell line stably expressing RFP-GFP-Atg8a. Together L. DeVorkin and I found that RNAi-mediated knockdown of all 13 candidates significantly increased the number of autolysosomes per cell following starvation (Figure 3-1B,C), indicating that these proteins negatively regulate starvation-induced autophagic flux *in vitro.* For an experimental control the formation of autolysosomes was monitored following RNAi-mediated knockdown of *Rheb* and *S6K* and found a significant increase and decrease, respectively, in the number of autolysosomes per cell (Figure 3-1D). As an additional control to test the efficacy of the RFP-GFP-Atg8a assay, cells were starved and treated with the late stage autophagy inhibitor Bafilomycin A1 where a significant increase in the number of autolysosomes became blocked (Figure 3-1E). Knockdown of all 13 candidates in fed conditions also led to a statistically significant, although modest, increase in autolysosomes, with the greatest effects observed among the four heat-shock proteins identified (Figure 3-1F,G).

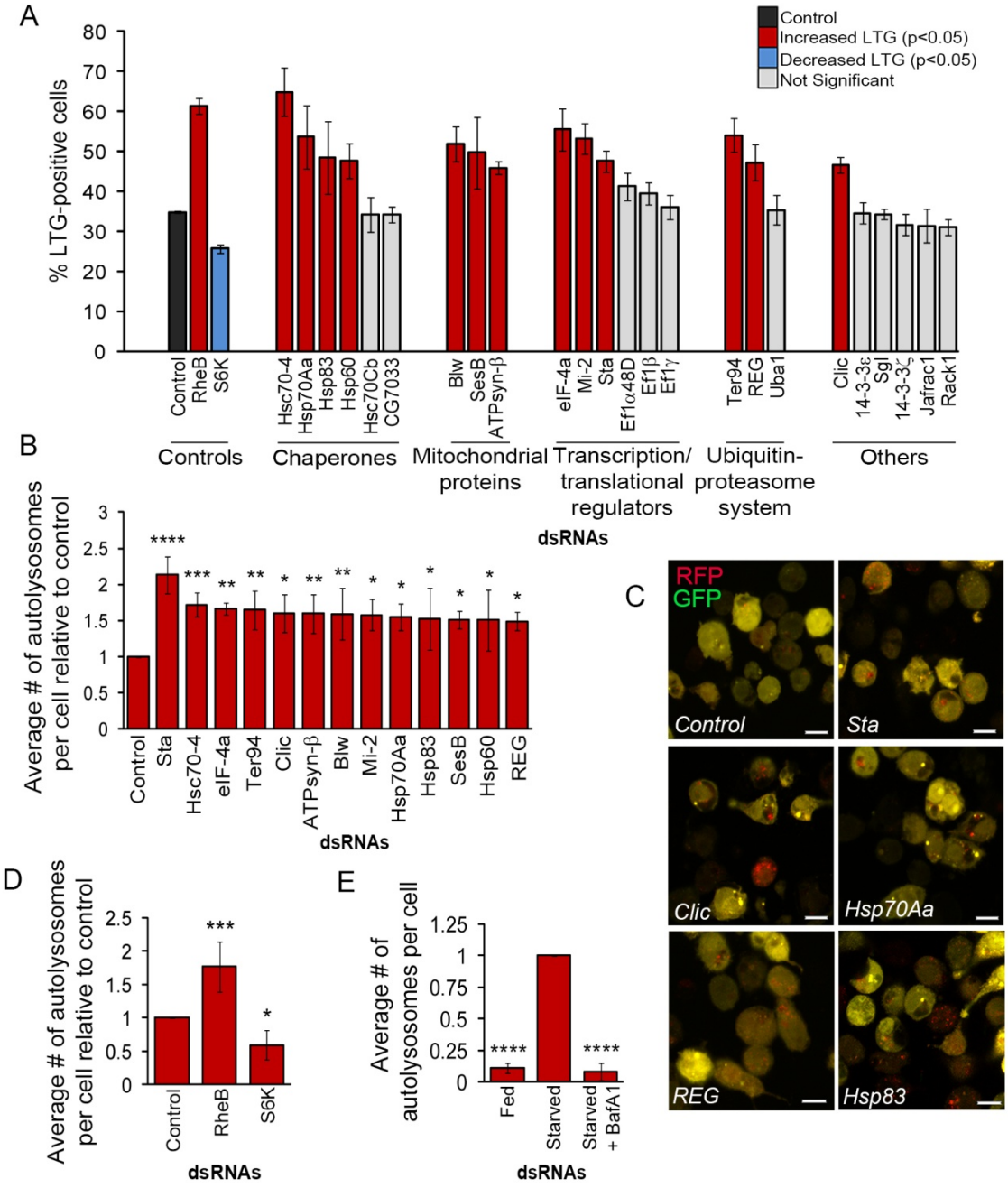

Figure 3-1 **Thirteen candidate Dcp-1 interactors modify LysoTracker® Green and autolysosomes *in vitro***

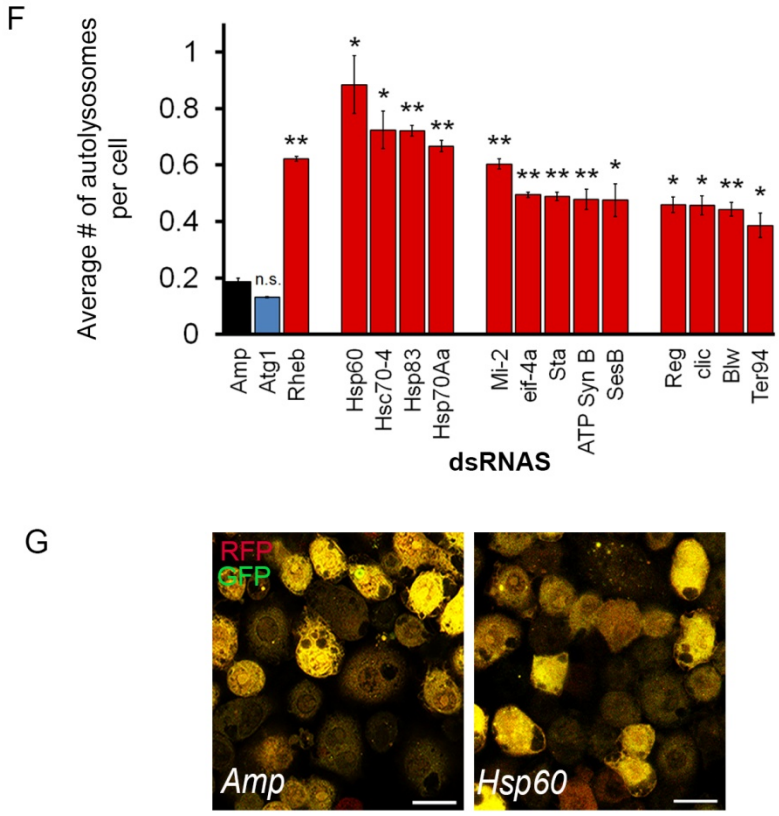

Figure 3-1 (cont'd)
(A) RNAi treated *l(2)mbn* cells stained with LysoTracker® Green (LTG) and starved to measure autophagy-associated activity via flow cytometry. Error bars represent ± S.E.M.(n=3). Statistical significance was determined using one-way ANOVA with a Dunnet post-test. Knockdown of targets that significantly increased LTG levels are indicated in red ($p<0.05$), and knockdown of targets that significantly decreased LTG levels are indicated in blue ($p<0.05$). All samples were compared to the negative control dsRNA (Ampicillin resistance gene) that is shown in black. (**B**-**G**) Analysis of RFP-GFP-Atg8a puncta in RNAi-treated *Drosophila* S2 cells. At least 50 cells were counted per treatment (n=3), and graphs represent the average number of autolysosomes per cell relative to the control. Error bars represent the average ± S.E.M, and statistical significance was determined using one-way ANOVA with a Dunnet post-test. (**B**) Cells were treated with indicated dsRNAs and subjected to starvation conditions for seven hours. *p<0.05, **p<0.01, ***p<0.001 ****p<0.0001. (**C**) Representative images of *S2-RFP-GFP-Atg8a* cells treated with indicated dsRNAs. Scale bars =10μm. (**D**) Cells were treated with *control*, *Rheb*, or *S6K* dsRNA and subjected to seven hours of starvation,*p<0.05, ***p<0.001. (**E**) Cells were subjected to nutrient rich or deprived conditions for seven hours in the presence or absence of 0.1μM Bafilomycin A1 (BafA1). ****p<0.0001. (**F**) Cells were treated with indicated dsRNAs in nutrient-rich conditions. dsRNAs *Rheb* and *Atg1* served as controls for an increase or a decrease in autophagy, respectively, and *Amp* served as a non-targeting control, *p<0.05,**p<0.01. (**G**) Representative image of the S2 RFP-GFP-Atg8a-expressing cells demonstrating a modest increase in puncta between *Hsp60* and the *Amp* control, scale bars =10 μm.

3.4. Loss of Hsp83 increases TUNEL staining, the percentage of mid-stage degenerating egg chambers (MSDECs) and autophagic flux.

In vitro autophagy assays revealed that Dcp-1 may regulate, or may be regulated by, one or more of the 13 identified negative regulators of starvation-induced autophagy. Of the interacting partners identified, I chose to focus on Hsp83. To further confirm the *in vitro* findings that Hsp83 acts as a negative regulator of autophagy, I designed additional *Hsp83* dsRNAs and analyzed LTG levels by flow cytometry (Figure 3-2A-C). Successful knockdown of a 65 - 80% reduction of Hsp83 confirmed that Hsp83 levels were lowered and that this resulted in a decrease in lysosomal staining.

For *in vivo* analyses, I chose to analyze *Drosophila* ovaries as it was shown that nutrient deprivation leads to both Dcp-1 dependent cell death and autophagy (DeVorkin et al., 2014; Laundrie et al., 2003). Loss-of-function studies were performed using transheterozygous (transhet) combinations of *Hsp83* mutant alleles since *Hsp83* homozygous mutant flies are lethal (Bandura et al., 2013; Yue et al., 1999). I examined the role of two transhet combinations with loss of function *Hsp83* alleles, $Hsp83^{e6A}$ with $Hsp83^{6-55}$ ($Hsp83^{e6A/6-55}$) and $Hsp83^{e6D}$ with $Hsp83^{6-55}$ ($Hsp83^{e6D/6-55}$), for their role in autophagy during *Drosophila* oogenesis by analyzing mid-stage egg chambers (MSECS). These alleles carry missense point mutations and the combinations were previously functionally screened by genetic complementation tests (Bandura et al., 2013). Ovaries from $Hsp83^{e6A/6-55}$ and $Hsp83^{e6D/6-55}$ flies contained an increase in the percentage of degenerating MSECs (MSDECS) that stained positively for LysoTracker® Red (LTR) and TUNEL relative to control flies and balanced monoallelic *Hsp83* mutants (Figure 3-2D-F). MSECs undergoing cell death are characterized by nurse cell nuclear condensation and fragmentation, uptake of the germline by follicle cells and follicle cell death (Giorgi and Deri, 1976). These findings suggest that there is an increase in lysosomal activity, a key feature of autophagy, in addition to cell death.

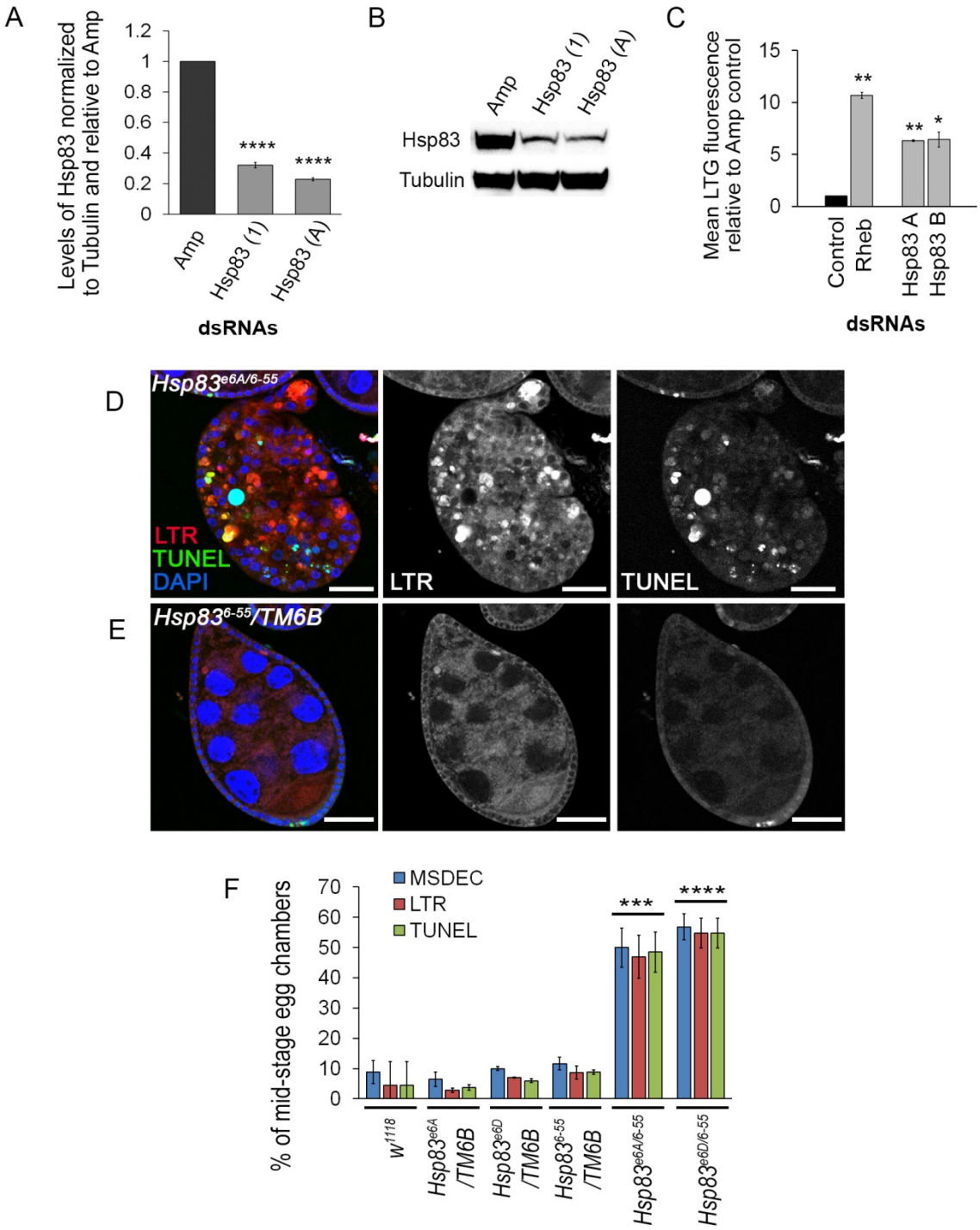

Figure 3-2 **Loss of Hsp83 function leads to an increase in lysosomal staining and cell death features in nutrient-rich conditions**

Figure 3-2 (figure legend continued from previous page)
(**A**) Quantification of levels of Hsp83 relative to actin and compared to the *Amp* control from western blots in *l(2)mbn* cells after being treated with indicated dsRNA. Error bars represent ± S.E.M. of n=4 and statistical significance was determined using a two-way Student's *t* test, ****p<0.0001. (**B**) Representative western blot showing the level of Hsp83 in comparison to tubulin following treatment with the indicated *Hsp83* dsRNA constructs. (**C**) *l(2)mbn* cells were treated with two additional non-overlapping Hsp83 dsRNAs and then stained with LTG. Fluorescence was measured by flow cytometry and their mean LTG fluorescence was normalized to *Amp* with *Rheb* being a positive control for a negative regulator *p<0.01, **p<0.001 (n=3). (**D**,**E**) Representative MSDECs and non-degenerating MSECs stained with LTR, TUNEL and DAPI, scale bars =25μm. (**D**) MSDEC from an $Hsp83^{e6A/6-55}$ ovariole that scored positive for LTR and TUNEL staining. (**E**) Non degenerating MSEC from $Hsp83^{6-55}/TM6B$ scored as negative for LTR and TUNEL (**F**) Mid-stage egg chambers (MSECS) scored as being TUNEL positive, LysoTracker® Red (LTR) positive or as having condensed degenerating nurse cell nuclei by DAPI (MSDEC) with percentages reported according to their genotype. At least 50 MSECs were counted per genotype (n=3). Error bars represent ± S.E.M. and statistical significance was determined using one-way ANOVA with a Bonferroni post-test and compared to w^{1118}, ***p<0.001, ****p<0.0001.

As an additional measure to examine autophagic flux specifically, I utilized the tandem-tagged Atg8a reporter system expressing GFP-mCherry-Atg8a in the germline of Hsp83 transhets in nutrient-rich conditions. Due to the nature of the cross, $Hsp83^{6-55}$/MKRS and either $Hsp83^{e6A}$/MKRS or $Hsp83^{e6D}$/MKRS were indistinguishable and thus analyzed together. First, I confirmed that expression of the Atg8a reporter construct did not affect the frequency of MSDECs (Figure 3-3A). $Hsp83^{e6A/6-55}$ and $Hsp83^{e6D/6-55}$ had very distinct MSDECs that had high levels of autolysosomes in comparison to the control Hsp83 heterozygotes (Figure 3-3B-D). Quantification showed that 75-90% of MSDECs had greater than five autolysosomes compared to only 15-20% when carrying one mutated *Hsp83* allele (Figure 3-3B). The non-degenerating MSECs in the mutant transhets and the controls looked morphologically normal and didn't appear to have high levels of autophagic flux (Figure 3-3E,F). From these studies I concluded that loss of Hsp83 enhances the percentage of MSDECs undergoing autophagic flux. To determine if the phenotype is affected by the stress of nutrient deprivation, the flies were fed a sucrose-only diet for four to five days. Both the control *Hsp83* heterozygotes and the mutant $Hsp83^{e6A/6-55}$ transhets showed an increase in autolysosomal activity in the early stage egg chambers. However, in the mutant *Hsp83* transhets, I observed an exacerbated phenotype of nearly obliterated mCherry-positive mid-stage egg chambers in contrast to the degenerating mid-stage egg chambers observed in fed conditions (Figure 3-4).

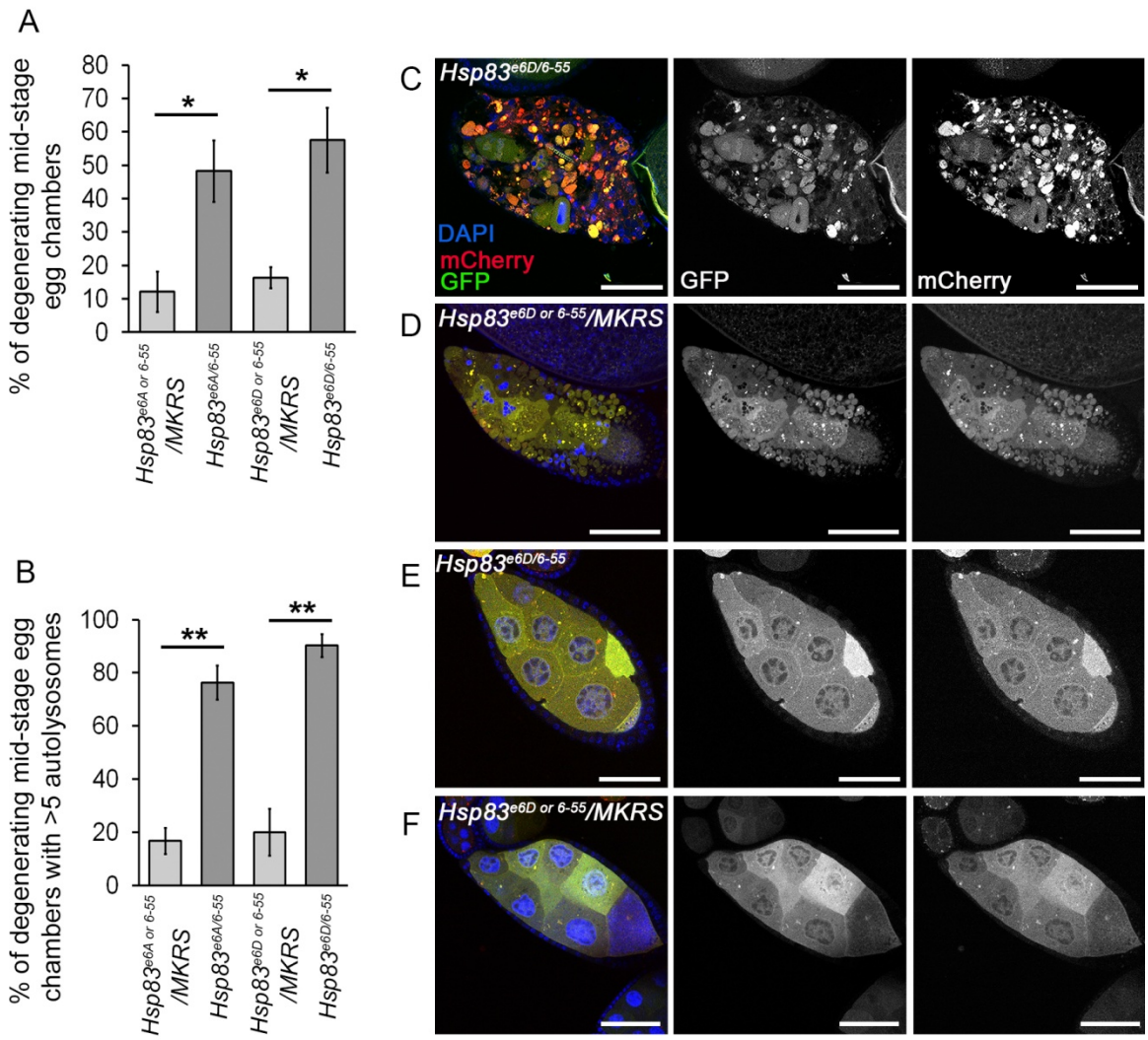

Figure 3-3 Loss of Hsp83 function leads to an increase in autophagy *in vivo* in nutrient rich conditions

MSECs were scored from flies expressing GFP-mCherry-Atg8a in the germline (*UAsp-GFP-mCherry-DrAtg8a* with single copies of the drivers *otu-GAL4* and *NGT-GAL4*). *Hsp83^{e6D}/MKRS* and *Hsp83$^{6-55}$/MKRS*, *Hsp83^{e6A}/MKRS* and *Hsp83$^{6-55}$/MKRS* from the same cross were analyzed together. (**A**) Percentage of MSDECs for the indicated genotypes is represented on the graph and reflects the mean of at least 100 MSECs scored per genotype(n=3). Error bars represent ± S.E.M. and statistical significance was determined using a two-tailed Student's *t* test, * p<0.05. (**B**) Flies expressing GFP-mCherry-Atg8a in the germline were scored as either having more than five autolysosomes or less than or equal to five autolysosomes. The percentages shown reflect the mean of at least 100 MSECs scored per genotype (n=3). Error bars represent ± S.E.M. and statistical significance was determined using a two-tailed Student's *t* test, **p<0.01. (**C**-**F**) Representative images of MSECs expressing the construct GFP-mCherry-Atg8a, scale bar = 25µm. MSDECS found in (**C**) *Hsp83$^{e6D/6-55\ flies}$* and (**D**) *Hsp83$^{e6D\ or\ 6-55}$/MKRS*. (**E**,**F**) Examples of non-degenerating MSECs from (**E**) *Hsp83$^{e6D/6-55\ flies}$* and (**F**) *Hsp83$^{e6D\ or\ 6-55}$/MKRS.*

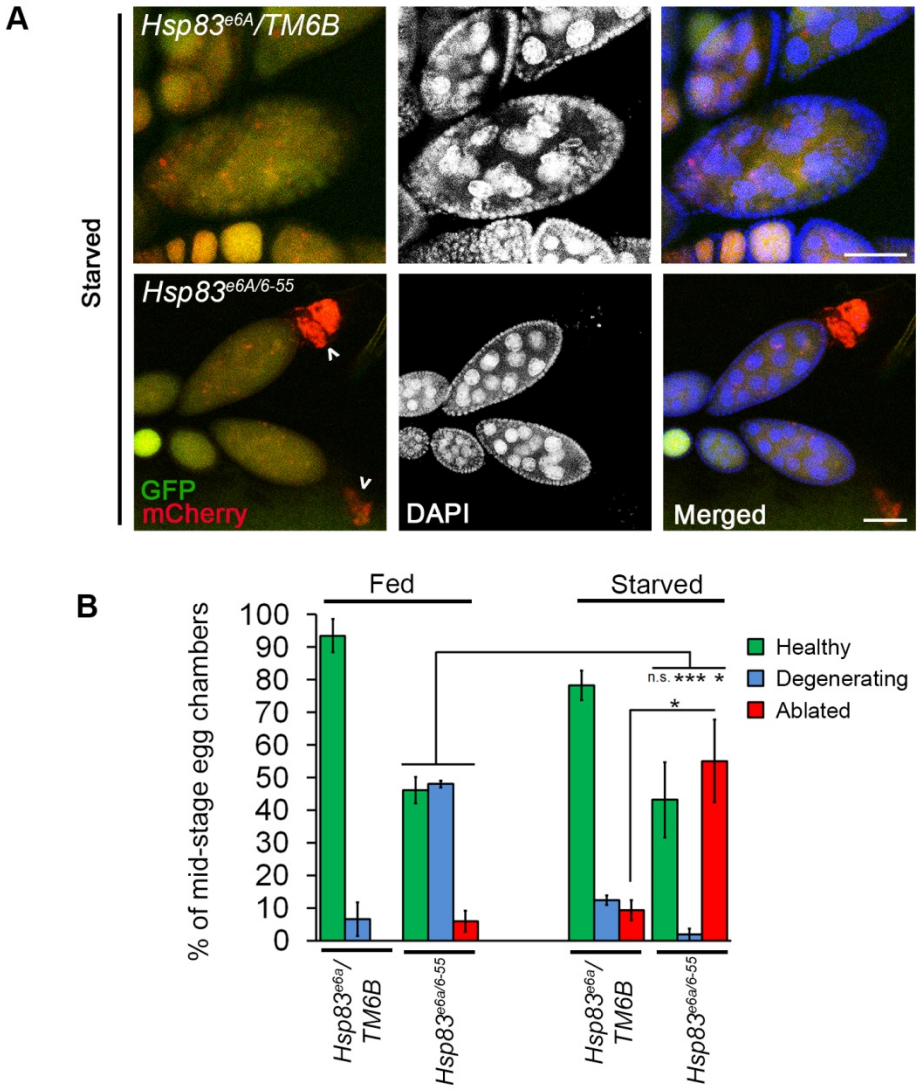

Figure 3-4 Loss of Hsp83 function increases impairment of oogenesis in starvation conditions

(**A**)Representative images of MSECs from flies expressing UAsp-GFP-mCherry-Atg8a with one copy of the maternal drivers *otu-GAL4* and *NGT-GAL* in the background of monoallelic *Hsp83*^{e6a} or *Hsp83*$^{e6a/6-55}$ transhets. Flies were incubated in tubes with yeast paste for two days then put in a vial with only 10% sucrose for 4-5 days after eclosion to be exposed to low nutrient or starved conditions. Arrows indicate strong aggregates of the mCherry channel in place of a MSEC. Scale bars = 25 µm (n=3). (**B**) MSECs were scored as being healthy, degenerating or ablated and compared in fed and starved conditions. Error bars represent the average ± S.E.M, and statistical significance was determined using one-way ANOVA with a Dunnet post-test, *p<0.05,***p<0.001 (n=3).

3.5. Hsp83 interacts with pro-Dcp-1 and regulates its levels

Previous analyses performed by L. DeVorkin and N. Go found that Hsp83 is not cleaved by Dcp-1 and that Hsp83 only associates with the zymogen form of Dcp-1, pro-Dcp-1. Since Dcp-1 does not cleave Hsp83 and they interact, I reasoned that Hsp83 might be affecting Dcp-1 since chaperones are known to stabilize proteins or facilitate their turnover. To better understand their interaction, I quantified levels of the zymogen pro-Dcp-1 in *Hsp83* flies by western blot analysis. *Hsp83*$^{e6A/6-55}$ and *Hsp83*$^{e6D/6-55}$ flies showed a significant increase in the levels of pro-Dcp-1 in comparison to wild-type and the single mutant alleles of *Hsp83* (Figure 3-5A,B). To determine if Hsp83 loss also led to elevated levels of catalytically active Dcp-1, I analyzed levels of cleaved Dcp-1 by scoring immunofluorescence with an antibody targeted against cleaved-Dcp-1 (IF). I found a statistically significant increase in the percentage of MSECS that stained positively for cleaved Dcp-1 in *Hsp83* mutants compared to controls (Figure 3-5C,D). The elevated levels of both pro-Dcp-1 and processed Dcp-1 indicate that loss of Hsp83 does not impair pro-Dcp-1 processing into its active form.

In order to test the possibility of transcriptional regulation as an explanation for the elevated Dcp-1, N. Go performed qRT-PCR on RNA extracts from *Hsp83* flies and found that there was no significant difference in Dcp-1 transcript levels between *Hsp83* transhets, *Hsp83* heterozygote controls and wild-type (Figure 3-6A). These data suggest that loss of functional Hsp83 leads to increased Dcp-1 that is independent of transcriptional regulation. Next, I explored the potential role of the Death-associated inhibitor of apoptosis 1 (Diap1) protein. Diap1 was shown previously to ubiquitylate and inhibit the activity of cleaved Dcp-1 without affecting its levels (Ditzel et al., 2008), but the consequences on pro-Dcp-1 levels are unknown. I overexpressed Diap1 *in vivo* and found that Diap1 overexpression did not have a significant effect on the protein levels of pro-Dcp-1 (Figure 3-6B,C). I also overexpressed Diap1 in the *Hsp83* transhet background and found no statistically significant difference in levels compared to the Hsp83 transhets (Figure 3-6D,E). These results taken together with the knowledge that Hsp83 only associates with the pro-form of Dcp-1, indicate that the regulation of pro-Dcp-1 levels in this context is largely independent of Diap1.

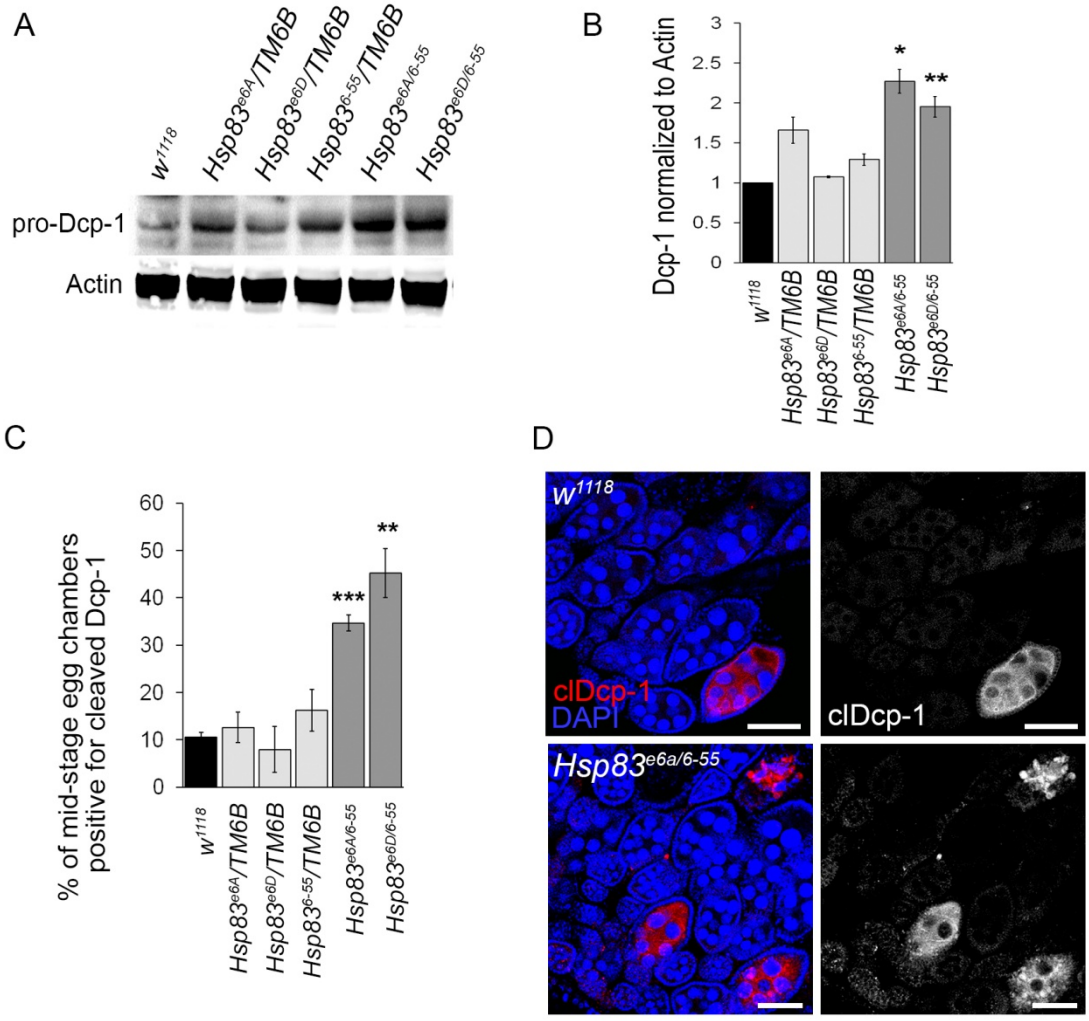

Figure 3-5 Loss of Hsp83 mutants have increased levels of pro-Dcp-1 and cleaved Dcp-1

(**A**) Representative western blot of whole body lysates from females of the specified genotypes; pro-Dcp-1 = 35kDa, actin = 42kDa. (**B**) Quantification of levels of pro-Dcp1 was determined by densitometry and normalized to levels of actin. The average relative levels of pro-Dcp-1 were determined with eight females per lysate (n=3). Error bars represent ± S.E.M. and statistical significance was determined by comparison to the w^{1118} control using one-way ANOVA with a Dunnet post-test, *p<0.05, **p<0.01. (**C**) MSECs were scored as being positive or negative for cleaved Dcp-1 (clDcp-1). The average percentage was determined by analyzing over 50 MSECs per genotype (n=3). Error bars represent ± S.E.M. and statistical significance was determined by comparison to w^{1118} using one-way ANOVA with a Dunnet post-test, **p<0.01,***p<0.001. (**D**) Representative images of *Drosophila* ovarioles that were stained with cleaved Dcp-1 antibody and DAPI for w^{1118} control and $Hsp83^{e6a/6-55}$, scale bars = 50 µm.

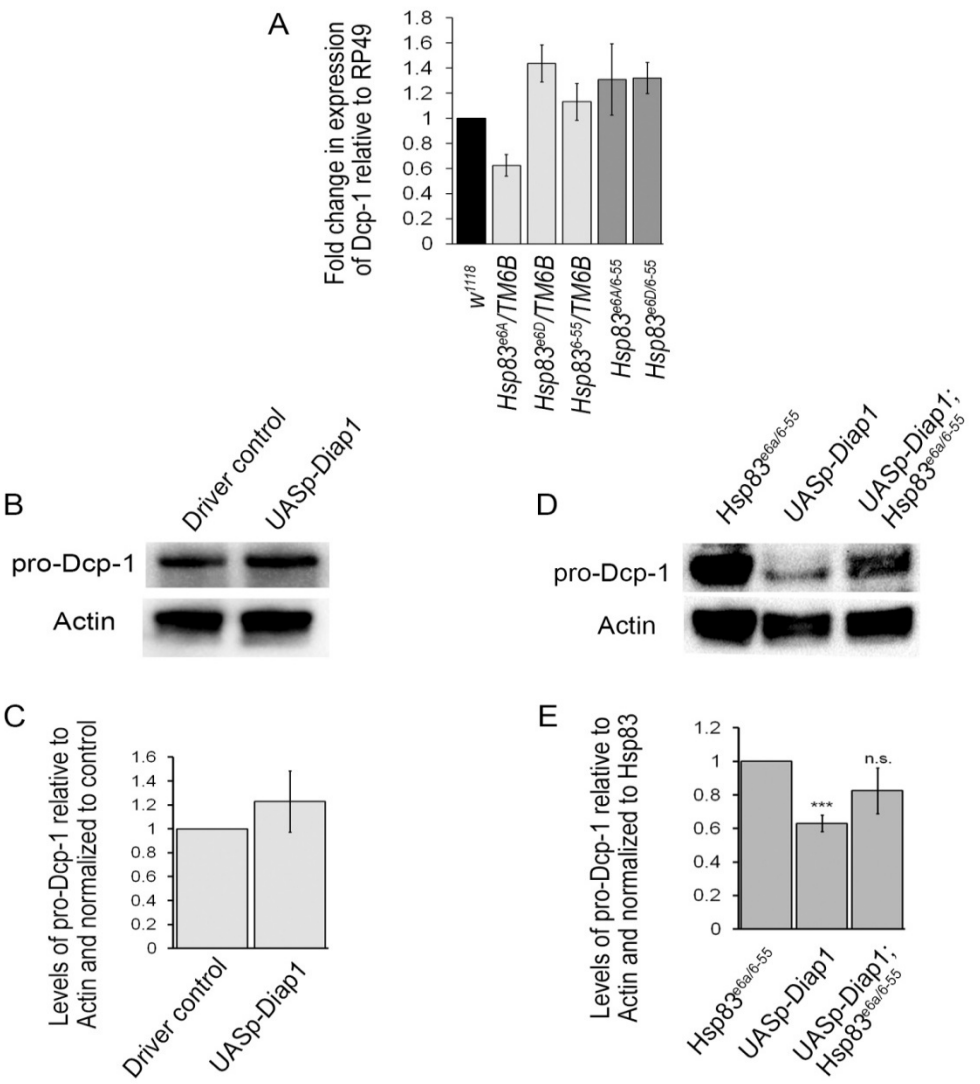

Figure 3-6 The elevated levels of Dcp-1 in *Hsp83* mutants are independent of regulation by transcription and inhibitor of apoptosis protein Diap1

(**A**) QRT-PCR was performed on mRNA extracts from eight animals each to determine levels of *Dcp-1* mRNA relative to the *RP49* control mRNA (n=3). The relative fold change was normalized to wild-type w^{1118} with error bars representing ± S.E.M. There was no significant difference in *Dcp-1* mRNA expression between genotypes. (**B**,**C**) Flies containing a single copy of the maternal driver *nosGal4* in the background of the *UASp-Diap1* construct or w^{1118} control were incubated at 25°C for 4 days before collection. (**B**) A representative blot probed with pro-Dcp-1 (35kDa) and actin (42kDa) (**C**) A quantitative graph analyzing densitometry showed no significant difference in the levels of pro-Dcp-1 relative to actin. Error bars represent ± S.E.M and statistical significance was determined using a two-way Student's *t* test (n=6). (**D**, **E**) Flies expressing one copy each of the drivers *otu-GAL4* and *NGT-GAL* in either a *Hsp83* transhet mutant background, *UASp-Diap1* background or a combination of both were collected after incubation at 25°C for 4 days . (**D**) A representative western blot probed with pro-Dcp-1 (35kDa) and actin (42kDa). (**E**) A quantitative graph analyzing densitometry of the western blots. Error bars represent ± S.E.M of n=4 with significance determined by a one-way ANOVA with a Bonferroni post-test and compared to *Hsp83* transhet, ***p<0.001.

3.6. Reduced proteasomal activity in Hsp83 mutants, proteasomal knockdown and inhibition led to an increase in Dcp-1

Homologs of Hsp83, yeast Hsp90 and human HSP90, were shown to be needed for 26S proteasomal assembly and for antigen processing, respectively (Imai et al., 2003; Yamano et al., 2008). To test whether altered proteasomal activity could be a possible explanation for the elevated levels of Dcp-1 observed in *Hsp83* mutants, I used a luminescence assay with proteasome-targeted substrates that react when cleaved. Luminescence was significantly decreased in flies harboring RNAi targeted against *Prosα1*, a subunit of the 20S proteasome, and in *Hsp83* transhets when compared to *Hsp83* heterozygote controls and wild-type flies (Figure 3-7A). To confirm the decreased proteasome activity in *Hsp83* transhets, I expressed the proteasome activity reporter CL1-GFP, a fusion protein with a degradation signal introduced into the otherwise stable GFP molecule (Bence et al., 2001), in the larval fat body using the larval midgut specific driver *cg-GAL4*. The *Hsp83* transhets had a marked increase in GFP expression relative to controls, indicating inefficient turnover of CL1-GFP (Figure 3-7B,C). The observed reduction in proteasomal activity could explain why Dcp-1 levels are elevated in the *Hsp83* transhet mutants.

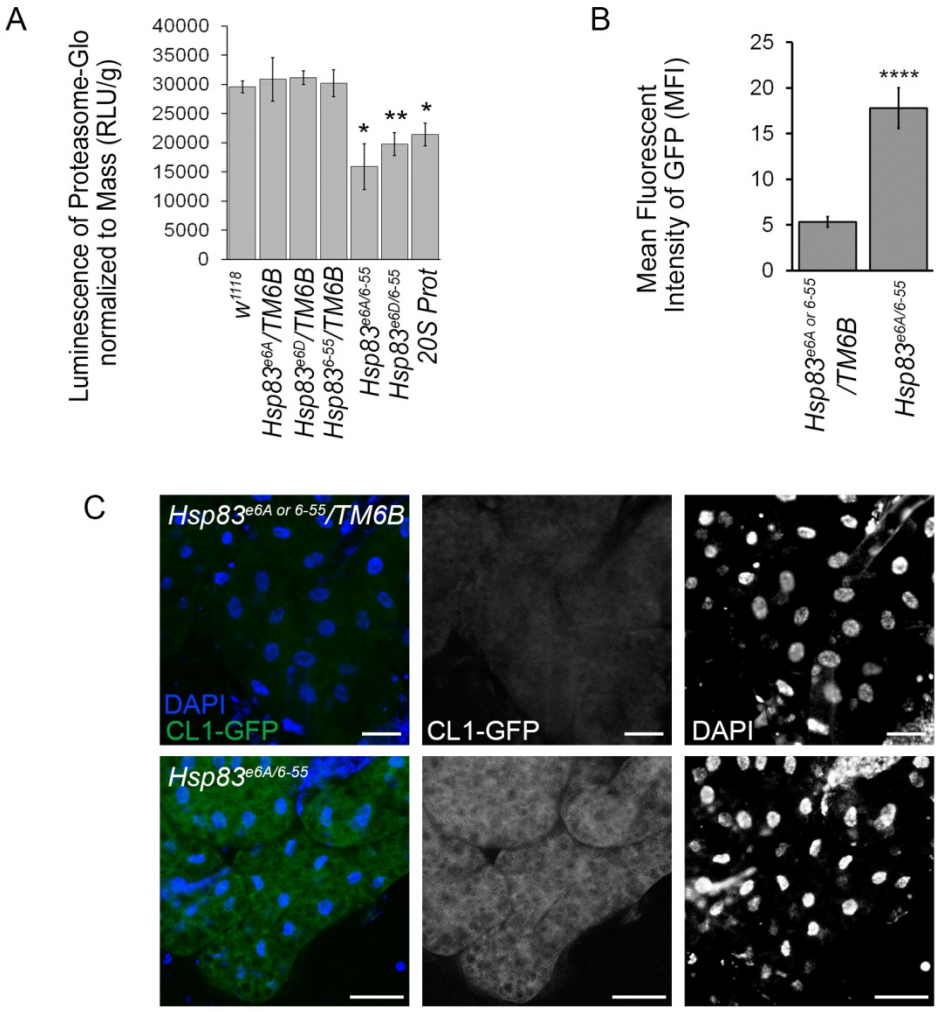

Figure 3-7 Functional loss of Hsp83 decreases proteasomal activity *in vivo*

(**A**) Proteasomal activity was measured in females from the indicated genotypes using luminescent output (RLU) produced from cleavage of proteasomal substrates (ProteasomeGlo kit) and made relative to mass. Error bars represent ± S.E.M. and statistical significance was determined using one-way ANOVA with a Bonferroni post-test and compared to w^{1118}, *p<0.05, **p<0.01.(n=5) (**B**,**C**) UAS-CL1-GFP expressed in the larval fat body using the driver *cg-GAL4* in transhet and monoallelic Hsp83 mutants and visualized with non-adjusted GFP channel images taken in the same experiment with identical confocal microscope settings (n=3). (**B**) Quantification of fluorescent intensity. Error bars represent ± S.E.M. and statistical significance was determined using a two-tailed Student's *t* test, **** p<0.0001. (**C**) Representatives images showing DAPI staining and CL1-GFP expression, scale bars = 50 µm.

To determine if Dcp-1 levels are affected by the proteasome, I quantified levels of Dcp-1 in an RNAi line targeted against *Rpn2*, a regulatory subunit of the 26S proteasome. RNAi knockdown was enhanced by expressing one copy of Dicer2 using the oogenesis specific driver *nosGAL4*. An increase in temperature enhances expression of Gal4-driven Dicer2 under the *UAsp* promoter and thus the knockdown is more efficacious. *Rpn2* RNAi flies (*Rpn2/Dcr*) or control flies (*Dcr*), were incubated at 18°C or 25°C for two days before collection. The enhanced knockdown of Rpn2 at 25°C correlated with a greater increase in pro-Dcp-1 levels in comparison to the *Dcr* flies (Figure 3-8A,B). In addition to genetic suppression of the proteasome, I tested pharmacological inhibition by feeding flies the proteasome inhibitor MG132. A significant decrease in proteasomal activity was observed in both wild-type and *Hsp83* transhets following MG132 treatment (Figure 3-8C). The levels of pro-Dcp-1 increased in wild-type with the addition of MG132, consistent with the decrease in proteasomal activity (Figure 3-8D,E). There was no further increase in the levels of pro-Dcp-1 in *Hsp83* transhets treated with MG132 compared to the DMSO control despite reduced proteasomal activity. Together, these results show that Dcp-1 levels are affected by the proteasome and that the reduction of Dcp-1 is dependent on functional Hsp83.

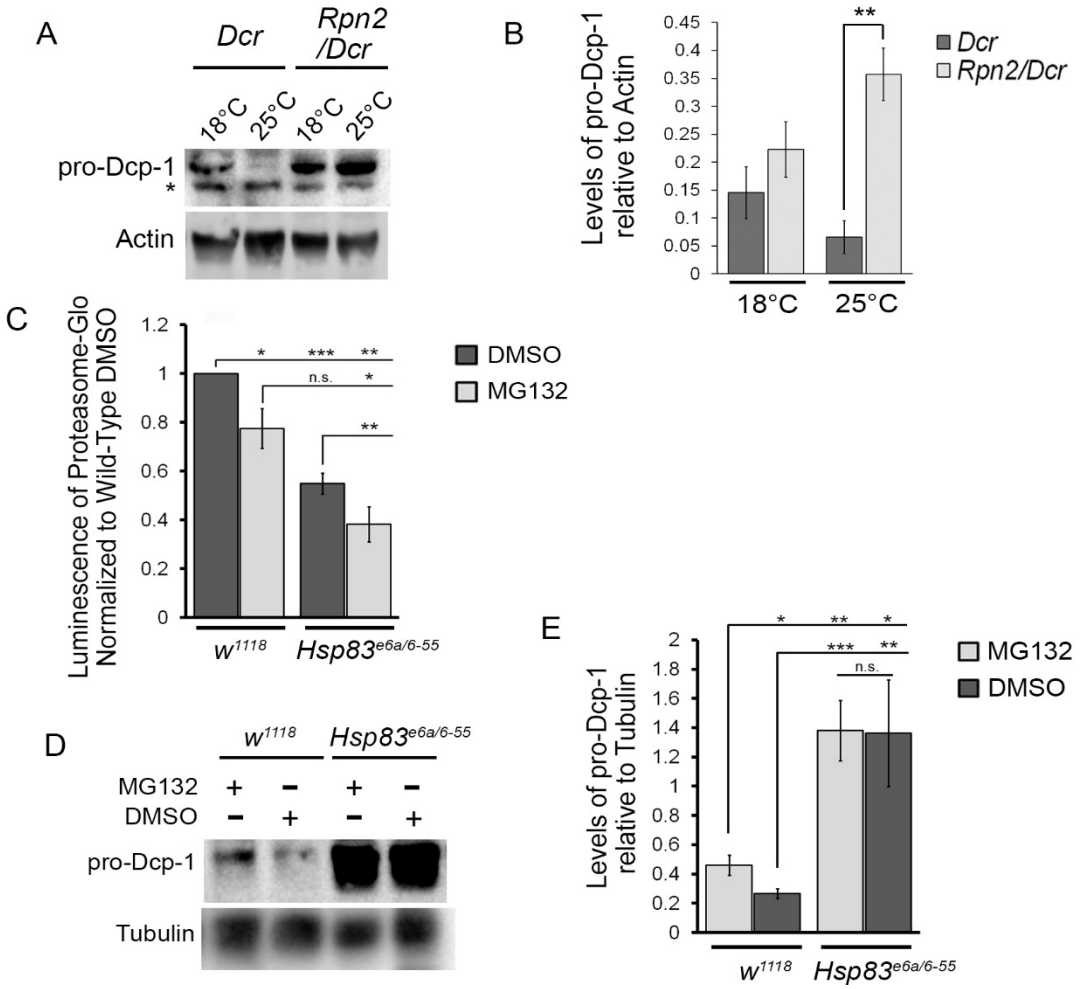

Figure 3-8 A decrease in proteasomal activity leads to an increase in levels of pro-Dcp-1 that is Hsp83 dependent

(**A**,**B**) Females with the maternal driver nosGAL4 were collected after two days of exposure to 18°C or 25°C with the genotypes *+/UAspDcr2; nosGAL4/+* (*Dcr*) and *Rpn2-RNAI/UAspDcr2;nosGAL4/+* (*Rpn2/Dcr*). (**A**) Representative western blot of pro-Dcp-1 and Actin levels in *Dcr* and *Rpn2/Dcr* pro-Dcp-1 = 35kDa, Actin = 42kDa, * represents a non-specific band detected by the Dcp-1 antibody. (**B**) Quantification of pro-Dcp-1 levels was performed by densitometry and normalized to levels of Actin. The average relative levels of pro-Dcp-1 were determined with eight females per lysate (n=3). Error bars represent ± S.E.M. and statistical significance was determined using a two-way Student's *t* test, **p<0.01. (**C**-**E**) $Hsp83^{e6A/6-55}$ and w^{1118} flies were fed proteasomal inhibitor MG132 or the control DMSO for 4 days. (**C**) Proteasomal activity was measured and normalized to w^{1118} flies fed with DMSO (n=3). Error bars represent ± S.E.M. and statistical significance was determined using a Student's *t* test, *p<0.05, **p<0.01, ***p<0.001. (**D**) Representative image of a western blot probed for pro-Dcp-1(35kDa) and Tubulin (55kDa). (**E**) Quantification of pro-Dcp-1 levels was performed by densitometry and normalized to levels of tubulin. The average relative levels of pro-Dcp-1 were determined with eight females per lysate(n=3). Error bars represent ± S.E.M. and statistical significance was determined using a two-way Student's *t* test, *p<0.05, **p<0.01, ***p<0.001.

3.7. Hsp83 loss induces Dcp-1-dependent compensatory autophagy that is required to maintain female fertility and larval viability

It was previously found that Dcp-1 levels are increased and induce autophagic flux in response to starvation (DeVorkin et al., 2014; Hou et al., 2008). To understand if the increased levels of autophagy in *Hsp83* mutants are dependent on Dcp-1, I performed an epistasis experiment. I created double mutants consisting of *Hsp83* transhets and the *Dcp-1^{Prev1}* loss-of-function alleles through multiple genetic crosses. Ovaries from *Dcp-1^{Prev1}* flies contain persisting nurse cell nuclei and premature loss of follicle cells (Laundrie et al., 2003). I found that the MSECs of double mutants *Dcp-1^{Prev1}; Hsp83$^{e6A/6-55}$* and *Dcp-1^{Prev1}; Hsp83$^{e6D/6-55}$* flies have a phenotype similar to *Dcp-1^{Prev1}* but with several differences (Figure 3-9A,B). The MSECs appear to have a premature loss of follicle cells, similar to *Dcp-1^{Prev1}* flies, but the nurse cell nuclei are only partially condensed relative to those observed in MSDECs from *Hsp83* transhet mutants. The nurse cell nuclei in *Hsp83; Dcp-1^{Prev1}* double mutant MSECs also stain positively for TUNEL similar to Hsp83 but fail to stain for LTR.

To determine if the relationship between Hsp83 and Dcp-1 occurs in other tissues I analyzed the larval fat body. Fat bodies from *Hsp83* transhets had increased TUNEL and LTR staining, similar to the ovaries. In addition, fat bodies from *Dcp-1;Hsp83* double mutants had only TUNEL staining whereas control *Hsp83* alleles*, Dcp-1^{Prev1}* and wild-type flies had no significant LTR or TUNEL (Figure 3-9C,D).

The *Hsp83;Dcp-1^{Prev1}* double mutants also affected fecundity as both females and males were sterile whereas only male *Hsp83* transhets are sterile and *Dcp-1^{Prev1}* flies are fertile. In addition, the double mutants showed a reduction in viability with a significant increase in the fraction of animals dying in the pharate adult stage and not being able to eclose, as quantified by the ratio of dead pharate adults to eclosed pupae ($p<0.01$) (Figure 3-9E). These results suggest that loss of Hsp83 can lead to activation of cell death through a pathway independent of Dcp-1, but that loss of Hsp83 induces compensatory autophagy through a pathway that requires Dcp-1.

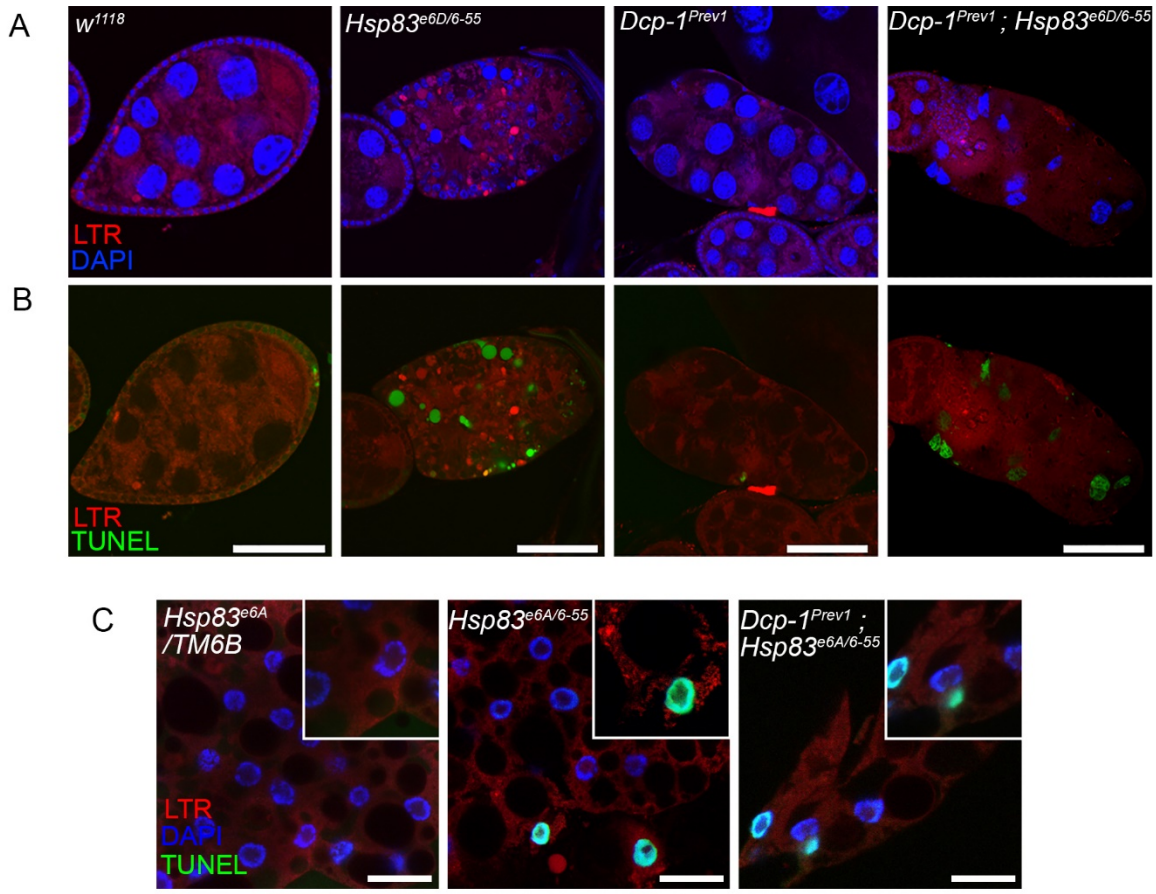

D

Genotype	Nuclei	LTR	TUNEL
w^{1118}	244	0	0
+; *Hsp83*^{e6A}/*TM6B*	328	1	21
+; *Hsp83*^{e6D}/*TM6B*	337	0	0
+; *Hsp83*$^{6-55}$/*TM6B*	234	0	4
+; *Hsp83* $^{e6A/6-55}$	222	**74**	**74**
+; *Hsp83* $^{e6D/6-55}$	262	**76**	**63**
Dcp-1^{Prev1};+	310	0	0
Dcp-1^{Prev1}; *Hsp83* $^{e6A/6-55}$	186	**0**	**37**
Dcp-1^{Prev1}; *Hsp83* $^{e6D/6-55}$	262	**0**	**55**

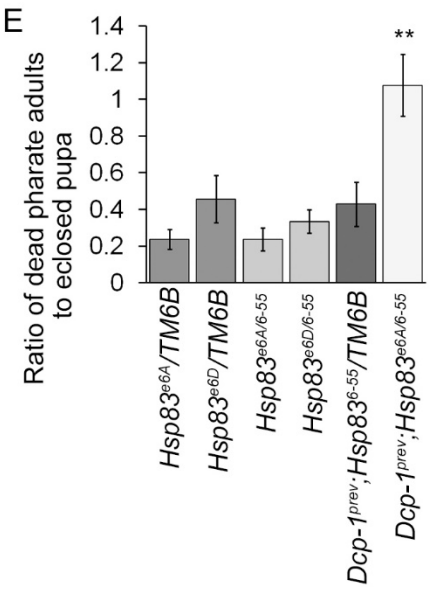

Figure 3-9 **Dcp-1 is required for autophagic flux and contributes to developmental viability but not cell death resulting from loss of Hsp83**

Figure 3-9 (figure legend continued from previous page)
(**A**,**B**) Representative images of MSECs for the genotypes w^{1118}, $Hsp83^{e6D/6-55}$, $Dcp\text{-}1^{Prev1}$ and $Dcp\text{-}1^{Prev1}$; $Hsp83^{e6D/6-55}$, stained with (**A**) LTR and DAPI or (**B**)LTR and TUNEL; experiments were performed on at least eight females per genotype (n=3), scale bars = 50 μm. (**C**)Representative images of first instar larval fat bodies stained with LTR, DAPI and TUNEL; scale bars =10 μm. (**D**) Quantification of the total number of cells, determined by DAPI staining, that stained positively for LTR and/or TUNEL in larval fat bodies from indicated genotypes. Experiments were performed in triplicate with the total number of cells assessed listed in the table. (**E**) The ratio of dead pharate adult pupae to eclosed pupae was counted in vials containing different combinations of mutant *Hsp83* and *Dcp-1* alleles. Vials were incubated at room temperature for 14 days past first fly eclosion and then ratios were counted for at least 80 animals (n=3). Error bars represent ± S.E.M. and statistical significance was determined using one-way ANOVA with a Dunnet post-test (**p<0.01)

To further validate the relationship between Hsp83 and Dcp-1, I conducted RNAi studies in the *S2-RFP-GFP-Atg8a* cell line as a more specific autophagy assay. As expected, *Atg1* and *Rheb* showed a relative decrease and increase in the numbers of autolysosomes, respectively, compared to the control (Figure 3-10). The decrease in autolysosomes seen in the *Dcp-1* RNAi-treated cells was reiterated in the combination knockdown of Hsp83 and Dcp-1 and was in stark contrast to the increase observed in *Hsp83* RNAi treated cells.

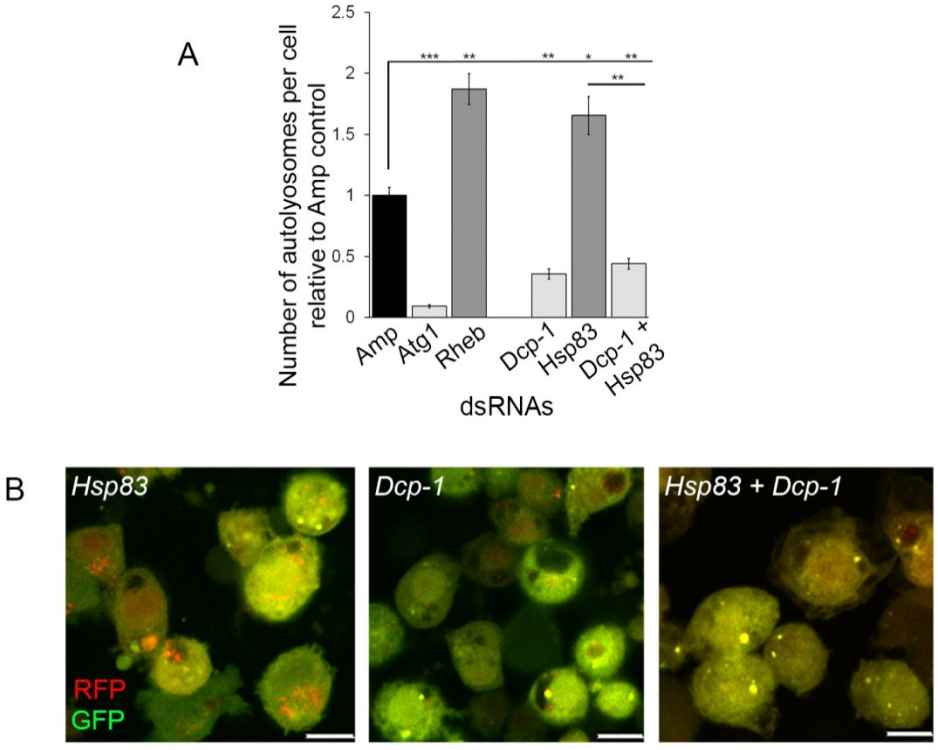

Figure 3-10 Dcp-1 is required for autophagic flux caused by loss of Hsp83 *in vitro*

The number of autolysosomes per cell was quantified in S2 cells stably expressing RFP-GFP-Atg8a and treated with the indicated dsRNAs. (**A**) All counts were normalized to the *Amp* dsRNA control. *Atg1* and *Rheb* dsRNA's served as controls for decreasing and increasing the number of autolysosomes, respectively (n=3). Error bars represent ± S.E.M. and statistical significance was determined using one-way ANOVA with a Dunnet post-test, *p<0.05, **p<0.01,***p<0.001. Over 100 cells were analyzed per treatment. (**B**) Representative images of RFP-GFP-Atg8a S2 cells following treatment with the indicated dsRNAs; scale bars =10 μm.

3.8. Proteasome disruption induces Dcp-1-dependent compensatory autophagy

To determine if Dcp-1 is required for compensatory autophagy following proteasome disruption specifically we used RNAi targeted against *Rpn11*, a *Drosophila* proteasome regulatory subunit, that was shown to compromise proteasomal activity (Lundgren et al., 2003). Similar to Hsp83-RNAi, the Rpn11-RNAi resulted in enhanced levels of autolysosomes that were significantly reduced in combination with Dcp-1 RNAi (Figure 3-10). Since mutant *Hsp83* transhets showed an increase in pro-Dcp-1, cleaved Dcp-1, and LTR staining, we investigated whether there was also an increase in cleaved Dcp-1 and LTR staining in proteasome-compromised flies in addition to the elevated pro-Dcp1 levels already observed (Figure 3-8,B). *Rpn2/Dcr* flies kept at 25°C showed a significant increase in the number of MSDECs expressing cleaved Dcp-1 that were LTR-positive (Figure 3-12A,B). To determine if LTR levels correlated with Dcp-1 levels, we quantified staining at both 18°C and 25°C, and found a significant increase ($p<0.05$) in LTR staining, along with increased Dcp-1 levels, at the higher temperature (Figure 3-12C). Together, these findings support that the increase in autophagy detected *in vitro* and *in vivo* in response to reduced proteasome function is regulated by Dcp-1.

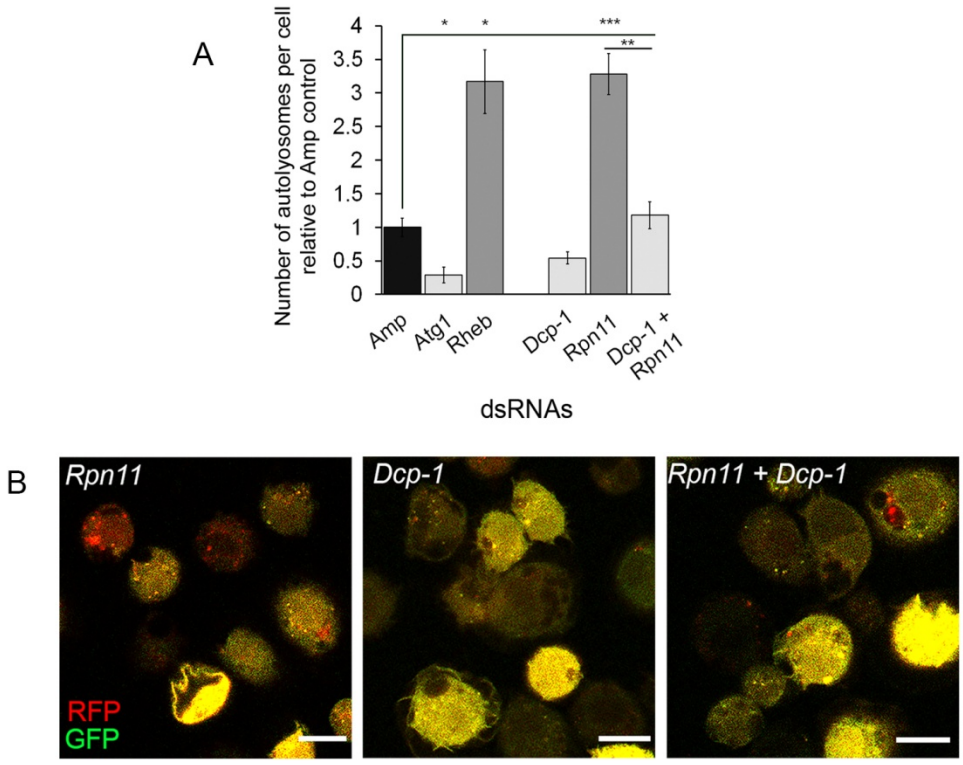

Figure 3-11 Proteasomal subunit loss results in Dcp-1-dependent compensatory autophagy *in vitro*

(**A**,**B**) The number of autolysosomes per cell was quantified in S2 cells stably expressing RFP-GFP-Atg8a and treated with the indicated dsRNAs. (**A**) Representative images of RFP-GFP-Atg8a S2 cells following treatment with the indicated dsRNAs; scale bars =10 μm. (**B**) All counts were normalized to the *Amp* dsRNA control. *Atg1* and *Rheb* dsRNA's served as controls for decreasing and increasing the number of autolysosomes, respectively. Error bars represent ± S.E.M. and statistical significance was determined using one-way ANOVA with a Dunnet post-test, *p<0.05, **p<0.01,***p<0.001

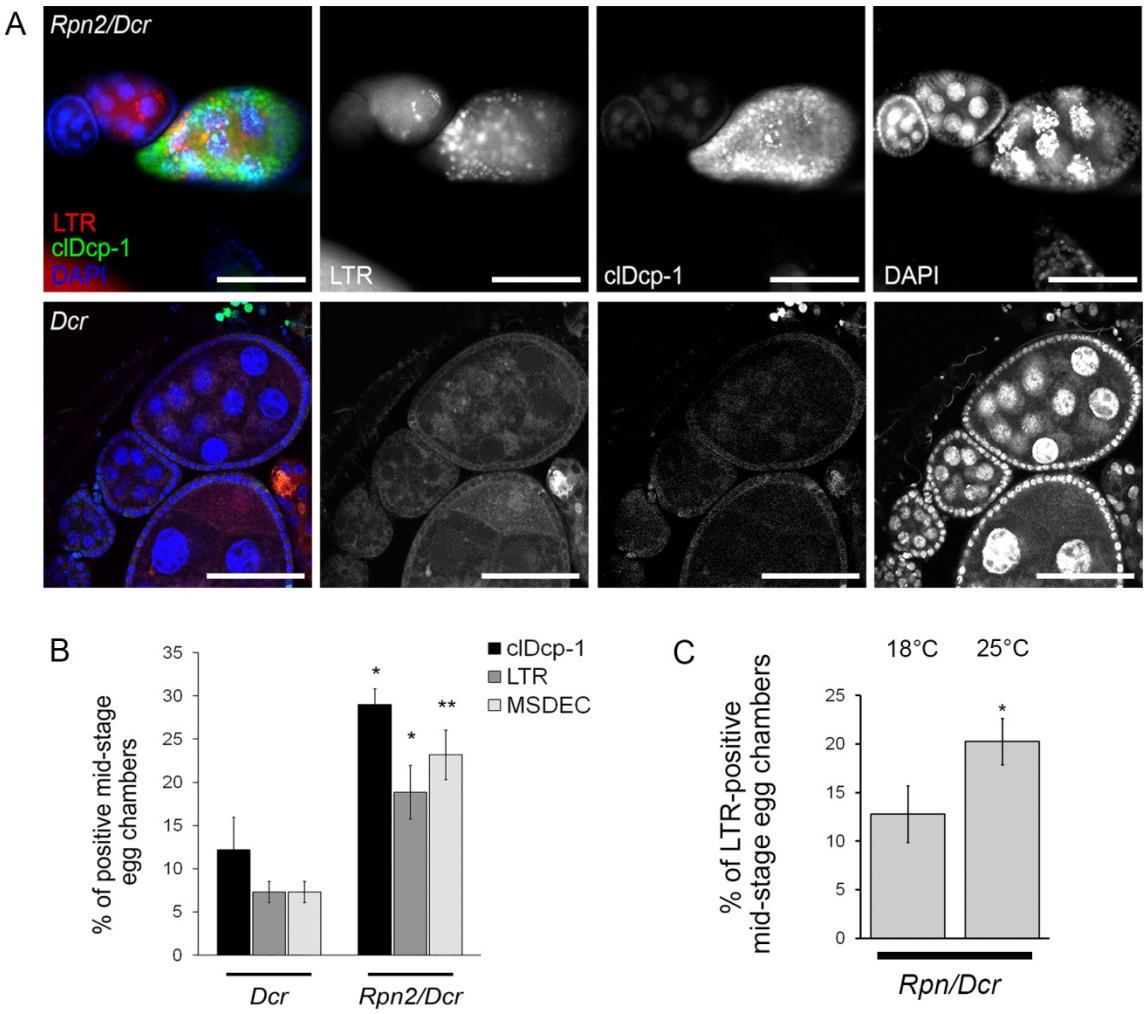

Figure 3-12 Proteasomal subunit loss results in Dcp-1-dependent compensatory autophagy

(**A**,**B**) Females were collected from flies with the UAS maternal driver kept at 25°C with the genotypes *UAspDcr2/+;* nosGAL4/+ (*Dcr*) and *Rpn2-RNAI/UAspDcr2;nosGAL4*/+ (*Rpn2/Dcr*). (**A**) Representative images of MSECs from *Rpn2/Dcr* and *Dcr* kept at 25°C. Ovaries were imaged with clDcp-1 antibody, LTR and DAPI; scale bars = 50µm. (**B**) MSECS from *Dcr* and *Rpn2/Dcr* flies were scored for cleaved Dcp-1 (clDcp-1), LTR and DAPI. The graph represents the average percentage of MSECs that scored positive for LTR, MSDEC or clDcp-1. Experiments were performed with at least eight females per genotype (n=3). Error bars represent ± S.E.M. and statistical significance was determined using two-way Student's *t* test, *p<0.05, **p<0.01 (**C**) MSECS in *Rpn2/Dcr* flies were scored for LTR positivity at 18°C and 25°C. At least 50 MSECS were analyzed per temperature (n=4). Error bars represent ± S.E.M. and statistical significance was determined using two-way Student's *t* test, *p<0.05.

3.9. Discussion

I assisted with the identification of 13 putative negative autophagy regulators that could be involved in Dcp-1-mediated autophagy via a RNAi flow cytometry screen and RFP-GFP-Atg8a microscopy assay. Of those interactors, I further characterized the role of Hsp83 and found that it negatively regulates autophagy and cell death in *Drosophila in vivo* and *in vitro*. Loss of Hsp83 function led to a decrease in proteasomal activity and an increase in Dcp-1 that was not transcriptionally regulated. Analysis of proteasome-compromised flies also showed an increase in levels of Dcp-1 and LTR staining supporting that Dcp-1 is regulated by the proteasome. The Dcp-1 observed in *Hsp83* mutants was found to be required for the ensuing compensatory autophagy, and contributed to both female fertility and development to adulthood. These findings highlight a novel role for Hsp83 in the proteasome-dependent regulation of pro-Dcp-1 that functions normally to prevent accumulation of Dcp-1 and the subsequent activation of autohpagy (Figure 3-13).

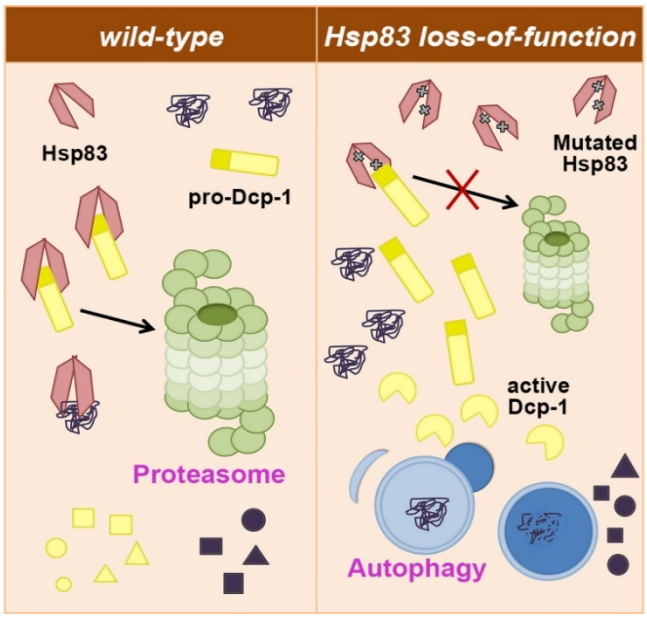

Figure 3-13 Proposed model in wild-type and loss-of-function *Hsp83* backgrounds

In a wild-type cell, we propose that Hsp83 promotes proteasomal activity. With an active proteasome, Dcp-1 and other proteins are regulated properly and proteostasis is maintained. Alternatively, in a cell with dysfunctional Hsp83 or a lack of Hsp83, the proteasome is less active which allows an accumulation of Dcp-1. The elevated levels of Dcp-1 induce compensatory autophagy as an alternative pathway to degrade proteins in an attempt to maintain proteostasis.

3.9.1. Putative Dcp-1 interactors identified

It is possible that the eleven additional proteins identified in the IP-MS study may also positively or negatively regulate autophagy, but due to potential incomplete knockdown by RNAi or functional redundancy, they did not show an effect on autophagy. It would be valuable to complete *in vivo* studies to validate the remaining genes identified in the RNAi screen for their autophagy-regulatory role during *Drosophila* oogenesis or in other tissues. Additionally, identification of potential Dcp-1 cleavage substrates specifically could be worthwhile as it was found that Dcp-1 catalytic activity is required to activate autophagy (DeVorkin et al., 2014).

3.9.2. pro-Dcp-1 levels are regulated by the proteasome

Caspases require constitutive regulation to prevent unwanted activation and cell death. Inhibitor of apoptosis proteins (IAPs) are one way caspases can be regulated, acting either through baculovirus inhibitor of apoptosis protein repeat (BIR) domain binding or E2/E3 ubiquitin ligase activity which can be degradative or non-degradative (Vaux and Silke, 2005). While the active (cleaved) form of Dcp-1 was shown previously to be regulated by Diap1 through non-degradative ubiquitylation (Ditzel et al., 2008), it was unknown how or if the zymogen form of Dcp-1 is regulated. We found that the elevated levels of pro-Dcp-1 in *Hsp83* mutants neither correspond to Diap1 levels nor to transcript levels. Instead, we found that pro-Dcp-1 levels were elevated following the loss of function of Hsp83, two different proteasomal subunits or pharmacological inhibition of the proteasome. While other *Drosophila* caspases Drice and Dronc were found not to be stabilized by proteasome inhibition (Ditzel et al., 2008; Lee et al., 2011, 2016), there is precedence for proteasome regulation of the cleaved form, but not the pro-form, of caspases 8 and 3 in human cell lines (Fiandalo et al., 2013; Suzuki et al., 2001b). Based on previous protein interaction studies that showed Hsp83 only interacts with the pro-form of Dcp1, I propose a model where Hsp83 acts at a relatively early stage, prior to Diap1, to regulate levels of pro-Dcp-1 via the proteasome in basal conditions. Functional loss of Hsp83 results in elevated pro-Dcp-1 that is available for the subsequent cleavage into active Dcp-1 and the induction of autophagy. Further studies are required to determine if pro-Dcp-1 itself is being directly processed by the proteasome or is instead indirectly

regulated by the proteasome through as of yet unknown molecular components. Another outstanding question is the threshold of Dcp-1 required for autophagy induction.

3.9.3. Hsp83 mediates proteasomal degradation.

It was shown previously that Hsp83 plays a role in promoting protein degradation involving a degradative complex function. Loss of Hsp83 led to a build-up of proteins targeted for degradation in the cell cycle due to inhibition of the anaphase-promoting complex/cyclosome (Bandura et al., 2013). In a *Drosophila* neurodegenerative disease model, Hsp83 was required for targeting the mutant protein $TPI^{sugarkill}$ for proteasomal degradation (Hrizo and Palladino, 2010), and, similarly, the human homolog HSP90 was required for the delivery of substrates to the proteasome (Oura et al., 2011). While proteasomal activity was further decreased in *Hsp83* transhets treated with MG132, the level of pro-Dcp-1 was not further increased, suggesting that Hsp83 specifically is a rate limiting step in the proteasomal processing that regulates pro-Dcp-1. Since Hsp83 and pro-Dcp-1 could have been immunoprecipitated in a complex involving the proteasome, further work is required to understand if pro-Dcp-1 requires Hsp83 for delivery or targeting to the proteasome or if Hsp83 might play a more direct role at the proteasome to facilitate degradation of pro-Dcp-1.

3.9.4. Dcp-1 regulates compensatory autophagy.

Proteostasis requires a balance between the two major degradative UPS and autophagy pathways. When proteasome activity is inhibited, as is the case in *Hsp83* mutants, there is increased autophagic flux known as compensatory autophagy (Lilienbaum, 2013). Previous to this study, Dcp-1 was reported to be a positive regulator of autophagy only in the context of starvation although overexpression was also shown to induce autophagy (DeVorkin et al., 2014; Hou et al., 2008; Kim et al., 2010).Here, we observed a Dcp-1 dependent increase in the number of autolysosomes or lysosomal staining with loss of Hsp83 or Rpn11, and thus reduced proteasomal activity, even in nutrient-rich conditions. In fly models compensatory autophagy was shown to occur when the UPS is inhibited (Hartl et al., 2011; Pandey et al., 2007), but this is the first time an effector caspase has been reported to be involved. The discovery that Dcp-1 is required

for compensatory autophagy when proteasomal activity is compromised begs further exploration into whether there are other forms of stresses or contexts, such as hypoxia, that also rely on Dcp-1 for autophagy induction.

3.9.5. Hsp83;Dcp-1 double mutants have effects on cell death, cell division, autophagy, fertility and development.

Loss of Dcp-1 prevents the autophagy that is otherwise induced in loss-of-function *Hsp83* mutants, indicating a Dcp-1-dependent role in the regulation of autophagy in this context. In addition to autophagy dysregulation, double *Dcp-1;Hsp83* mutants had other surprising phenotypes involving cell death and division. *Dcp-1;Hsp83* flies had an abnormal number of persisting nurse cell nuclei that showed partial condensation and stained positively for TUNEL. This suggests that the cell death associated with Hsp83 loss is Dcp-1-independent and that Dcp-1 contributes at least partially to the pyknosis observed. The double mutants also rendered females sterile and did not rescue the male sterility observed in *Hsp83* mutants, indicating an increasingly impaired phenotype. Furthermore, there was an increase in animals with developmental defects as more *Hsp83/Dcp-1* flies died in the pharate adult stage. This divergence between control of cell death and autophagy with Dcp-1 and Hsp83 is a unique and surprising finding. Discovery of this relationship provides a potential avenue for further understanding the complex cross-talk between autophagy and apoptosis, as well as for exploitation of promoting cell death without autophagy by counterintuitively targeting an effector caspase in the presence of Hsp83/HSP90 genetic or pharmacologic inhibition.

Chapter 4. Hsp60 controls autophagic response to nutrient deprivation by altering subcellular localization of caspase-3.

Adapted and expanded from: Courtney Choutka, Nancy Erro Go, and Sharon M. Gorski. “Hsp60 controls autophagic response to nutrient deprivation by altering subcellular localization of caspase-3.” *Manuscript in preparation.*

I conceived, designed, and conducted all experiments as well as prepared the manuscript in collaboration with SG. NG constructed the RFP-GFP-LC3 stable cell lines.

4.1. Abstract

The cell survival process of autophagy and cell death program of apoptosis have a complex relationship with several points of intersection. For example, caspases were found in many different contexts to either inhibit or promote autophagic flux. One area not yet explored is the role of effector caspases in starvation-induced autophagy in the context of human cells. Based on previous findings in *Drosophila,* here I identify a functionally conserved role for caspase-3 in the activation of starvation-induced autophagy in human cells. I also show that caspase-3 translocation between the mitochondria and the cytosol is controlled by Heat-shock protein 60 in response to nutritional status. My results highlight a novel function for caspase-3 in starvation-induced autophagy in humans and illustrate how this response is regulated by subcellular localization.

4.2. Introduction

It is becoming increasingly clear that while cellular caspases are traditionally associated with apoptosis, they have important roles in many other cellular processes such as immunity, cell proliferation, differentiation, tumour suppression, development and aging (Kuranaga and Miura, 2007; Launay et al., 2005; Shalini et al., 2015). One of the complex relationships emerging is a role for caspases in the cross-talk between autophagy and apoptosis.

Caspases were found to both promote and inhibit autophagic flux. The initiator caspases, caspase-2, caspase-8, caspase-9, and caspase-10 have been largely identified as suppressors of autophagy (Bell et al., 2008; Cho et al., 2009; Oral et al., 2012; Tiwari et al., 2011, 2014; You et al., 2013) although caspase-9 was shown to increase autophagy by enhancing the priming and lipidation of the key autophagy protein light-chain 3B/LC3B through formation of a complex with autophagy protein ATG7 (Han et al., 2014; Jeong et al., 2011). Similarily, the effector caspases, caspase-3, caspase-6, and caspase-7, have been linked to suppression of autophagy (Cho et al., 2009; Norman et al., 2010; Pagliarini et al., 2012; Sirois et al., 2012; Wirawan et al., 2010; You et al., 2013). In contrast, it was suggested that caspase-3 could upregulate autophagy by cleavage and subsequent activation of ATG4D (Betin and Lane, 2009). While *in vitro* cleavage of autophagy proteins by effector caspases was shown in human cells in response to cell death stimuli, there is very little known about caspase regulation of autophagy in other cellular contexts. Our previous discovery in *Drosophila* of an effector caspase Dcp-1 responsible for upregulation of autophagy under nutrient deprivation (DeVorkin et al., 2014; Hou et al., 2008) led us to investigate whether this functional relationship is conserved amongst higher eukaryotes.

Here I investigate the potential evolutionary conservation of a caspase-activated autophagic response in human cells. I report that caspase-3 (CASP3) is required for the upregulation of autophagic flux in response to nutrient deprivation in several human tissue culture cell lines. I further characterize how CASP3 is regulated in response to starvation, and show that its subcellular localization and activation state are affected by the molecular chaperone heat-shock protein 60 (HSP60).

4.3. CASP3 partially localizes to the mitochondria and is required for starvation-induced autophagy

The mitochondrial localization and autophagy-activating role of *Drosophila* effector caspase Dcp-1 (DeVorkin et al., 2014; Hou et al., 2008) were used as the basis to screen for functional conservation of caspases in human cells. I initially screened the initiator caspases, CASP8 and CASP9, and the effector caspases, CASP3, CASP6 and CASP7, to determine if they partially localized to the mitochondria using the human breast cancer

line SKBR3. Both CASP8 and CASP9 had undetectable levels in mitochondrial fractions (*data not shown*) but CASP3, CASP6 and CASP7 appeared to at least partially localize to mitochondria. A mitochondrial fractionation and Proteinase K assay was performed to determine if the zymogen form of any of these effector caspases localized inside of mitochondria, similar to previous observations of the zymogen pro-Dcp-1. The Proteinase K assay revealed that only the CASP3 zymogen partially localized inside of mitochondria (Figure 4-1A) whereas the degradation of CASP6 and CASP7 indicated that they primarily associated with the outer mitochondrial membrane in these conditions (Figure 4-1B,C).

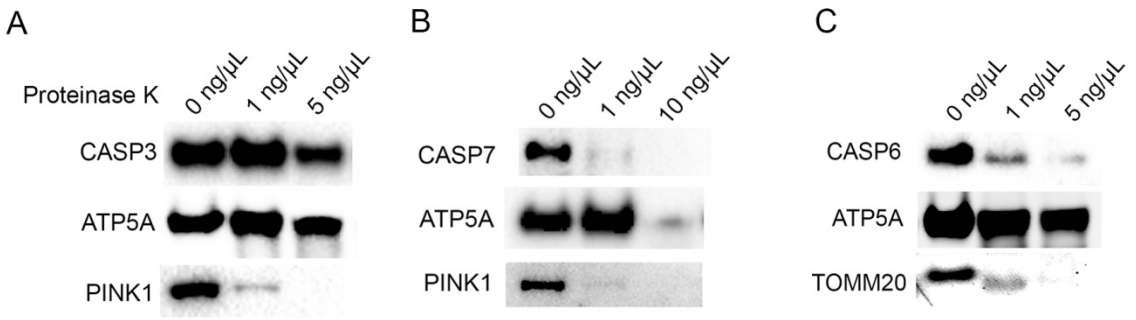

Figure 4-1 CASP3 partially localizes inside of mitochondria in SKBR3 cells while CASP6 and CASP7 do not

(**A**-**C**) Representative western blot images of mitochondrial-enriched fractions treated with increasing concentrations of Proteinase K showing immunodetection of (**A**) CASP3 (32kDa), (**B**) CASP7 (35kDa) or (**C**) CASP6 (35kDa). ATP5A (53 kDa) is an inner mitochondrial protein control while PINK1 (63kDa) and TOMM20 (16kDa) are outer mitochondrial protein controls. (n=3).

Next, to determine if CASP3 was involved in the induction of starvation-induced autophagy, I utilized the common autophagy protein marker LC3B for two flux assays. First, I depleted CASP3 levels using siRNA knockdown and subjected mRFP-eGFP-LC3B expressing SKBR3 cells to total starvation for two hours. I analyzed the average number of autolysosomes per cell following treatment with the siRNA control or the three distinct CASP3 siRNAs and found that cells with reduced CASP3 were significantly impaired in their autophagic response to starvation ($p<0.001$) (Figure 4-2A,B). As an additional autophagy assay, SKBR3 cells were subjected to complete starvation or nutritient-rich condtions and treated with Bafilomycin A, a compound that blocks autophagic flux by preventing acidification of the lysosomes, to analyze levels of autophagy induction by

comparing LC3B lipidation states. Under starvation conditions, cells treated with CASP3 siRNAs failed to accumulate the lipidated form of LC3B, LC3BII, when compared to the scramble control (Figure 4-2,D). These observations together support that CASP3 loss results in a block in autophagy at an early step in the pathway.

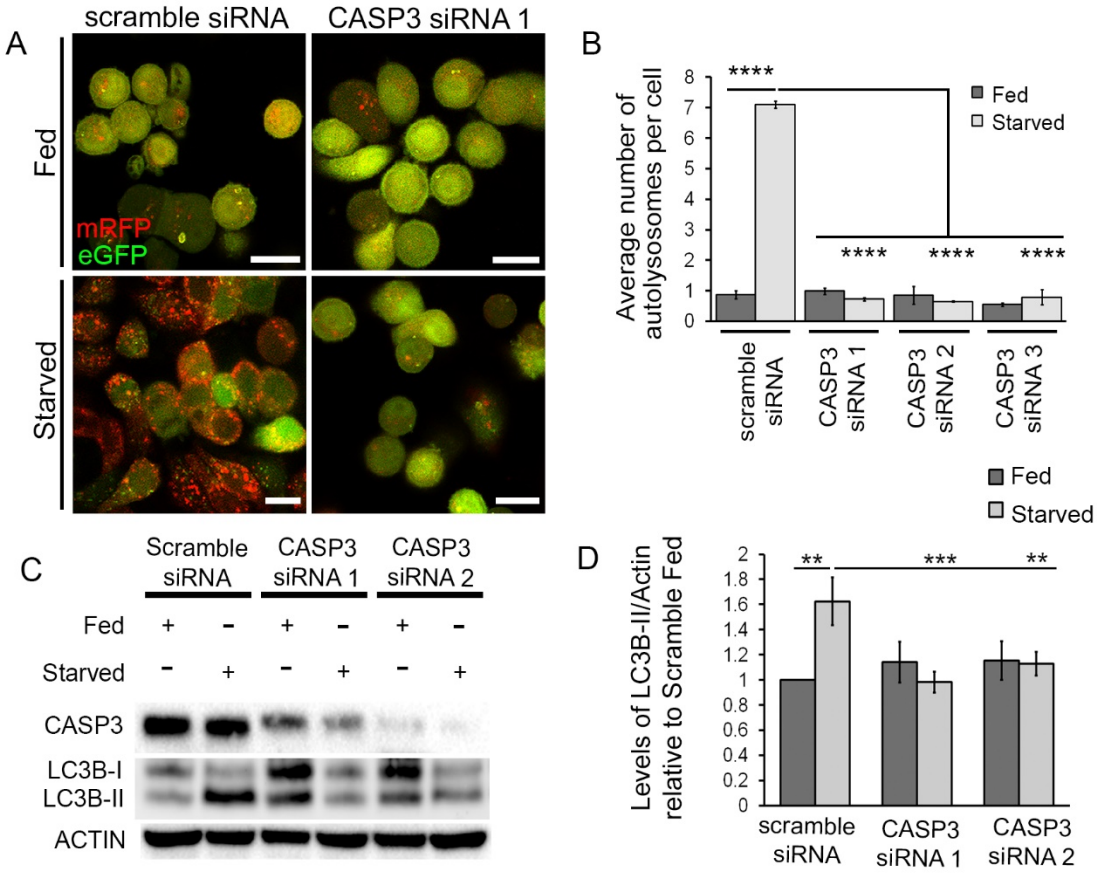

Figure 4-2 CASP3 is required for starvation-induced autophagy in SKBR3 cells

(**A**,**B**) mRFP-eGFP-LC3B expressing SKBR3 cells were subjected to control scramble or CASP3 siRNA in fed and starved conditions. (**A**) Representative images, scale bars = 20μM (**B**) Quantification of average number of autolysosomes per cell for control scramble siRNA and three CASP3 siRNA constructs. At least 50 cells were counted per treatment and error bars represent the mean ± S.E.M; statistical significance was determined using one-way ANOVA with a Bonferroni post-test, ****p<0.0001 (n=4). (**C**,**D**) SKBR3 cells were treated with scramble or CASP3 siRNA, cultured in fed or starved conditions and incubated with Baf for 2 hours. (**C**) A representative blot with CASP3 (32kDa), LC3BI/LC3BII (19kDa, 17kDa), ACTIN (42kDa). (**D**) Levels of LC3B-II normalized to ACTIN and shown relative to the scramble Fed control. Error bars represent the mean ± S.E.M; statistical significance was determined using one-way ANOVA with a Bonferroni post-test, **p<0.01, ***p<0.001 (n=3).

4.4. CASP3-mediated autophagy response to nutrient deprivation is context dependent

Four human cell lines in addition to SKBR-3 were screened for their ability to induce CASP3-regulated autophagy in response to nutrient deprivation: human embryonic kidney line HEK293, human triple-negative breast adenocarcinoma line MDA-MB-231, pancreatic ductal epitheliod carcinoma line PANC1, and lung squamous cell carcinoma line NCI-H2170. All of these lines were transfected to stably express mRFP-eGFP-LC3B and treated with control and CASP3 siRNAs in fed and nutrient-deprived conditions to determine autophagic flux. MDA-MB-231 cells had a higher level of basal autophagic flux compared to SKBR3 cells, yet MDA-MB-231 cells treated with CASP3 siRNA similarily failed to induce increased autolysosomes in response to starvation as observed in control siRNA-treated MDA-MB-231 cells (Figure 4-3). PANC1 cells had the highest levels of basal autophagy in nutrient-rich conditions, but similar to MDA-MB-231, failed to further upregulate autophagic flux in response to nutrient deprived conditions when CASP3 was depleted (Figure 4-4). NCI-H2170 also failed to induce a signficant increase in autolysosomes, compared to the siRNA control, when CASP3 was depleted in starvation conditions, although the CASP3-depleted starved cells still appeared to show a modest but not statistically significant increase in autolysosome number compared to the CASP3-depleted fed cells (Figure 4-5). HEK293 displayed a contrasting response in comparison to the other four lines. There was no decrease of autophagic flux in response to starvation in the context of CASP3 knockdown and one CASP siRNA construct intensified the autophagic response (Figure 4-6). These results together indicate that CASP3 is required for the upregulation of autophagy in response to nutrient deprivation in some contexts, but does not have a significant effect on the levels of basal autophagy in fed conditions. These findings also indicate that CASP3 regulation of autophagy in response to starvation does not occur in every tissue or context.

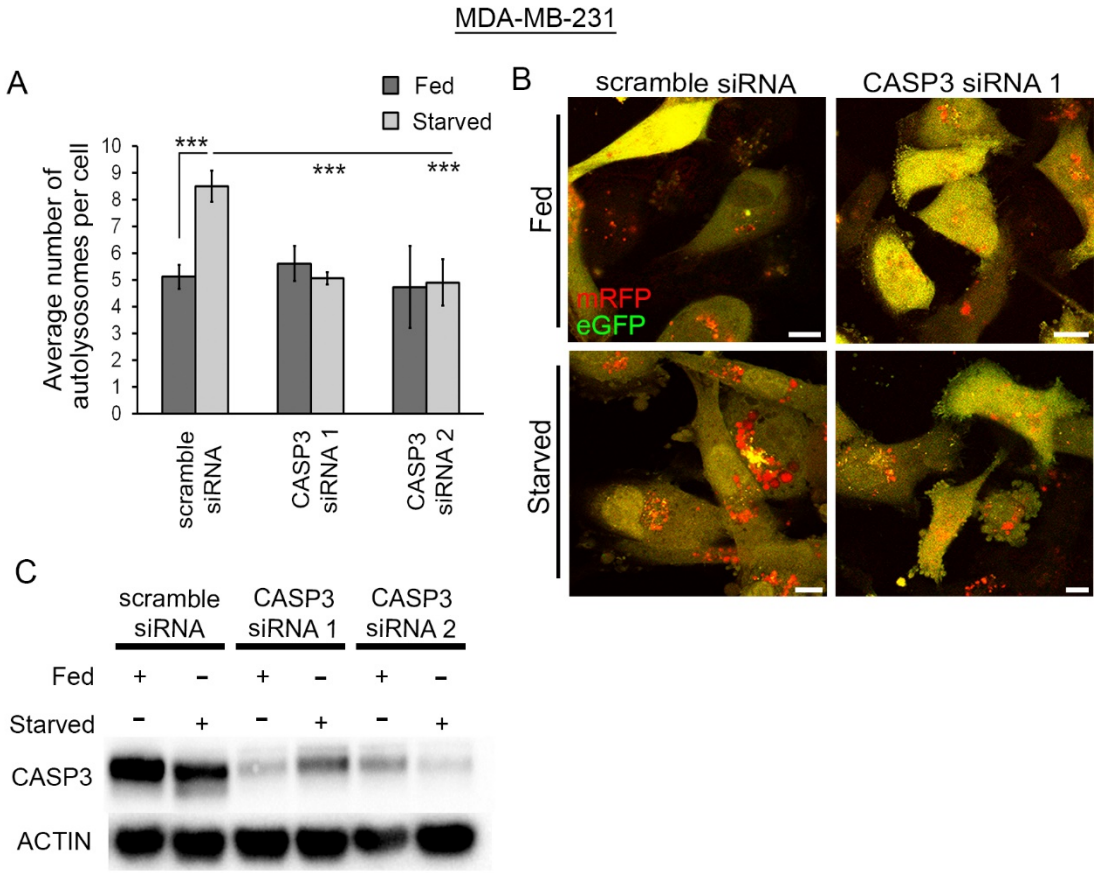

Figure 4-3 CASP3 knockdown effects on starvation induced autophagy in MDA-MB-231 cells

MDA-MB-231 cells stably expessing mRFP-eGFP-LC3B were treated with scramble or CASP3 siRNAs in fed and starved conditions. (**A**) Quantification of average number of autolysosomes per cell for control scramble siRNA and two CASP3 siRNA constructs. At least 50 cells were counted per treatment and error bars represent the mean ± S.E.M; statistical significance was determined using one-way ANOVA with a Bonferroni post-test, ***p<0.001.(**B**) Representative images, scale bars = 10μM. (**C**) Representative blot of CASP3 siRNA efficacy with CASP3 (32kDa) and ACTIN (42kDa).

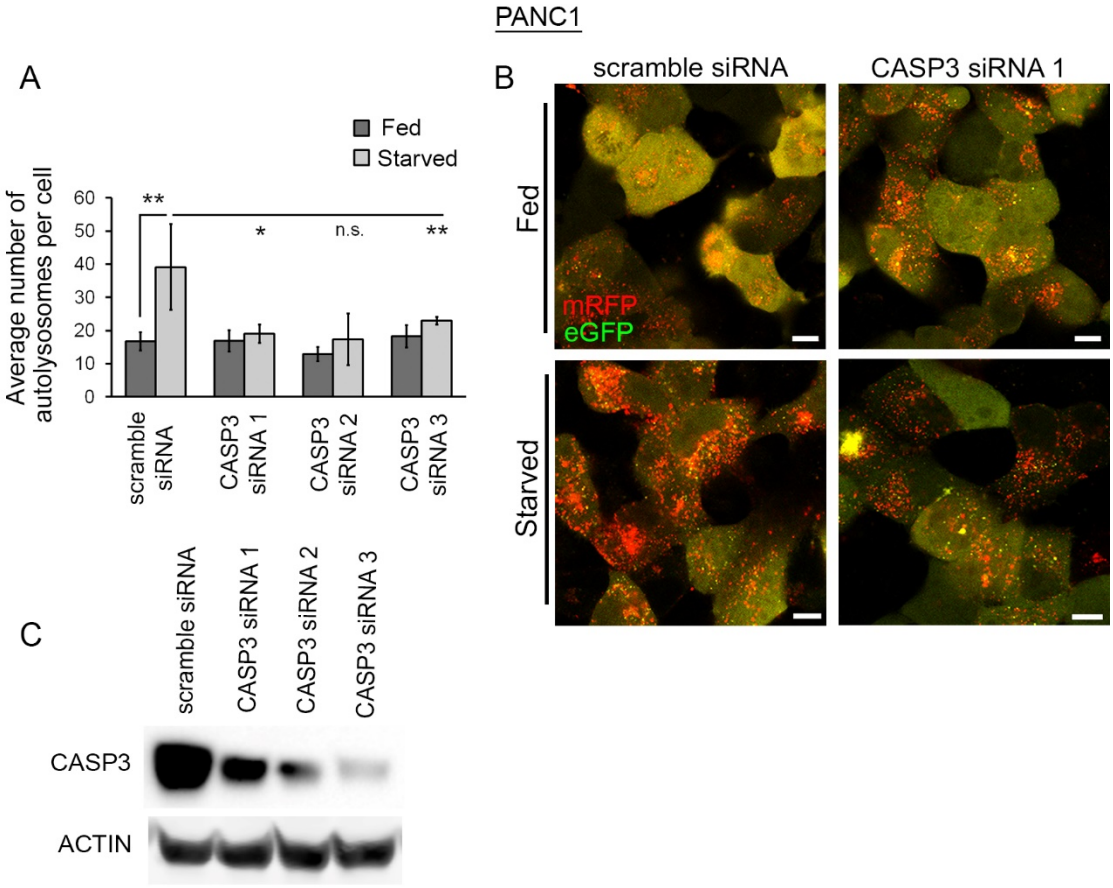

Figure 4-4 CASP3 knockdown effects on starvation induced autophagy in PANC1 cells

PANC1 cells stably expessing mRFP-eGFP-LC3B were treated with scramble or CASP3 siRNAs in fed and starved conditions. (A) Quantification of average number of autolysosomes per cell for control scramble siRNA and three CASP3 siRNA constructs. At least 50 cells were counted per treatment and error bars represent the mean ± S.E.M; statistical significance was determined using one-way ANOVA with a Bonferroni post-test, n.s. $p \geq 0.05$, *$p < 0.05$, **$p < 0.01$ (B) Representative images, scale bars = 10μM. (C) Representative blot of CASP3 siRNA efficacy with CASP3 (32kDa) and ACTIN (42kDa).

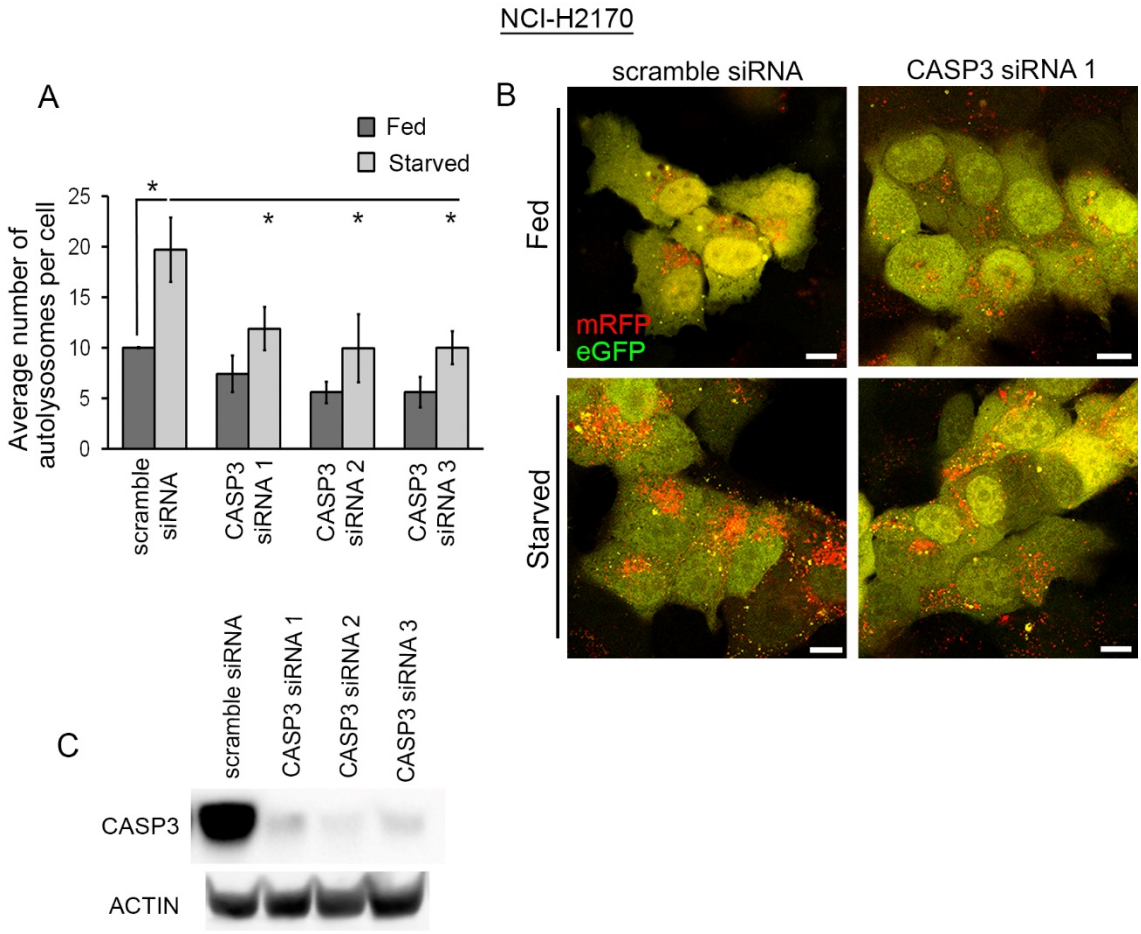

Figure 4-5 CASP3 knockdown effects on starvation induced autophagy in NCI-H2170 cells

NCI-H2170 cells stably expessing mRFP-eGFP-LC3B were treated with scramble or CASP3 siRNAs in fed and starved conditions. (A) Quantification of average number of autolysosomes per cell for control scramble siRNA and three CASP3 siRNA constructs. At least 50 cells were counted per treatment and error bars represent the mean ± S.E.M; statistical significance was determined using one-way ANOVA with a Bonferroni post-test, *$p<0.05$ (B) Representative images, scale bars = 10μM. (C) Representative blot of CASP3 siRNA efficacy with CASP3 (32kDa) and ACTIN (42kDa).

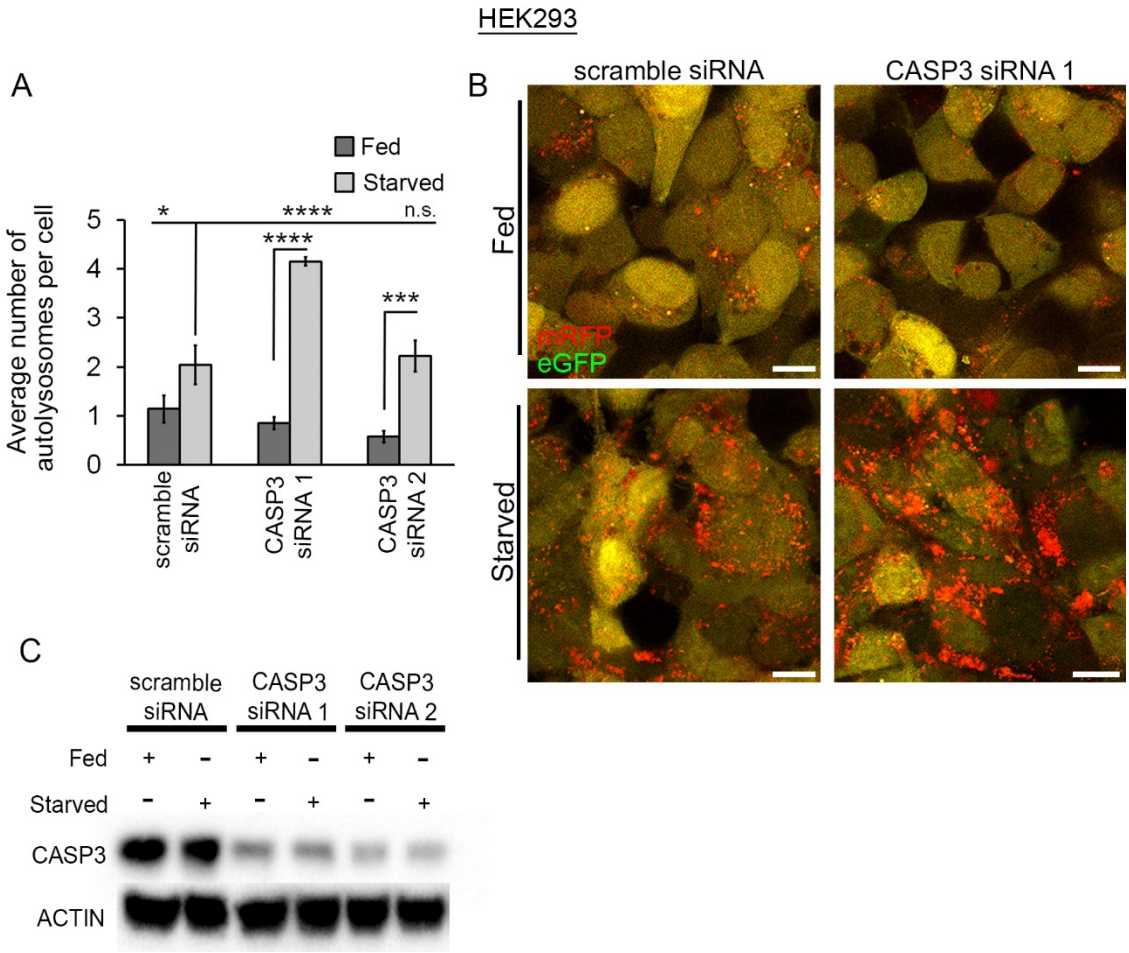

Figure 4-6 CASP3 knockdown effects on starvation induced autophagy in HEK293 cells

HEK293 cells stably expessing mRFP-eGFP-LC3B were treated with scramble or CASP3 siRNAs in fed and starved conditions. (A) Quantification of average number of autolysosomes per cell for control scramble siRNA and two CASP3 siRNA constructs. At least 50 cells were counted per treatment and error bars represent the mean ± S.E.M; statistical significance was determined using one-way ANOVA with a Bonferroni post-test, n.s. p≥0.05, *p<0.05, ***p<0.001, ****p<0.0001 (B) Representative images, scale bars = 10μM. (C) Representative blot of CASP3 siRNA efficacy with CASP3 (32kDa) and ACTIN (42kDa).

4.5. HSP60 associates with CASP3 in starvation conditions

I used the *Drosophila* Dcp-1 IP-MS experiment data that identified interacting proteins (Table 1.1) to choose three human homologs to characterize as candidate CASP3 interactors. All three proteins are classically associated with the mitochondria and were identified as putative negative regulators of autophagy (Figure 3-1). The first was adenine nucleotide translocase 2/ANT2, which is the closest human isoform, based on protein sequence identity (83%) to the *Drosophila* adenine nucleotide translocase SesB, and is located in the inner mitochondrial membrane. This translocase was found to function downstream of Dcp-1 in autophagy regulation (DeVorkin et al., 2014). Heat-shock protein Hsp83, which partially localizes to mitochondria, was described in the previous chapter to be a negative regulator of autophagy and involved in the regulation of pro-Dcp-1, so I investigated its human homolog heat-shock protein 90 alpha/HSP90AA1 (protein sequence identity 78%). Lastly, I examined HSP60/heat-shock protein 60, the human homolog to *Drosophila* Hsp60. Hsp60 is a predominantly mitochondrial chaperone that was also identified as a putative negative regulator of autophagy in *Drosophila* (Figure 3-1). To determine if any of these three proteins interacted with CASP3, I performed an immunoprecipitation (IP) experiment to isolate CASP3 and its interactors from SKBR3 cells exposed to two hours of complete starvation. HSP90AA1 was detectable in the whole cell lysates but not in the CASP3 immunoprecipitate. ANT2 was faintly detectable in the whole cell lysates but not in the CASP3 immunoprecipitate, while HSP60 was clearly detectable in both the whole cell lysates and the CASP3 immunoprecipitate. This result suggests that there is an interaction between the CASP3 and HSP60 proteins under these conditions (Figure 4-7A). To confirm the interaction, I performed a reciprocal IP using an HSP60 antibody in starvation conditions. CASP3 was identified in both the whole cell lysates and in the HSP60 pull-down, confirming the interaction between HSP60 and CASP3 (Figure 4-7B).

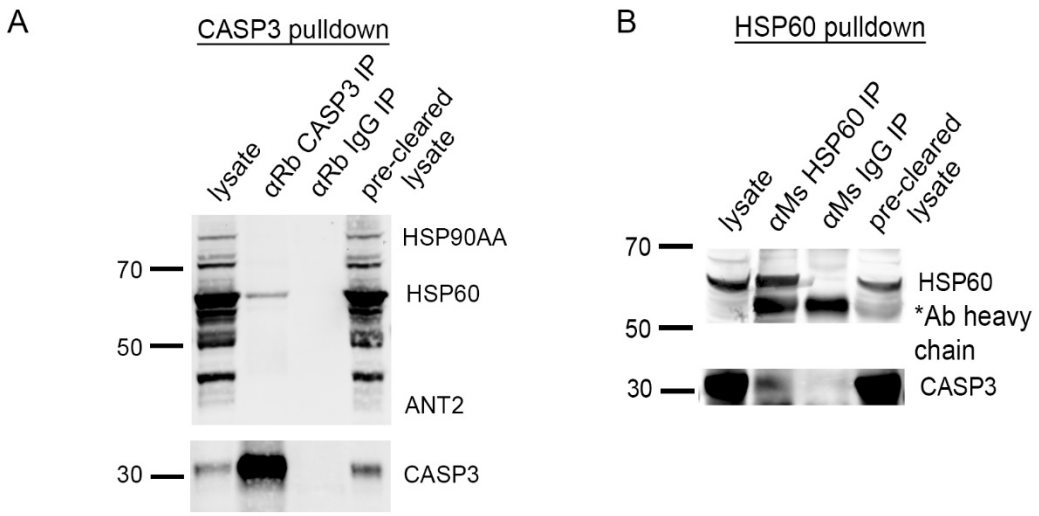

Figure 4-7 HSP60 interacts with CASP3 in starvation conditions in SKBR3 cells

(**A**) Representative blot from SKBR3 cells subjected to starvation conditions and then incubated with either αRb-CASP3 antibody or control αRb-IgG antibody. Pre-cleared lysate (right) is the original lysate (left) after incubation with Sepharose 4B Beads and before being incubated with antibodies. Proteins probed include CASP3 (32kDa), ANT2 (37kDa) HSP60 (60kDa), and HSP90AA (90kDa) (n=2). (**B**) Representative blot from SKBR3 cells subjected to starvation conditions and then incubated with either αMsHSP60 antibody or control αMsIgG antibody. Pre-cleared lysate (right) is the original lysate (left) after incubation with Sepharose 4B Beads and before being incubated with antibodies. Proteins probed include CASP3 (32kDa) and HSP60 (60kDa) *heavy chain of the antibody detected (n=2).

4.6. HSP60 is a negative regulator of autophagy and maintains levels of pro-CASP3

HSP60 was knocked down in mRFP-eGFP-LC3B expressing SKBR3 cells to determine its effects on autophagic flux. HSP60 knockdown resulted in an increase in autolysosomes in cells under fed conditions in comparison to the siRNA control which had typical low levels of autophagic flux (Figure 4-8A,B). There was no further increase in the number of autolysosomes per cell in starved HSP60 knockdown compared to starved scramble siRNA control cells, indicating autophagic flux levels could be saturated. To confirm this finding, a western blot based flux assay in the presense of Bafilomycin A1 was performed. LC3B-II accumulated in HSP60 knockdown cells even in fed conditions in comparison to the scramble control siRNA cells (Figure 4-8C,D). Both LC3B assays indicate an increase in autophagy upon HSP60 knockdown in SKBR3 cells under fed conditions. Next, we tested whether HSP60 acts to control the levels of pro-CASP3. Knockdown of HSP60 resulted in decreased levels of pro-CASP3 (Figure 4-8E,F), supporting that HSP60 is needed to sustain the levels of pro-CASP3 in the cell.

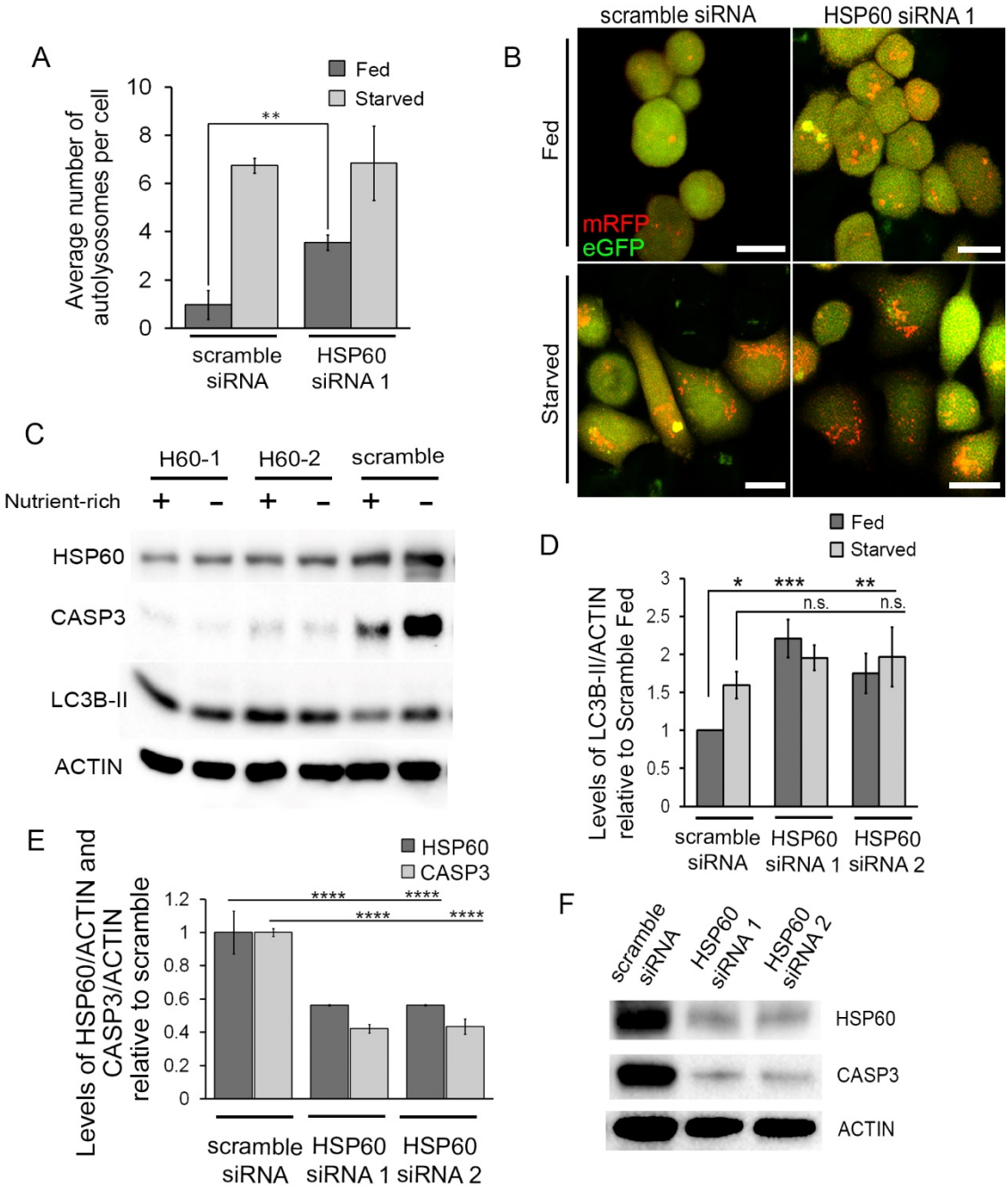

Figure 4-8 HSP60 negatively regulates autophagy and maintains pro-CASP3 levels in SKBR3 cells

Figure 4-8 (figure legend continued from previous page)
(**A**,**B**) HSP60 was knocked down in mRFP-eGFP-LC3B expressing SKBR3 cells in fed and starved conditions. (**A**) Autolysosomes were quantified per cell with at least 50 cells counted per treatment and error bars represent the mean ± S.E.M; statistical significance was determined using a using a two-tailed Student's *t* test, **p<0.01 (n=3) (**B**) Respresentative images, scale bar = 20μm. (**C**,**D**) SKBR3 cells were treated with two HSP60 siRNA constructs and one scramble siRNA in fed and starved conditions and all treated with Baf (**C**) A representative blot of LC3B-II (17kDa), ACTIN (42kDa), CASP3 (32kDa) and HSP60 (60kDa) (**D**) Levels of LC3B-II normalized to ACTIN and shown relative to the scramble Fed control. Error bars represent the mean ± S.E.M; statistical significance was determined using one-way ANOVA with a Bonferroni post-test, n.s. p≥0.05, *p<0.05, **p<0.01, ***p<0.001 (n=3). (**E**,**F**) SKBR3 cells were treated with two HSP60 siRNA constructs and then assessed for levels of HSP60 and CASP3 relative to ACTIN. (**E**) Levels of HSP60 and CASP3 quantified and normalized to ACTIN. Error bars represent the mean ± S.E.M; statistical significance was determined using a using a two-tailed Student's *t* test, ****p<0.0001 (n=4). (**F**) A representative blot with ACTIN (42kDa), CASP3 (32kDa) and HSP60 (60kDa).

4.7. HSP60 depletion requires CASP3 for the increase in autophagy observed and results in an increase in cleaved CASP3.

To determine if HSP60 acts downstream or upstream of CASP3 in autophagy regulation I performed an epistasis analysis by knocking down both HSP60 and CASP3 to observe the effects on autophagic flux in mRFP-eGFP-LC3B expressing SKBR3 cells. The cells treated with both CASP3 and HSP60 siRNAs had similar levels of autophagy to the CASP3 knockdown alone in both fed and starved conditions, indicating that CASP3 acts downstream of HSP60 to increase autophagy (Figure 4-9A,B). Since pro-CASP3 levels were reduced when CASP3-dependent autophagy was increased in response to HSP60 knockdown (Figure 4-8C,E,F), I suspected that there was a concomitant increase in the cleaved form of CASP3 (cl-CASP3). To test this, I ran a high percentage gel with three times the amount of protein to enable detection of the cleaved fragment. Following HSP60 knockdown, I observed an increase in cl-CASP3 that coincided with the decrease in pro-CASP3 and HSP60 (Figure 4-9C,D).

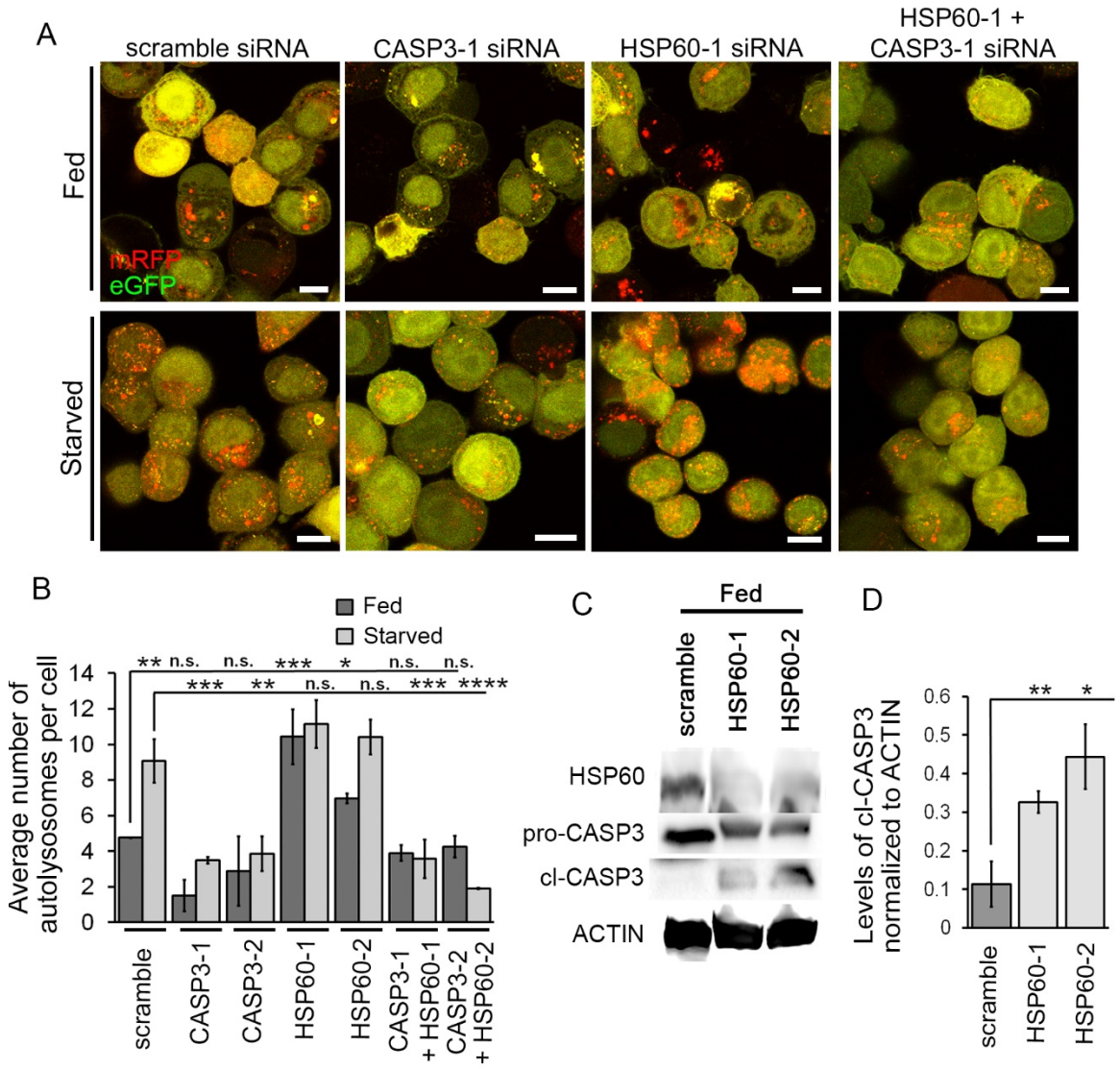

Figure 4-9 HSP60 knockdown causes a CASP3-dependent increase in autophagy and increased levels of cl-CASP3 in SKBR3 cells

(**A**,**B**) SKBR3 cells expressing mRFP-eGFP-LC3B treated with scramble, CASP3, HSP60 or HSP60 and CASP3 siRNAs in fed and starved conditions. (**A**) Representatives images, scale bars = 10μm (**B**) Autolysosome quantification per cell for each treatment. At least 50 cells were counted per treatment and error bars represent the mean ± S.E.M; statistical significance was determined using one-way ANOVA with a Bonferroni post-test, n.s. p≥0.05, *p<0.05, **p<0.01, ***p<0.001, ****p<0.0001 (n=3). (**C,D**) SKBR3 cells were treated with one of two different HSP60 siRNA constructs or a scramble siRNA control. (**C**) A representative blot probed for ACTIN (42kDa), proCASP3 (32kDa), cl-CASP3 (20kDa) and HSP60 (60kDa) (n=3). (**D**) Levels of cl-CASP3 normalized to ACTIN. Error bars represent the mean ± S.E.M; statistical significance was determined using a two-tailed Student's *t* test, *p<0.05, **p<0.01 (n=3).

4.8. HSP60 and nutrient levels control subcellular localization of CASP3

Mitochondrial fractionation following HSP60 knockdown revealed that pro-CASP3 levels were reduced in the cytosol and the mitochondria upon HSP60 siRNA treatment (Figure 4-10A). Additionally, cleaved CASP3 was enhanced in the cytosol (Figure 4-10A), indicating that HSP60 might control CASP3 activation through subcellular localization. Since HSP60 was previously implicated in mitochondrial transport and subcellular localization of CASP3 during cell death (Samali et al., 1999; Xanthoudakis et al., 1999), I hypothesized that HSP60 was responsible for the subcellular localization and subsequent activation of CASP3 during starvation. Cells were fractionated into mitochondrial and cytosolic fractions following exposure to nutrient deprivation at different time intervals to analyse levels of HSP60, pro-CASP3 and cleaved CASP3. Levels of HSP60, pro-CASP3 and cleaved CASP3 all increased in the cytosol with increasing timed exposures to starvation conditions (Figure 4-10B).

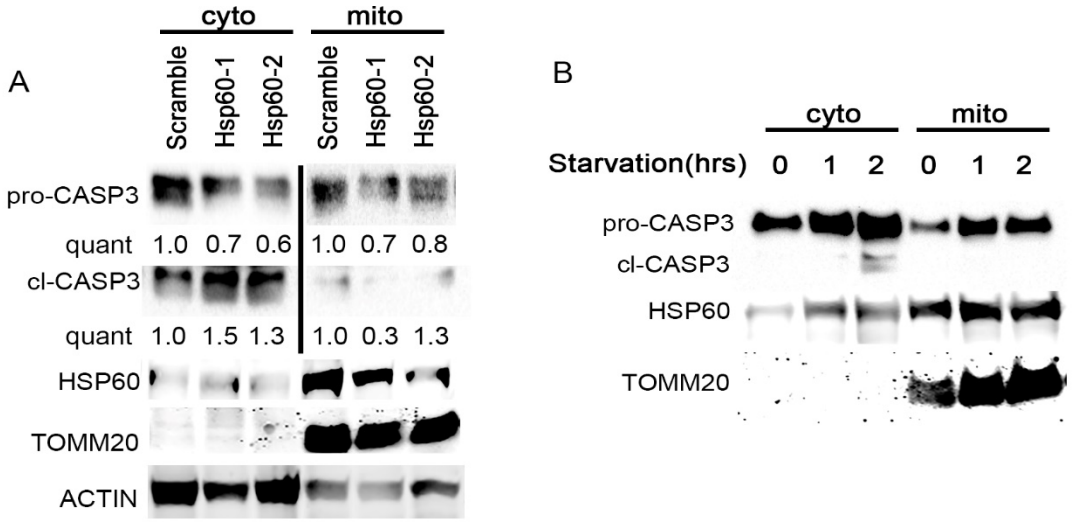

Figure 4-10 Loss of HSP60 or starvation cause an increase of cl-CASP3 in the cytoplasm

(**A**) A representative blot of mitochondrial and cytosolic enriched fractions from well-fed SKBR3 cells treated with either of two HSP60 siRNA constructs or one scramble siRNA. Blots were probed for ACTIN (42kDa), proCASP3 (32kDa), cl-CASP3 (20kDa), HSP60 (60kDa) and mitochondrial marker TOMM20 (16kDa) (n=2). Quant represents the levels of above protein normalized to ACTIN or TOMM20 for cyto and mito, respectively and relative to scramble control. *note: vertical line distinguishes different exposure times for the same blot (**B**) A representative blot of mitochondrial and cytosolic enriched fractions from SKBR3 cells exposed to well-fed, one hour complete starvation or two hours of complete starvation and probed for pro-CASP3 (32kDa), cl-CASP3 (20kDa), HSP60 (60kDa) and mitochondrial marker TOMM20 (16kDa) (n=3).

4.9. Discussion

Here I demonstrated that CASP3 has a context-dependent role in the upregulation of starvation-induced autophagy in human cell lines. Furthermore, I showed that a decrease in the levels of HSP60 can lead to an increase in autophagic flux and decrease in the pro-form of CASP3. In fed conditions, the increase in autophagic flux following HSP60 knockdown is reliant on CASP3 and correlates with an increase in cl-CASP3. The increase in cl-CASP3 suggests that pro-CASP3 is being more readily processed or the turnover of cl-CASP3 is decreased and is preventing pro-CASP3 production. Additionally, an increase in the cl-CASP3, pro-CASP3 and HSP60 levels specifically in the cytosol during starvation demonstrate how subcellular localization of these proteins in response to nutrient deprivation controls the autophagic response. This information taken together supports a model where HSP60 maintains levels of pro-CASP3 in the mitochondria through retention or reception of pro-CASP3 inside the mitochondria under nutritionally stable conditions (Figure 4-11). However, upon the cellular stress of nutrient deprivation, HSP60 and pro-CASP3 translocate to the cytosol where pro-CASP3 can be processed to cl-CASP3 and act to upregulate autophagy.

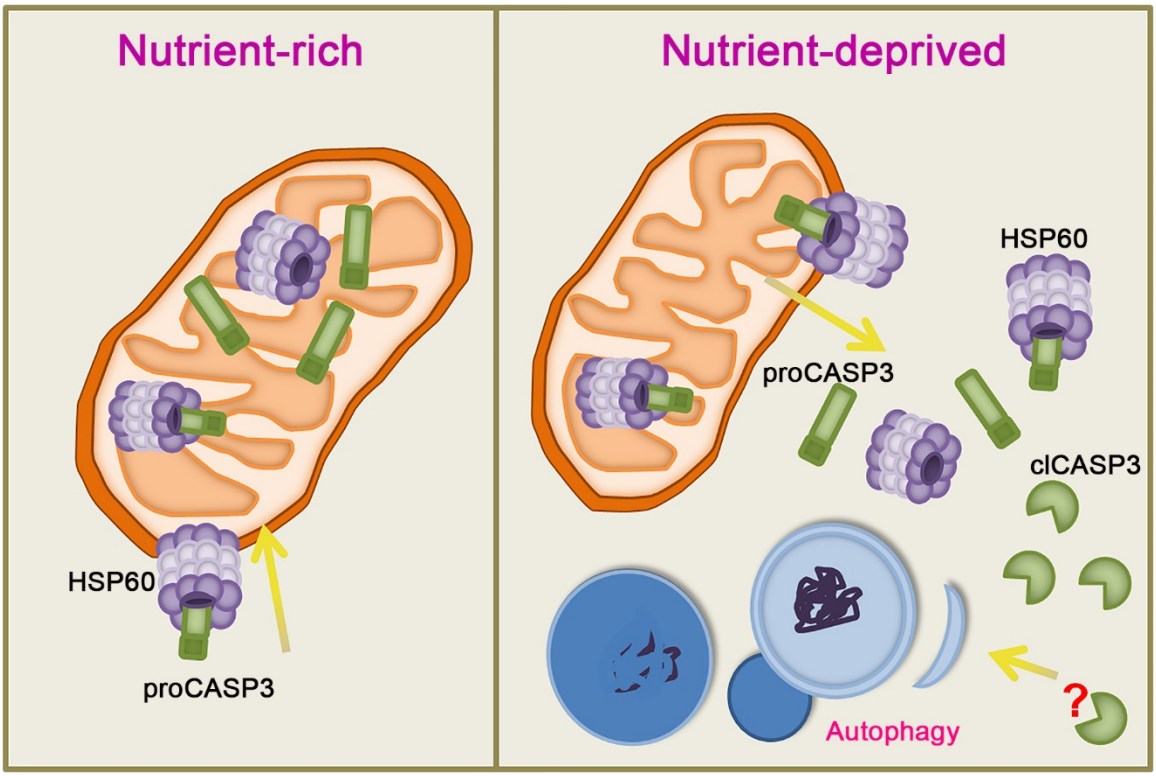

Figure 4-11 Proposed model of subcellular localization of HSP60 and CASP3 in nutrient-rich and nutrient-deprived conditions

When cells are well fed, a pool of HSP60 and proCASP3 is maintained in mitochondria either by HSP60 retaining proCASP3 in the mitochondria or through assisted mitochondrial delivery. However, once a cell experiences the cellular stress of starvation, it allows a release of HSP60 and proCASP3 into the cytosol. Accumulation of proCASP3 triggers activation where clCASP3 cleaves a substrate to induce autophagy.

These findings could help provide an explanation of how cells can gradually increase the levels of active caspases until an apoptotic threshold is achieved (Florentin and Arama, 2012). Previously HSP60 and CASP3 were associated in the context of cell death (Samali et al., 1999; Xanthoudakis et al., 1999), but our study identifies a new context where mitochondria act as a CASP3 reservoir in which HSP60 is the gatekeeper and controls the response to nutrient stress. The cytosolic increase in HSP60 in response to starvation mimics other findings in previous reports that suggest HSP60 exits the mitochondria in response to cell death stimuli before the mitochondrial membrane potential changes (Samali et al., 1999). Another report indicated that in response to cell death stimuli, an increase in HSP60 can result from mitochondrial export but that this effect was cell line dependent (Chandra et al., 2007). Clarification of the subcellular origin of

HSP60 in starvation conditions as well as the potential role of HSP60 in the retention and/or reception of pro-CASP3 in the mitochondria requires further study.

Many studies have demonstrated previously that upon exposure to cell death stimuli effector caspases can cleave autophagy proteins to inhibit autophagy (Cho et al., 2009; Norman et al., 2010; Pagliarini et al., 2012; Sirois et al., 2012; Wirawan et al., 2010; You et al., 2013). What is poorly understood is the role that effector caspases play in response to other cellular stresses such as starvation. Based on previousy studies in *Drosophila* (DeVorkin et al., 2014; Hou et al., 2008), here I identified human CASP3 as a regulator of starvation induced autophagy in several different cellular contexts. Outstanding questions include whether there is functional redundancy among human caspases, and specifically whether the other effector caspases, CASP6 and CASP7, also play a role in the regulation of autophagy. Additionally, the *Drosophila* effector caspase Dcp-1 was shown to upregulate autophagy in response to proteasome inhibition (Chapter 3), so it would be of interest to determine if CASP3 or other effector caspases are also able to regulate this mode of compensatory autophagy.

The IP western experiment did not identify ANT-2 or HSP90 as CASP3-interacting proteins, although their Drosophila homologs SesB and Hsp83, respectively, were shown to interact with Dcp-1 (DeVorkin et al., 2014). There are several potential explanations for this: i) I performed an IP in starvation conditions and perhaps they only interact in fed conditions, ii) other isoforms of the homologs could play a role instead, iii) there were insufficient levels of the proteins to be detected, iv) there was poor antibody recognition, and v) CASP3 could have varied upstream and downstream pathways of regulation in comparison to Dcp-1. One downstream pathway or proteins of particular interest are the cleavage substrates of CASP3 that function to regulate autophagy. Candidate cleavage targets of Dcp-1 in autophagy regulation currently remain unknown. One potential mammalian candidate of CASP3 cleavage during starvation is autophagy protein ATG4D. It was reported that CASP3 could cleave ATG4D to enhance the lipidation of GABARAP and increase autophagy in this manner (Betin and Lane, 2009), but it has yet to been shown if this happens in a cellular context or in any of the cell lines used in this study.

While this work investigated five human tissue cell lines, the only line that seemed to have a significant contrasting effect was embryonic HEK293. HEK293 is unlike the other lines as it was not derived from a human cancer but rather from a healthy, developing fetus. The HEK293 specific cell type is unknown as it could be endothelial, epithelial or fibroblasts but mRNA profiling also indicates it could be neuronal – a cell type that is recognized as having unique pathways of autophagy regulation (Tsvetkov et al., 2009). Further studies are required to ascertain whether CASP3 regulation of autophagy could be a cancer adaptation, whether it occurs during development, or if it occurs *in vivo*.

This research contributes several new connections between HSP60 and CASP3 in the context of autophagy and importantly sheds light on how certain cellular stress proteins react or adapt to nutritional stress.

Chapter 5. General Discussion

5.1. Summary and significance

In this thesis, my aims were (1) to characterize the regulatory relationship between Dcp-1 and Hsp83 in the context of autophagy and (2) to discover if there was an effector caspase in humans that could also positively regulate starvation-induced autophagy. The purpose of these aims was to better understand the factors and mechanisms involved in autophagy regulation in *Drosophila* and to understand if this novel regulatory role for an effector caspase is an important evolutionarily conserved mechanism present in higher eukaryotes and more specifically humans.

5.1.1. Specific Aim 1 – Characterization of Hsp83 and Dcp-1 in autophagy

In order to better understand the role of Dcp-1 in autophagy regulation, I utilized previous IP-MS results from a catalytically inactive Dcp-1 pull-down experiment that identified candidate Dcp-1 interacting proteins. I furthered the initial RNAi/LysoTracker® Green/Flow cytometry screen of these interactors by designing additional dsRNAs to validate the effects of protein knockdown. I then added to the initial RNAi/RFP-GFP-Atg8a/starvation assay by performing the experiment in fed conditions to observe whether the identified regulators of starvation-induced autophagy were also negative regulators of autophagy under basal conditions. Following these studies, Hsp83 remained a protein of interest since it was shown to be a negative regulator of autophagy in both fed and starved conditions using the tandem-fluorescent Atg8a assay as well as the LTG assay. The results from the assays in fed conditions also suggested a new relationship between heat-shock proteins and the maintenance of low levels of basal autophagy (Figure 3-1).

To further elucidate the role of Hsp83, I looked to *in vivo* models to determine if there was an effect on autophagy. Utilizing already available and well-characterized transheterozygous loss-of-function mutant combinations of *Hsp8* (Bandura et al., 2013), I was able to further evaluate the contribution of Hsp83 to autophagy during mid-oogenesis and in the larval fat body. Interestingly, the two transheterozygous mutant combinations

showed similar phenotypes of an increase in autolyosomes and cell death (Figure 3-2, Figure 3-3) which became increasingly degenerative in starvation conditions (Figure 3-4). To understand the relationship between Dcp-1 and Hsp83, I examined whether Dcp-1 levels were affected by loss of Hsp83 *in vivo,* since previous experiments conducted in our laboratory showed that Hsp83 was not cleaved by Dcp-1 (L. Devorkin, N. Go). Overall levels of Dcp-1, both the zymogen and the cleaved form, were increased in the *Hsp83* transhets showing that Hsp83 normally functions to suppress levels of Dcp-1 (Figure 3-5). These experiments ascribed Hsp83 as a negative regulator of autophagy in *Drosophila* for the first time and showed that Hsp83 controlled stability of Dcp-1.

To explain the increased levels of Dcp-1 in the *Hsp83* mutant background, I experimentally ruled out transcriptional control or regulation through the known inhibitor of cleaved Dcp-1, Diap1 (Figure 3-6). Based on literature describing roles for Hsp83 homologs in proteasomal degradation in humans and yeast, I discovered that proteasomal activity was similarly compromised in *Hsp83* transhet flies using two separate assays (Figure 3-7). Supporting experiments targeting the proteasome using RNAi or a small molecule inhibitor then demonstrated that Dcp-1 zymogen levels were increased upon proteasome inhibition in a manner that was Hsp83-dependent (Figure 3-8). The regulation of the cleaved form of Dcp-1 has been well-characterized by non-degradative ubiquitylation by Diap1 (Ditzel et al., 2008), but my discovery that the Dcp-1 zymogen form is negatively affected by the proteasome is a novel finding. My research also further supports the association between Hsp83 and proteasomal processing of specific substrates in *Drosophila* that was introduced by Hrizo and Palladino, 2010.

My epistasis experiments further elucidated the nature of the Dcp-1/Hsp83 relationship and the respective roles of Dcp-1 and Hsp83 in autophagy regulation and cell death. Ovaries in mutants lacking Dcp-1 and with reduced Hsp83 function had very unique characteristics in that they had abnormal cell division, partially condensed and persisting nurse cell nuclei, premature loss of follicle cells, and positive staining for TUNEL but not for LysoTracker® Red (Figure 3-9). The double mutants rendered an increasingly impaired phenotype with female infertility and decrease in developmental viability. The LysoTracker® and TUNEL phenotypes were reiterated in the larval fat body, indicating that Hsp83 loss results in activation of a cell death pathway that is independent of Dcp-1

but activation of an autophagy pathway that is dependent on Dcp-1. Decreased autophagy was also observed following reduction of both Dcp-1 and Hsp83 in cultured cells (Figure 3-10). The double mutant analyses really highlighted the complex relationship between these two proteins, with the plethora of interesting phenotypes and in particular the unexpected divergence between cell death and autophagy. Lastly, when I inhibited the proteasome I observed an increase in autophagy and cleaved Dcp-1 that was mitigated when I additionally knocked down Dcp-1 (Figure 3-11, Figure 3-12); this demonstrates that proteasomal inhibition upregulates compensatory autophagy that is dependent on Dcp-1. While compensatory autophagy in this context was previously described, it was never before connected to Dcp-1 nor shown to be dependent on Dcp-1.

Altogether, these studies illustrate a novel proteostatic relationship where Dcp-1 levels are basally suppressed through Hsp83-mediated proteasomal activity and when Hsp83 or the proteasome is inhibited, Dcp-1 is responsible for the ensuing autophagy (Figure 3-13).

5.1.2. Specific Aim 2 – Conservation of an autophagy-inducing effector caspase in human cells

To address my second aim, I began by screening human effector caspases for potential localization to the inner mitochondrial matrix since Dcp-1 was shown to localize predominantly to that subcellular localization as well as have a distinct effect on mitochondrial morphology and ATP levels (DeVorkin et al., 2014). In doing so, I found that only CASP3, but not the effector caspases 6 or 7, was partially localized inside of mitochondria in the human breast cancer line SKBR3 (Figure 4-1). Knockdown of CASP3 then revealed that it was required for starvation-induced autophagy through analysis of two separate assays (Figure 4-2). To determine if this role was unique to SKBR3, I screened four other cell lines, three of distinct cancer tissue origins and one from embryonic development. I found that the cancer cell lines required CASP3 for upregulation of autophagy in response to nutrient-deprivation (Figure 4-3 - Figure 4-6). These are the first reported findings, to our knowledge, that reveal CASP3 as a context-dependent positive regulator of starvation-induced autophagy in human cells.

To better understand CASP3 regulation of autophagy, I performed an IP experiment to test whether CASP3 interacted with the human homlogs of three mitochondrial-related Dcp-1 interacting proteins. One of the three homologs, HSP60, was clearly identified as an interactor via pull down and reciprocal pulldown assays with CASP3 (Figure 4-7). Hsp60 was identified as a putative negative regulator of autophagy in *Drosophila* (Figure 3-1) so I ventured to characterize the potential role of HSP60 in autophagy regulation in SKBR3 cells. I discovered by two separate assays that HSP60 is a negative regulator of autophagy and that its loss in fed conditions can cause an induction of autophagy (Figure 4-8). Through an epistasis experiment I discovered that the induction of autophagy from HSP60 knockdown requires CASP3 (Figure 4-9). Interestingly, when HSP60 was knocked down, there was a decrease in levels of pro-CASP3, but there was also an increase in the cleaved form of CASP3 signifying an increase in CASP3 activation (Figure 4-8, Figure 4-9). Fractionation studies under starvation conditions or HSP60 knockdown revealed an increase in cleaved CASP3 within the cytosolic fraction (Figure 4-10). Additionally, in starvation conditions there was an increase in cytosolic HSP60 and pro-CASP3 supporting the model that HSP60 relocates to the cytosol with CASP3 (Figure 4-10). These findings support a new role for HSP60 where it acts to control and maintain the subcellular reservoir of pro-CASP3 in the mitochondria to manage stress responses.

The findings from my second aim support a model (Figure 4-11) whereby a modest increase in cytosolic active CASP3 is mediated by HSP60 and pro-CASP3 relocation to the cytosol. This cytosolically active CASP3 induces an upregulation of autophagy by targeting a currently unknown substrate and can be induced in response to starvation or HSP60 loss.

5.2. Strengths, limitations and future avenues

The basis of this thesis was largely dependent on the outcomes of the Dcp-1 IP-MS data (Table 1.1) and additional screening of interactors for autophagy regulation (Figure 3-1). The assays were subject to stringent conditions for selection of candidates and secondary screening was thorough with two distinct dsRNAs targeting each candidate for LTR staining that was followed up with a specific autophagy assay. While this approach was thorough and systematic, there are notable limitations to these experiments which

are important to consider. Firstly, the candidate interactors of Dcp-1 were not stratified for association in nutrient-rich versus nutrient-deprived conditions which increased the difficulty of distinguishing which could be important regulators of starvation-induced autophagy versus general interactors with Dcp-1 under basal conditions. Additionally, the construct used for IP expressed the pro-domain of Dcp-1 as well as the mutated active site to render it catalytically inactive; these features could provide limited pull-down of potential cleavage targets due to weaker interactions from the mutated amino acid as well as enrich for interactors that stabilize specifically the pro-form through interaction with the pro-domain. The initial LTR screening was limited in that there could have been incomplete knockdown, functional redundancy, or a long half-life of the proteins which could cause no discernible change in autophagy regulation and might have prematurely identified some interactors as false negatives. The screen was successful in narrowing the scope as it accurately identified at least two negative regulators of autophagy involved in Dcp-1-mediated autophagy, SesB and Hsp83, but it is important to note it is likely to be an incomplete list of putative regulators.

The original screen was strengthened with the addition of RNAi treatments under fed conditions in the S2 RFP-GFP-Atg8a expressing cell line as an extra step to identify which of the candidates function in basal conditions to negatively modulate autophagy (Figure 3-1). This experiment helped distinguish genes that function to downregulate basal autophagy and those that displayed an effect due to already being sensitized to starvation conditions. In fed conditions, the difference in autophagic flux between control-siRNA and experimental-siRNA cells was significant but minor and exposed a linkage between chaperones from the heat-shock family and their effect of normally suppressing autophagy by mitigating general cellular stress and not specifically starvation-induced autophagy. The weak autophagy induction response in fed conditions when negative regulators of autophagy were targeted also supports that Dcp-1 cleavage targets or regulators of starvation-induced autophagy might have gone unrepresented in the original screen as a stronger autophagic response might be expected.

The focus on Hsp83 allowed extensive and comprehensive studies *in vivo* and *in vitro* of its regulation of autophagy. The *in vivo* experiments were performed using two different transheterozygote combinations with three corresponding monoallelic controls

and one wild-type control. Additionally, assays were performed in two different developmental tissue types, the ovaries and the larval fat body. The transheterozygotes still expressed Hsp83 but with different loss-of-function point mutations and both combinations relying on one copy of the *Hsp83*$^{6\text{-}55}$ allele (Bandura et al., 2013). The two mutant transhet combinations had similar phenotypes in my studies which could emphasize the importance of the *Hsp83*$^{6\text{-}55}$ point mutation site for its functions related to autophagy and cell survival but raises the question about what different effects the *Hsp83*^{e6A} and *Hsp83*^{e6D} alleles contribute to the phenotypes. Regardless, the use of LTR and RFP-GFP-Atg8a analyzed in several contexts convincingly illustrated the role of Hsp83 as a suppressor of autophagy under basal conditions.

The *Hsp83*;*Dcp-1* double mutants provided many important phenotypic observations highlighting how Dcp-1 and Hsp83 can congruently affect several different pathways. It would be of particular interest to further investigate the observed phenotypes to understand how cell division is specifically affected, to identify how Dcp-1 contributes to pyknosis, and lastly to characterize the Dcp-1-independent cell death.

The role of the proteasome in Hsp83 mutants and its effects on Dcp-1 were clearly demonstrated through *in vitro* and *in vivo* means in this project. Using two separate proteasomal activity assays, I was able to show that proteasomal processing was diminished in both *Hsp83* transhet combinations. Further support of proteasome control of Dcp-1 levels and proteasome dependency on Hsp83 was shown genetically and chemically with a proteasomal RNAi knockdown strain, Rpn2-RNAi, and with drug treatment by feeding flies the proteasomal inhibitor MG132. While I made strong links between Hsp83, Dcp-1 and the proteasome, there are several more potential avenues of investigation. Dcp-1 was shown to be affected by levels of proteasomal activity, but further studies are required to understand if Dcp-1 is regulated directly or indirectly through the proteasome. The role of Hsp83 in proteasomal activity requires further elucidation as it could be involved at several different levels, such as substrate delivery and proteasomal assembly in *Drosophila*. Additionally, it remains unknown if the physical interaction shown between the pro-form of Dcp-1 and Hsp83 is necessary for the regulation of Dcp-1 or if Hsp83 independently supports proteasomal activity.

For my second aim, the mitochondrial localization experiment assisted with prioritization of potential human effector caspases to analyze further, and confirmed that the SKBR3 cell line has detectable levels of CASP3. By focusing on CASP3, I was able to confirm its autophagic regulatory role with two separate autophagy assays as well as test for similar effects in four other human cell lines. One issue with concentrating solely on CASP3 is that it excluded further analysis of the other effector caspases, CASP6 and CASP7, which could also play roles in autophagy regulation. It would be important in future experiments to determine if there is functional redundancy among the human effector caspases in their autophagy regulation as there is known functional redundancy among caspases in other contexts (Zheng et al., 2000). The investigation of the other cell lines was limited as it was restricted to only one autophagy assay so it would be ideal to complete additional autophagic flux assays in the different cell lines. Additionally, variable responses between the pathogenic lines and the fetal-derived line support the need for screening more cell lines to understand the general impact and ubiquity of CASP3 in this role. It would also be ideal to test if HSP60 is a negative regulator of autophagy in other lines, and if it functions similarly with respect to its subcellular localization roles in response to starvation. Ultimately, the goal of these studies would be to test the CASP3 findings in primary human samples or xenograft models to determine whether my findings have a biologically relevant application or if they are a phenomenon of cell culture. Another related avenue of interest would be to examine autophagy responses in CASP3 knockout mice or tissues (Le et al., 2002).

One outstanding question is if Dcp-1 and CASP3-regulated autophagy is induced through cleavage of a substrate. Previous experiments in *Drosophila* demonstrated that in order to rescue autophagy in *Dcp-1*^{Prev} mutants, catalytic activity of Dcp-1 was required; this supports the concept that cleavage of a substrate mediates the autophagy function (DeVorkin et al., 2014). Furthermore, my findings in the SKBR3 cell line showed that autophagy levels correlate with cleaved cytosolic CASP3 levels, indicating that its activation could be important for autophagy regulation. Currently, I am pursuing experiments to answer this question by identifying potential cleavage targets that negatively regulate autophagy. I plan to investigate two previously identified negative regulators of autophagy in human cells that are also potential CASP3 cleavage targets. One of the proteins I am investigating is RUBCN (Rubicon/Run domain Beclin-1-

interacting and cysteine-rich domain-containing protein) which was identified as a PI3K complex protein that interacts with UVRAG and Vps34 to block PI3K complex kinase activity under basal conditions and thus inhibit autophagy (Matsunaga et al., 2009; Sun et al., 2010, 2011). RUBCN became a target of interest after a caspase cleavage prediction database (Kumar et al., 2014) identified it as a high likelihood substrate of CASP3 due to its sequence containing a canonical DEVD CASP3 peptide recognition sequence. The other protein of potential interest, 14-3-3ζ, has a *Drosophila* homolog of the same name that was one of the 24 proteins identified in the Dcp-1 IP/MS (Table 1.1). Although it wasn't recognized as a negative regulator in the RNAi/LTR/Flow screen, this could be potentially due to incomplete knockdown. Mammalian 14-3-3ζ is a part of the 14-3-3 family of regulatory proteins that inhibits the PI3K complex by association with Vps34 under basal conditions to prevent its kinase activity (Pozuelo-Rubio, 2011). 14-3-3ζ does not contain the canonical DEVD sequence but its paralog, 14-3-3ε, was shown to be cleaved at a noncanonical sequence of MQGD by CASP3 (Won et al., 2003). 14-3-3ζ shares high sequence identity with 14-3-3ε and has a similar sequence of TQGD flanked by conserved residues making it possible that it is also cleaved at the aspartic acid. If neither 14-3-3ζ nor RUBCN prove to be viable cleavage targets of CASP3 in the context of autophagy regulation, I plan to conduct an IP/MS experiment in starvation conditions with a catalytically inactive CASP3 that lacks the pro-domain to identify other putatitve associations with the autophagy pathway. Additionally, to confirm that CASP3 is required to cleave a target in this context, it would be ideal to create a CASP3 knockout in SKBR3 and then conduct a rescue experiment with wild-type or catalytically inactive CASP3 to determine if the increase in starvation-induced autophagy can be restored.

Dcp-1 and CASP3 have both been identified as positive regulators of autophagy but their respective mechanisms of regulation have not been evaluated for conservation. There is currently more known about the regulation of Dcp-1 as Hsp83 has now been identified as an upstream regulator, and SesB was previously recognized as a downstream regulator (DeVorkin et al., 2014). I first attempted to examine potential functional conservation with these proteins but due to complications such as the many isoforms of HSP90, the human homolog to Hsp83, and the several members from the ANT family, homologs of SesB, I didn't manage to successfully design and execute experiments before further pursuing my investigation with HSP60. It would be pertinent to

study if these pathways are conserved and, if so, at what levels. For example: Is CASP3 regulated by the proteasome? Can CASP3 induce compensatory autophagy? Is there a similar mitochondrial morphology/ATP effect with human CASP3 or do these organisms have evolutionarily diversified pathways? Conversely, it would be interesting to test if *Drosophila* Hsp60 plays a role similar to human HSP60 regarding the subcellular localization of Dcp-1 in response to nutrient starvation. In addition, it would be interesting to determine if autophagy-related cleavage substrates of CASP3 are conserved as autophagy-related substrates of Dcp-1 in *Drosophila*.

5.3. Potential applications

My thesis elucidated novel relationships between caspases and heat-shock proteins in response to cellular stresses in two eukaryotic organisms. In addition to a better understanding of how cells manage stress, this data provides insights into how cells function under basal conditions or how they could function in developmental processes. The use of two organisms with similar nonapoptotic caspase-mediated responses also sheds light into possible evolutionary conservation of stress adaptation mechanisms. The acquired knowledge from my project pertaining to basic biological stress responses could be extrapolated to disease contexts. For example, it could help explain what might be going wrong in a diseased cell or could even further be applied to improve drug design with better comprehension of cellular and molecular consequences. To help illustrate the potential applications of my project I highlight below how my findings can be translated into two disease types commonly associated with autophagy and its dysregulation: cancer and neurodegenerative diseases.

5.3.1. Cancer

Autophagy is beneficial in healthy cells to mitigate damage and prevent maladies such as cancer. However, autophagy can also aid an established tumour by helping it survive stressful conditions such as hypoxia and limited nutrient availability that can be caused by poor vascularisation (Degenhardt et al., 2006). Targeting autophagy as a chemotherapeutic adjuvant has been a fairly recent endeavour with limited success mostly due to nonspecific and low potency drugs that target lysosomes (such as

hydroxychloroquine), systemic side effects and limited understanding regarding optimal patients and treatment schedules (Rebecca and Amaravadi, 2016). My study reveals a previously unforeseen opportunity of targeting a cell death protein, CASP3, to enhance chemotherapeutic outcomes by preventing cancer cells from upregulating autophagy to enable survival in response to stressful tumour conditions. There is already precedent that high levels of active CASP3 could be a cancer-related phenotype as several studies have shown that cancers -such as gastric, ovarian, cervical, colorectal, skin, and breast - with higher levels of active CASP3 are associated with a poorer patient prognosis (Jäger and Zwacka, 2010; Liu et al., 2015, 2013; O'Donovan et al., 2003; Woenckhaus et al., 2003). My findings contribute a possible explanation: the active levels of CASP3 may induce autophagy in the cancer cells or the protective stroma around the cancer that can aid survival and proliferation of cancers. The approach of targeting CASP3 in cancer was previously proposed as it was shown to increase cell death in tumours in a mouse lung xenograft model (Kim et al., 2008), although the connection to autophagy has not been made. CASP3 could be particularly beneficial as a target since it doesn't appear to have an effect on basal levels of autophagy. This is important because it could then affect poorly vascularized tumours with limited access to nutrients that are addicted to autophagy, while leaving the basal levels of autophagy intact in healthy cells. Such a strategy would avoid the potential negative effects associated with systemic autophagy inhibition such as neurodegeneration (Amaravadi and Debnath, 2014).

HSP90 is currently a popular drug target for cancers because it stabilizes many oncogenic proteins such as transcription factors and signalling kinases that can contribute to aberrant proliferation (Whitesell and Lindquist, 2005). More specifically, it was found that mitochondrial-localized HSP90 could be an ideal target as it plays a pivotal role in mitochondrial proteostasis specifically in tumour cells (Altieri, 2013; Siegelin et al., 2011). One issue with targeting HSP90 has been that it can induce autophagy in addition to apoptosis (Mori et al., 2015). Translation of findings from my Hsp83 studies supports targeting the putative functional homolog of Dcp-1, CASP3, in conjunction with targeting HSP90. I demonstrated that loss of the effector caspase Dcp-1 in the context of *Hsp83* loss-of-function mutants still showed evidence of cell death phenotypes but not autophagy. The translation of this finding to humans supports a new counterintuitive combination treatment approach. By targeting HSP90 and CASP3, it may be possible to inhibit autophagy but still induce a cell death pathway independent of CASP3. Furthermore, the

knowledge that inhibition of HSP90 function could affect proteasomal activity and induce caspase-dependent compensatory autophagy is particularly pertinent. Treatment with the small molecule bortezomib, a proteasomal inhibitor, was shown to induce autophagy in melanomas (Selimovic et al., 2013). Using bortezomib with the adjuvant hydroxychloroquine to suppress autophagy has shown some promising effectd in Phase I trials in melanoma (Vogl et al., 2014) and could be improved upon potentially by specifically targeting autophagy through CASP3.

HSP60 was considered as a potential target for chemotherapeutic adjuvants as it was found to be highly expressed in some cancer cells where it acts to maintain mitochondrial proteostasis (Ghosh et al., 2008). Notably, HSP60 was found to accumulate predominantly in the cytosol in some cancer types (Cappello et al., 2008) indicating its potential adaptational response to stress. This change in subcellular localization could lead to an activation of CASP3-induced autophagy according to my model and thus the subcellular localization of HSP60 might be useful as a marker for identifying which cancers are susceptible to treatments that inhibit CASP3 or autophagy.

5.3.2. Neurodegeneration

Neurons are highly reliant on autophagy because of their limited capacity to manage damage resulting from protracted axonal cytoplasm and low amounts of cell division. Loss of autophagy is associated with several neurodegenerative disorders due to defective clearance of aggregated or dysfunctional proteins and organelles (Nixon, 2013). Mutations in ATG proteins at different stages in the autophagy pathway have been associated with Alzheimer's disease (AD), amyotrophic lateral sclerosis (ALS) and familial Parkinson's disease (PD) (Nixon, 2013). While I did not study neuronal cells, if my findings are applicable in that context, then they would suggest potential new disease-related factors. During the process of aging and in many neurodegenerative diseases there is an observable increase of heat-shock proteins (Lu et al., 2004) which may be what is limiting autophagy induction. High levels of HSP90 maintain the correct folding and solubilisation of proteins to help mitigate damage that would contribute to neurodegenerative diseases (Daturpalli et al., 2013; Dou et al., 2003) but, similar to cancer, could play a negative role once the onset of neurodegeneration has begun. HSP60, on the other hand, has important roles in mitochondrial homeostasis and there is generally a correlation of loss or mutated

HSP60 with neuronal impairment (Bross et al., 2012). For these reasons, HSP60 is perhaps not an ideal target. Furthermore, since many neurodegenerative diseases have degeneration that is mediated by apoptosis, CASP3 was seen as a potential target to limit neuronal loss (Vila and Przedborski, 2003). With enhanced knowledge, there is a growing awareness that CASP3 has several nonapoptotic roles and thus might not be a suitable target (D'Amelio et al., 2012). If CASP3 does contribute to stress induced autophagy in neurons, then targeting CASP3 might actually cause more harm than good if autophagy regulation is impaired.

Altogether, my research uncovers novel molecular relationships that shed light on cellular stress adaptation and its evolutionary conservation. Additionally, there are potential applications from my work that could provide solutions or explain limitations to current therapies in diseases affected by autophagy regulation such as neurodegeneration and cancer.

References

Abraham, M.C., and Shaham, S. (2004). Death without caspases, caspases without death. Trends in Cell Biology *14*, 184–193.

Ahlberg, J., and Glaumann, H. (1985). Uptake--microautophagy--and degradation of exogenous proteins by isolated rat liver lysosomes. Effects of pH, ATP, and inhibitors of proteolysis. Exp. Mol. Pathol. *42*, 78–88.

Altieri, D.C. (2013). Mitochondrial HSP90s and tumor cell metabolism. Autophagy *9*, 244–245.

Altieri, D.C., Stein, G.S., Lian, J.B., and Languino, L.R. (2012). TRAP-1, the mitochondrial Hsp90. Biochim. Biophys. Acta *1823*, 767–773.

Amaravadi, R., and Debnath, J. (2014). Mouse models address key concerns regarding autophagy inhibition in cancer therapy. Cancer Discov *4*, 873–875.

Ashoor, R., Yafawi, R., Jessen, B., and Lu, S. (2013). The Contribution of Lysosomotropism to Autophagy Perturbation. PLOS ONE *8*, e82481.

Axe, E.L., Walker, S.A., Manifava, M., Chandra, P., Roderick, H.L., Habermann, A., Griffiths, G., and Ktistakis, N.T. (2008). Autophagosome formation from membrane compartments enriched in phosphatidylinositol 3-phosphate and dynamically connected to the endoplasmic reticulum. J. Cell Biol. *182*, 685–701.

Azeez, O.I., Meintjes, R., and Chamunorwa, J.P. (2014). Fat body, fat pad and adipose tissues in invertebrates and vertebrates: the nexus. Lipids Health Dis *13*, 71.

Bandura, J.L., Jiang, H., Nickerson, D.W., and Edgar, B.A. (2013). The Molecular Chaperone Hsp90 Is Required for Cell Cycle Exit in Drosophila melanogaster. PLoS Genet *9*, e1003835.

Bandyopadhyay, U., Kaushik, S., Varticovski, L., and Cuervo, A.M. (2008). The Chaperone-Mediated Autophagy Receptor Organizes in Dynamic Protein Complexes at the Lysosomal Membrane. Mol. Cell. Biol. *28*, 5747–5763.

Bang, S., Jeong, E.-J., Kim, I.-K., Jung, Y.-K., and Kim, K.-S. (2000). Fas- and Tumor Necrosis Factor-mediated Apoptosis Uses the Same Binding Surface of FADD to Trigger Signal Transduction A TYPICAL MODEL FOR CONVERGENT SIGNAL TRANSDUCTION. J. Biol. Chem. *275*, 36217–36222.

Barth, J.M.I., Szabad, J., Hafen, E., and Köhler, K. (2011). Autophagy in Drosophila ovaries is induced by starvation and is required for oogenesis. Cell Death Differ. *18*, 915–924.

Bauckman, K.A., Owusu-Boaitey, N., and Mysorekar, I.U. (2015). Selective Autophagy: Xenophagy. Methods *75*, 120–127.

Beisner, D.R., Ch'en, I.L., Kolla, R.V., Hoffmann, A., and Hedrick, S.M. (2005). Cutting edge: innate immunity conferred by B cells is regulated by caspase-8. J. Immunol. *175*, 3469–3473.

Bell, B.D., Leverrier, S., Weist, B.M., Newton, R.H., Arechiga, A.F., Luhrs, K.A., Morrissette, N.S., and Walsh, C.M. (2008). FADD and caspase-8 control the outcome of autophagic signaling in proliferating T cells. Proc. Natl. Acad. Sci. U.S.A. *105*, 16677–16682.

Ben Moshe, T., Barash, H., Kang, T.-B., Kim, J.-C., Kovalenko, A., Gross, E., Schuchmann, M., Abramovitch, R., Galun, E., and Wallach, D. (2007). Role of caspase-8 in hepatocyte response to infection and injury in mice. Hepatology *45*, 1014–1024.

Bence, N.F., Sampat, R.M., and Kopito, R.R. (2001). Impairment of the ubiquitin-proteasome system by protein aggregation. Science *292*, 1552–1555.

Betin, V.M.S., and Lane, J.D. (2009). Caspase cleavage of Atg4D stimulates GABARAP-L1 processing and triggers mitochondrial targeting and apoptosis. J Cell Sci *122*, 2554–2566.

Boatright, K.M., and Salvesen, G.S. (2003). Mechanisms of caspase activation. Curr. Opin. Cell Biol. *15*, 725–731.

Borkovich, K.A., Farrelly, F.W., Finkelstein, D.B., Taulien, J., and Lindquist, S. (1989). hsp82 is an essential protein that is required in higher concentrations for growth of cells at higher temperatures. Mol Cell Biol *9*, 3919–3930.

Bortnik, S., Choutka, C., Horlings, H.M., Leung, S., Baker, J.H.E., Lebovitz, C., Dragowska, W.H., Go, N.E., Bally, M.B., Minchinton, A.I., et al. (2016). Identification of breast cancer cell subtypes sensitive to ATG4B inhibition. Oncotarget *7*, 66970–66988.

Boya, P., Reggiori, F., and Codogno, P. (2013). Emerging regulation and functions of autophagy. Nat Cell Biol *15*, 713–720.

Britton, J.S., Lockwood, W.K., Li, L., Cohen, S.M., and Edgar, B.A. (2002). Drosophila's insulin/PI3-kinase pathway coordinates cellular metabolism with nutritional conditions. Dev. Cell *2*, 239–249.

Bross, P., Magnoni, R., and Bie, A.S. (2012). Molecular chaperone disorders: defective Hsp60 in neurodegeneration. Curr Top Med Chem *12*, 2491–2503.

Broz, P., and Monack, D.M. (2013). Noncanonical inflammasomes: caspase-11 activation and effector mechanisms. PLoS Pathog. *9*, e1003144.

Calamita, P., and Fanto, M. (2011). Slimming down fat makes neuropathic hippo: the Fat/Hippo tumor suppressor pathway protects adult neurons through regulation of autophagy. Autophagy *7*, 907–909.

Cappello, F., Conway de Macario, E., Marasà, L., Zummo, G., and Macario, A.J.L. (2008). Hsp60 expression, new locations, functions and perspectives for cancer diagnosis and therapy. Cancer Biol. Ther. *7*, 801–809.

Cavaliere, V., Taddei, C., and Gargiulo, G. (1998). Apoptosis of nurse cells at the late stages of oogenesis of Drosophila melanogaster. Dev Gene Evol *208*, 106–112.

Chai, J., Wu, Q., Shiozaki, E., Srinivasula, S.M., Alnemri, E.S., and Shi, Y. (2001). Crystal structure of a procaspase-7 zymogen: mechanisms of activation and substrate binding. Cell *107*, 399–407.

Chandra, D., Choy, G., and Tang, D.G. (2007). Cytosolic accumulation of HSP60 during apoptosis with or without apparent mitochondrial release: evidence that its pro-apoptotic or pro-survival functions involve differential interactions with caspase-3. J. Biol. Chem. *282*, 31289–31301.

Chang, H.Y., and Yang, X. (2000). Proteases for cell suicide: functions and regulation of caspases. Microbiol. Mol. Biol. Rev. *64*, 821–846.

Chang, Y.-Y., and Neufeld, T.P. (2009). An Atg1/Atg13 complex with multiple roles in TOR-mediated autophagy regulation. Mol. Biol. Cell *20*, 2004–2014.

Cheong, H., Nair, U., Geng, J., and Klionsky, D.J. (2008). The Atg1 kinase complex is involved in the regulation of protein recruitment to initiate sequestering vesicle formation for nonspecific autophagy in Saccharomyces cerevisiae. Mol. Biol. Cell *19*, 668–681.

Chikte, S., Panchal, N., and Warnes, G. (2014). Use of LysoTracker dyes: a flow cytometric study of autophagy. Cytometry A *85*, 169–178.

Cho, D.-H., Jo, Y.K., Hwang, J.J., Lee, Y.M., Roh, S.A., and Kim, J.C. (2009). Caspase-mediated cleavage of ATG6/Beclin-1 links apoptosis to autophagy in HeLa cells. Cancer Lett. *274*, 95–100.

Ciehanover, A., Hod, Y., and Hershko, A. (1978). A heat-stable polypeptide component of an ATP-dependent proteolytic system from reticulocytes. Biochem. Biophys. Res. Commun. *81*, 1100–1105.

Clare, D.K., and Saibil, H.R. (2013). ATP-Driven Molecular Chaperone Machines. Biopolymers *99*, 846–859.

Cuervo, A.M., and Dice, J.F. (1996). A receptor for the selective uptake and degradation of proteins by lysosomes. Science *273*, 501–503.

Cuervo, A.M., Dice, J.F., and Knecht, E. (1997). A population of rat liver lysosomes responsible for the selective uptake and degradation of cytosolic proteins. J. Biol. Chem. *272*, 5606–5615.

D'Amelio, M., Sheng, M., and Cecconi, F. (2012). Caspase-3 in the central nervous system: beyond apoptosis. Trends in Neurosciences *35*, 700–709.

Daturpalli, S., Waudby, C.A., Meehan, S., and Jackson, S.E. (2013). Hsp90 inhibits α-synuclein aggregation by interacting with soluble oligomers. J. Mol. Biol. *425*, 4614–4628.

De Duve, C., and Wattiaux, R. (1966). Functions of lysosomes. Annu. Rev. Physiol. *28*, 435–492.

Degenhardt, K., Mathew, R., Beaudoin, B., Bray, K., Anderson, D., Chen, G., Mukherjee, C., Shi, Y., Gélinas, C., Fan, Y., et al. (2006). Autophagy promotes tumor cell survival and restricts necrosis, inflammation, and tumorigenesis. Cancer Cell *10*, 51–64.

Degterev, A., Boyce, M., and Yuan, J. (2003). A decade of caspases. Oncogene *22*, 8543–8567.

Denecker, G., Ovaere, P., Vandenabeele, P., and Declercq, W. (2008). Caspase-14 reveals its secrets. J. Cell Biol. *180*, 451–458.

DeVorkin, L., and Gorski, S.M. (2014a). Monitoring autophagy in Drosophila using fluorescent reporters in the UAS-GAL4 system. Cold Spring Harb Protoc *2014*, 967–972.

DeVorkin, L., and Gorski, S.M. (2014b). LysoTracker staining to aid in monitoring autophagy in Drosophila. Cold Spring Harb Protoc *2014*, 951–958.

DeVorkin, L., Go, N.E., Hou, Y.-C.C., Moradian, A., Morin, G.B., and Gorski, S.M. (2014). The Drosophila effector caspase Dcp-1 regulates mitochondrial dynamics and autophagic flux via SesB. J. Cell Biol. *205*, 477–492.

Di Bartolomeo, S., Corazzari, M., Nazio, F., Oliverio, S., Lisi, G., Antonioli, M., Pagliarini, V., Matteoni, S., Fuoco, C., Giunta, L., et al. (2010). The dynamic interaction of AMBRA1 with the dynein motor complex regulates mammalian autophagy. J. Cell Biol. *191*, 155–168.

Díaz-Troya, S., Pérez-Pérez, M.E., Florencio, F.J., and Crespo, J.L. (2008). The role of TOR in autophagy regulation from yeast to plants and mammals. Autophagy *4*, 851–865.

Dice, J.F., Terlecky, S.R., Chiang, H.L., Olson, T.S., Isenman, L.D., Short-Russell, S.R., Freundlieb, S., and Terlecky, L.J. (1990). A selective pathway for degradation of cytosolic proteins by lysosomes. Semin. Cell Biol. *1*, 449–455.

Ding, W.-X., Ni, H.-M., Gao, W., Yoshimori, T., Stolz, D.B., Ron, D., and Yin, X.-M. (2007). Linking of autophagy to ubiquitin-proteasome system is important for the regulation of endoplasmic reticulum stress and cell viability. Am. J. Pathol. *171*, 513–524.

Ditzel, M., Broemer, M., Tenev, T., Bolduc, C., Lee, T.V., Rigbolt, K.T.G., Elliott, R., Zvelebil, M., Blagoev, B., Bergmann, A., et al. (2008). Inactivation of effector caspases through nondegradative polyubiquitylation. Mol. Cell *32*, 540–553.

Dou, F., Netzer, W.J., Tanemura, K., Li, F., Hartl, F.U., Takashima, A., Gouras, G.K., Greengard, P., and Xu, H. (2003). Chaperones increase association of tau protein with microtubules. Proc. Natl. Acad. Sci. U.S.A. *100*, 721–726.

Drummond-Barbosa, D., and Spradling, A.C. (2001). Stem cells and their progeny respond to nutritional changes during Drosophila oogenesis. Dev. Biol. *231*, 265–278.

de Duve, C., Pressman, B.C., Gianetto, R., Wattiaux, R., and Appelmans, F. (1955). Tissue fractionation studies. 6. Intracellular distribution patterns of enzymes in rat-liver tissue. Biochem J *60*, 604–617.

Echeverría, P.C., Bernthaler, A., Dupuis, P., Mayer, B., and Picard, D. (2011). An Interaction Network Predicted from Public Data as a Discovery Tool: Application to the Hsp90 Molecular Chaperone Machine. PLoS ONE *6*, e26044.

Ertürk, A., Wang, Y., and Sheng, M. (2014). Local pruning of dendrites and spines by caspase-3-dependent and proteasome-limited mechanisms. J. Neurosci. *34*, 1672–1688.

Etlinger, J.D., and Goldberg, A.L. (1977). A soluble ATP-dependent proteolytic system responsible for the degradation of abnormal proteins in reticulocytes. Proc. Natl. Acad. Sci. U.S.A. *74*, 54–58.

Fan, Y., and Bergmann, A. (2008). Distinct mechanisms of apoptosis-induced compensatory proliferation in proliferating and differentiating tissues in the Drosophila eye. Dev. Cell *14*, 399–410.

Feng, Y., He, D., Yao, Z., and Klionsky, D.J. (2014). The machinery of macroautophagy. Cell Res. *24*, 24–41.

Fenton, W.A., Kashi, Y., Furtak, K., and Horwich, A.L. (1994). Residues in chaperonin GroEL required for polypeptide binding and release. Nature *371*, 614–619.

Fernando, P., Kelly, J.F., Balazsi, K., Slack, R.S., and Megeney, L.A. (2002). Caspase 3 activity is required for skeletal muscle differentiation. Proc. Natl. Acad. Sci. U.S.A. *99*, 11025–11030.

Fiandalo, M.V., Schwarze, S.R., and Kyprianou, N. (2013). Proteasomal regulation of caspase-8 in cancer cell apoptosis. Apoptosis *18*, 766–776.

Florentin, A., and Arama, E. (2012). Caspase levels and execution efficiencies determine the apoptotic potential of the cell. J Cell Biol *196*, 513–527.

Fraser, A.G., and Evan, G.I. (1997). Identification of a Drosophila melanogaster ICE/CED-3-related protease, drICE. EMBO J. *16*, 2805–2813.

Freimuth, J., Bangen, J.-M., Lambertz, D., Hu, W., Nevzorova, Y.A., Sonntag, R., Gassler, N., Riethmacher, D., Trautwein, C., and Liedtke, C. (2013). Loss of caspase-8 in hepatocytes accelerates the onset of liver regeneration in mice through premature nuclear factor kappa B activation. Hepatology *58*, 1779–1789.

Fujita, J., Crane, A.M., Souza, M.K., Dejosez, M., Kyba, M., Flavell, R.A., Thomson, J.A., and Zwaka, T.P. (2008a). Caspase activity mediates the differentiation of embryonic stem cells. Cell Stem Cell *2*, 595–601.

Fujita, N., Itoh, T., Omori, H., Fukuda, M., Noda, T., and Yoshimori, T. (2008b). The Atg16L complex specifies the site of LC3 lipidation for membrane biogenesis in autophagy. Mol. Biol. Cell *19*, 2092–2100.

Geng, J., and Klionsky, D.J. (2008). The Atg8 and Atg12 ubiquitin-like conjugation systems in macroautophagy. “Protein modifications: beyond the usual suspects” review series. EMBO Rep. *9*, 859–864.

Ghosh, J.C., Dohi, T., Kang, B.H., and Altieri, D.C. (2008). Hsp60 Regulation of Tumor Cell Apoptosis. J. Biol. Chem. *283*, 5188–5194.

Giorgi, F., and Deri, P. (1976). Cell death in ovarian chambers of Drosophila melanogaster. J Embryol Exp Morphol *35*, 521–533.

Goessling, W., North, T.E., Loewer, S., Lord, A.M., Lee, S., Stoick-Cooper, C.L., Weidinger, G., Puder, M., Daley, G.Q., Moon, R.T., et al. (2009). Genetic interaction of PGE2 and Wnt signaling regulates developmental specification of stem cells and regeneration. Cell *136*, 1136–1147.

Hamasaki, M., Furuta, N., Matsuda, A., Nezu, A., Yamamoto, A., Fujita, N., Oomori, H., Noda, T., Haraguchi, T., Hiraoka, Y., et al. (2013). Autophagosomes form at ER-mitochondria contact sites. Nature *495*, 389–393.

Han, J., Hou, W., Goldstein, L.A., Stolz, D.B., Watkins, S.C., and Rabinowich, H. (2014). A Complex between Atg7 and Caspase-9: A NOVEL MECHANISM OF CROSS-REGULATION BETWEEN AUTOPHAGY AND APOPTOSIS. J. Biol. Chem. *289*, 6485–6497.

Hanada, T., Noda, N.N., Satomi, Y., Ichimura, Y., Fujioka, Y., Takao, T., Inagaki, F., and Ohsumi, Y. (2007). The Atg12-Atg5 conjugate has a novel E3-like activity for protein lipidation in autophagy. J. Biol. Chem. *282*, 37298–37302.

Hannigan, A.M., and Gorski, S.M. (2009). Macroautophagy. Autophagy *5*, 140–151.

Hara, T., Nakamura, K., Matsui, M., Yamamoto, A., Nakahara, Y., Suzuki-Migishima, R., Yokoyama, M., Mishima, K., Saito, I., Okano, H., et al. (2006). Suppression of basal autophagy in neural cells causes neurodegenerative disease in mice. Nature *441*, 885–889.

Hara, T., Takamura, A., Kishi, C., Iemura, S.-I., Natsume, T., Guan, J.-L., and Mizushima, N. (2008). FIP200, a ULK-interacting protein, is required for autophagosome formation in mammalian cells. J. Cell Biol. *181*, 497–510.

Hartl, F.U., Bracher, A., and Hayer-Hartl, M. (2011). Molecular chaperones in protein folding and proteostasis. Nature *475*, 324–332.

Hawkins, C.J., Yoo, S.J., Peterson, E.P., Wang, S.L., Vernooy, S.Y., and Hay, B.A. (2000). The Drosophila caspase DRONC cleaves following glutamate or aspartate and is regulated by DIAP1, HID, and GRIM. J. Biol. Chem. *275*, 27084–27093.

Hay, B.A., Huh, J.R., and Guo, M. (2004). The genetics of cell death: approaches, insights and opportunities in Drosophila. Nat. Rev. Genet. *5*, 911–922.

Hayashi-Nishino, M., Fujita, N., Noda, T., Yamaguchi, A., Yoshimori, T., and Yamamoto, A. (2009). A subdomain of the endoplasmic reticulum forms a cradle for autophagosome formation. Nat. Cell Biol. *11*, 1433–1437.

He, H., Dang, Y., Dai, F., Guo, Z., Wu, J., She, X., Pei, Y., Chen, Y., Ling, W., Wu, C., et al. (2003). Post-translational modifications of three members of the human MAP1LC3 family and detection of a novel type of modification for MAP1LC3B. J. Biol. Chem. *278*, 29278–29287.

He, L., Wang, X., and Montell, D.J. (2011). Shining light on Drosophila oogenesis: live imaging of egg development. Current Opinion in Genetics & Development *21*, 612–619.

Heinemeyer, W., Fischer, M., Krimmer, T., Stachon, U., and Wolf, D.H. (1997). The active sites of the eukaryotic 20 S proteasome and their involvement in subunit precursor processing. J. Biol. Chem. *272*, 25200–25209.

Hemmingsen, S.M., Woolford, C., van der Vies, S.M., Tilly, K., Dennis, D.T., Georgopoulos, C.P., Hendrix, R.W., and Ellis, R.J. (1988). Homologous plant and bacterial proteins chaperone oligomeric protein assembly. Nature *333*, 330–334.

Henderson, B., Fares, M.A., and Lund, P.A. (2013). Chaperonin 60: a paradoxical, evolutionarily conserved protein family with multiple moonlighting functions. Biol Rev *88*, 955–987.

Hengartner, M.O. (2000). The biochemistry of apoptosis. Nature *407*, 770–776.

Hershko, A., Ciechanover, A., Heller, H., Haas, A.L., and Rose, I.A. (1980). Proposed role of ATP in protein breakdown: conjugation of protein with multiple chains of the polypeptide of ATP-dependent proteolysis. Proc. Natl. Acad. Sci. U.S.A. *77*, 1783–1786.

Hershko, A., Heller, H., Elias, S., and Ciechanover, A. (1983). Components of ubiquitin-protein ligase system. Resolution, affinity purification, and role in protein breakdown. J. Biol. Chem. *258*, 8206–8214.

Hershko, A., Ciechanover, A., and Varshavsky, A. (2000). Basic Medical Research Award. The ubiquitin system. Nat. Med. *6*, 1073–1081.

Hou, Y.-C.C., Chittaranjan, S., Barbosa, S.G., McCall, K., and Gorski, S.M. (2008). Effector caspase Dcp-1 and IAP protein Bruce regulate starvation-induced autophagy during Drosophila melanogaster oogenesis. J Cell Biol *182*, 1127–1139.

Houde, C., Banks, K.G., Coulombe, N., Rasper, D., Grimm, E., Roy, S., Simpson, E.M., and Nicholson, D.W. (2004). Caspase-7 Expanded Function and Intrinsic Expression Level Underlies Strain-Specific Brain Phenotype of Caspase-3-Null Mice. J. Neurosci. *24*, 9977–9984.

Hough, R., Pratt, G., and Rechsteiner, M. (1987). Purification of two high molecular weight proteases from rabbit reticulocyte lysate. J. Biol. Chem. *262*, 8303–8313.

Hoyt, M.A., and Coffino, P. (2004). Ubiquitin-free routes into the proteasome. Cell. Mol. Life Sci. *61*, 1596–1600.

Hrizo, S.L., and Palladino, M.J. (2010). Hsp70 and Hsp90 mediated proteasomal degradation underlies TPIsugarkill pathogenesis in Drosophila. Neurobiol Dis *40*, 676–683.

Huh, J.R., Guo, M., and Hay, B.A. (2004). Compensatory proliferation induced by cell death in the Drosophila wing disc requires activity of the apical cell death caspase Dronc in a nonapoptotic role. Curr. Biol. *14*, 1262–1266.

Hyman, B.T., and Yuan, J. (2012). Apoptotic and non-apoptotic roles of caspases in neuronal physiology and pathophysiology. Nat. Rev. Neurosci. *13*, 395–406.

Imai, J., Maruya, M., Yashiroda, H., Yahara, I., and Tanaka, K. (2003). The molecular chaperone Hsp90 plays a role in the assembly and maintenance of the 26S proteasome. EMBO J *22*, 3557–3567.

Ishizaki, Y., Jacobson, M.D., and Raff, M.C. (1998). A Role for Caspases in Lens Fiber Differentiation. The Journal of Cell Biology *140*, 153–158.

Itakura, E., Kishi, C., Inoue, K., and Mizushima, N. (2008). Beclin 1 forms two distinct phosphatidylinositol 3-kinase complexes with mammalian Atg14 and UVRAG. Mol. Biol. Cell *19*, 5360–5372.

Iwata, A., Riley, B.E., Johnston, J.A., and Kopito, R.R. (2005). HDAC6 and microtubules are required for autophagic degradation of aggregated huntingtin. J. Biol. Chem. *280*, 40282–40292.

Jäger, R., and Zwacka, R.M. (2010). The Enigmatic Roles of Caspases in Tumor Development. Cancers *2*, 1952–1979.

Jakob, U., Lilie, H., Meyer, I., and Buchner, J. (1995). Transient Interaction of Hsp90 with Early Unfolding Intermediates of Citrate Synthase IMPLICATIONS FOR HEAT SHOCK IN VIVO. J. Biol. Chem. *270*, 7288–7294.

Janzen, V., Fleming, H.E., Riedt, T., Karlsson, G., Riese, M.J., Lo Celso, C., Reynolds, G., Milne, C.D., Paige, C.J., Karlsson, S., et al. (2008). Hematopoietic stem cell responsiveness to exogenous signals is limited by caspase-3. Cell Stem Cell *2*, 584–594.

Jeong, H.-S., Choi, H.Y., Lee, E.-R., Kim, J.-H., Jeon, K., Lee, H.-J., and Cho, S.-G. (2011). Involvement of caspase-9 in autophagy-mediated cell survival pathway. Biochim. Biophys. Acta *1813*, 80–90.

Jewell, J.L., Russell, R.C., and Guan, K.-L. (2013). Amino acid signalling upstream of mTOR. Nat Rev Mol Cell Biol *14*, 133–139.

Juhász, G., Csikós, G., Sinka, R., Erdélyi, M., and Sass, M. (2003). The Drosophila homolog of Aut1 is essential for autophagy and development. FEBS Letters *543*, 154–158.

Jung, C.H., Jun, C.B., Ro, S.-H., Kim, Y.-M., Otto, N.M., Cao, J., Kundu, M., and Kim, D.-H. (2009). ULK-Atg13-FIP200 complexes mediate mTOR signaling to the autophagy machinery. Mol. Biol. Cell *20*, 1992–2003.

Kabeya, Y., Mizushima, N., Ueno, T., Yamamoto, A., Kirisako, T., Noda, T., Kominami, E., Ohsumi, Y., and Yoshimori, T. (2000). LC3, a mammalian homologue of yeast Apg8p, is localized in autophagosome membranes after processing. EMBO J. *19*, 5720–5728.

Kadowaki, M., and Karim, M.R. (2009). Cytosolic LC3 ratio as a quantitative index of macroautophagy. Meth. Enzymol. *452*, 199–213.

Kamada, Y., Funakoshi, T., Shintani, T., Nagano, K., Ohsumi, M., and Ohsumi, Y. (2000). Tor-mediated induction of autophagy via an Apg1 protein kinase complex. J. Cell Biol. *150*, 1507–1513.

Kamada, Y., Yoshino, K., Kondo, C., Kawamata, T., Oshiro, N., Yonezawa, K., and Ohsumi, Y. (2010). Tor Directly Controls the Atg1 Kinase Complex To Regulate Autophagy. Mol. Cell. Biol. *30*, 1049–1058.

Kang, B.H., Plescia, J., Dohi, T., Rosa, J., Doxsey, S.J., and Altieri, D.C. (2007). Regulation of tumor cell mitochondrial homeostasis by an organelle-specific Hsp90 chaperone network. Cell *131*, 257–270.

Kanuka, H., Kuranaga, E., Takemoto, K., Hiratou, T., Okano, H., and Miura, M. (2005). Drosophila caspase transduces Shaggy/GSK-3beta kinase activity in neural precursor development. EMBO J. *24*, 3793–3806.

Kaur, J., and Debnath, J. (2015). Autophagy at the crossroads of catabolism and anabolism. Nat Rev Mol Cell Biol *16*, 461–472.

Keller, L.C., Cheng, L., Locke, C.J., Müller, M., Fetter, R.D., and Davis, G.W. (2011). Glial-derived prodegenerative signaling in the Drosophila neuromuscular system. Neuron *72*, 760–775.

Kerr, J.F., Wyllie, A.H., and Currie, A.R. (1972). Apoptosis: a basic biological phenomenon with wide-ranging implications in tissue kinetics. Br. J. Cancer *26*, 239–257.

Kihara, A., Noda, T., Ishihara, N., and Ohsumi, Y. (2001). Two distinct Vps34 phosphatidylinositol 3-kinase complexes function in autophagy and carboxypeptidase Y sorting in Saccharomyces cerevisiae. J. Cell Biol. *152*, 519–530.

Kijanska, M., Dohnal, I., Reiter, W., Kaspar, S., Stoffel, I., Ammerer, G., Kraft, C., and Peter, M. (2010). Activation of Atg1 kinase in autophagy by regulated phosphorylation. Autophagy *6*, 1168–1178.

Kim, K.W., Moretti, L., and Lu, B. (2008). M867, a novel selective inhibitor of caspase-3 enhances cell death and extends tumor growth delay in irradiated lung cancer models. PLoS ONE *3*, e2275.

Kim, Y.-I., Ryu, T., Lee, J., Heo, Y.-S., Ahnn, J., Lee, S.-J., and Yoo, O. (2010). A genetic screen for modifiers of Drosophila caspase Dcp-1 reveals caspase involvement in autophagy and novel caspase-related genes. BMC Cell Biol. *11*, 9.

Kimura, S., Noda, T., and Yoshimori, T. (2007). Dissection of the autophagosome maturation process by a novel reporter protein, tandem fluorescent-tagged LC3. Autophagy *3*, 452–460.

King, R.C. (1970). Ovarian development in Drosophila melanogaster (Academic Press).

Kirilly, D., and Xie, T. (2007). The Drosophila ovary: an active stem cell community. Cell Res *17*, 15–25.

Kirisako, T., Ichimura, Y., Okada, H., Kabeya, Y., Mizushima, N., Yoshimori, T., Ohsumi, M., Takao, T., Noda, T., and Ohsumi, Y. (2000). The reversible modification regulates the membrane-binding state of Apg8/Aut7 essential for autophagy and the cytoplasm to vacuole targeting pathway. J. Cell Biol. *151*, 263–276.

Klionsky, D.J. (2014). Citing recent declines in the discovery of new ATG genes, some scientists now suggest that the end of autophagy research may be within sight. Autophagy *10*, 715–716.

Klionsky, D.J., Cuervo, A.M., Dunn, W.A., Levine, B., van der Klei, I., and Seglen, P.O. (2007). How shall I eat thee? Autophagy *3*, 413–416.

Klionsky, D.J., Elazar, Z., Seglen, P.O., and Rubinsztein, D.C. (2008). Does bafilomycin A1 block the fusion of autophagosomes with lysosomes? Autophagy *4*, 849–850.

Klionsky, D.J., Abdelmohsen, K., Abe, A., Abedin, M.J., Abeliovich, H., Acevedo Arozena, A., Adachi, H., Adams, C.M., Adams, P.D., Adeli, K., et al. (2016). Guidelines for the use and interpretation of assays for monitoring autophagy (3rd edition). Autophagy *12*, 1–222.

Knorr, R.L., Nakatogawa, H., Ohsumi, Y., Lipowsky, R., Baumgart, T., and Dimova, R. (2014). Membrane morphology is actively transformed by covalent binding of the protein Atg8 to PE-lipids. PLoS ONE *9*, e115357.

Koenig, U., Eckhart, L., and Tschachler, E. (2001). Evidence that caspase-13 is not a human but a bovine gene. Biochem. Biophys. Res. Commun. *285*, 1150–1154.

Koll, H., Guiard, B., Rassow, J., Ostermann, J., Horwich, A.L., Neupert, W., and Hartl, F.U. (1992). Antifolding activity of hsp60 couples protein import into the mitochondrial matrix with export to the intermembrane space. Cell *68*, 1163–1175.

Komatsu, M., Waguri, S., Ueno, T., Iwata, J., Murata, S., Tanida, I., Ezaki, J., Mizushima, N., Ohsumi, Y., Uchiyama, Y., et al. (2005). Impairment of starvation-induced and constitutive autophagy in Atg7-deficient mice. J. Cell Biol. *169*, 425–434.

Kondo, S., Senoo-Matsuda, N., Hiromi, Y., and Miura, M. (2006). DRONC coordinates cell death and compensatory proliferation. Mol. Cell. Biol. *26*, 7258–7268.

Kovalenko, A., Kim, J.-C., Kang, T.-B., Rajput, A., Bogdanov, K., Dittrich-Breiholz, O., Kracht, M., Brenner, O., and Wallach, D. (2009). Caspase-8 deficiency in epidermal keratinocytes triggers an inflammatory skin disease. J. Exp. Med. *206*, 2161–2177.

Kumar, S., and Doumanis, J. (2000). The fly caspases. Cell Death Differ. *7*, 1039–1044.

Kumar, S., van Raam, B.J., Salvesen, G.S., and Cieplak, P. (2014). Caspase Cleavage Sites in the Human Proteome: CaspDB, a Database of Predicted Substrates. PLoS ONE *9*, e110539.

Kuo, C.T., Zhu, S., Younger, S., Jan, L.Y., and Jan, Y.N. (2006). Identification of E2/E3 ubiquitinating enzymes and caspase activity regulating Drosophila sensory neuron dendrite pruning. Neuron *51*, 283–290.

Kuranaga, E., and Miura, M. (2007). Nonapoptotic functions of caspases: caspases as regulatory molecules for immunity and cell-fate determination. Trends in Cell Biology *17*, 135–144.

Labbadia, J., and Morimoto, R.I. (2015). The Biology of Proteostasis in Aging and Disease. Annual Review of Biochemistry *84*, 435–464.

Launay, S., Hermine, O., Fontenay, M., Kroemer, G., Solary, E., and Garrido, C. (2005). Vital functions for lethal caspases. Oncogene *24*, 5137–5148.

Laundrie, B., Peterson, J.S., Baum, J.S., Chang, J.C., Fileppo, D., Thompson, S.R., and McCall, K. (2003). Germline cell death is inhibited by P-element insertions disrupting the dcp-1/pita nested gene pair in Drosophila. Genetics *165*, 1881–1888.

Le, D.A., Wu, Y., Huang, Z., Matsushita, K., Plesnila, N., Augustinack, J.C., Hyman, B.T., Yuan, J., Kuida, K., Flavell, R.A., et al. (2002). Caspase activation and neuroprotection in caspase-3- deficient mice after in vivo cerebral ischemia and in vitro oxygen glucose deprivation. Proc. Natl. Acad. Sci. U.S.A. *99*, 15188–15193.

Lebovitz, C.B., Bortnik, S.B., and Gorski, S.M. (2012). Here, There Be Dragons: Charting Autophagy-Related Alterations in Human Tumors. Clin Cancer Res *18*, 1214–1226.

Lee, C.Y., and Baehrecke, E.H. (2001). Steroid regulation of autophagic programmed cell death during development. Development *128*, 1443–1455.

Lee, C.-Y., Cooksey, B.A.K., and Baehrecke, E.H. (2002). Steroid regulation of midgut cell death during Drosophila development. Dev. Biol. *250*, 101–111.

Lee, T.V., Fan, Y., Wang, S., Srivastava, M., Broemer, M., Meier, P., and Bergmann, A. (2011). Drosophila IAP1-mediated ubiquitylation controls activation of the initiator caspase DRONC independent of protein degradation. PLoS Genet. *7*, e1002261.

Lee, T.V., Kamber Kaya, H.E., Simin, R., Baehrecke, E.H., and Bergmann, A. (2016). The initiator caspase Dronc is subject of enhanced autophagy upon proteasome impairment in Drosophila. Cell Death Differ *23*, 1555–1564.

Leonard, J.R., Klocke, B.J., D'sa, C., Flavell, R.A., and Roth, K.A. (2002). Strain-Dependent Neurodevelopmental Abnormalities in Caspase-3-Deficient Mice. J Neuropathol Exp Neurol *61*, 673–677.

Levine, B., and Kroemer, G. (2008). Autophagy in the Pathogenesis of Disease. Cell *132*, 27–42.

Li, Z., and Srivastava, P. (2004). Heat-shock proteins. Curr Protoc Immunol *Appendix 1*, Appendix 1T.

Li, F., Huang, Q., Chen, J., Peng, Y., Roop, D.R., Bedford, J.S., and Li, C.-Y. (2010a). Apoptotic cells activate the "phoenix rising" pathway to promote wound healing and tissue regeneration. Sci Signal *3*, ra13.

Li, W., Li, J., and Bao, J. (2012). Microautophagy: lesser-known self-eating. Cell. Mol. Life Sci. *69*, 1125–1136.

Li, Z., Jo, J., Jia, J.-M., Lo, S.-C., Whitcomb, D.J., Jiao, S., Cho, K., and Sheng, M. (2010b). Caspase-3 activation via mitochondria is required for long-term depression and AMPA receptor internalization. Cell *141*, 859–871.

Liang, X.H., Jackson, S., Seaman, M., Brown, K., Kempkes, B., Hibshoosh, H., and Levine, B. (1999). Induction of autophagy and inhibition of tumorigenesis by beclin 1. Nature *402*, 672–676.

Liedtke, C., Bangen, J.-M., Freimuth, J., Beraza, N., Lambertz, D., Cubero, F.J., Hatting, M., Karlmark, K.R., Streetz, K.L., Krombach, G.A., et al. (2011). Loss of caspase-8 protects mice against inflammation-related hepatocarcinogenesis but induces non-apoptotic liver injury. Gastroenterology *141*, 2176–2187.

Lilienbaum, A. (2013). Relationship between the proteasomal system and autophagy. Int J Biochem Mol Biol *4*, 1–26.

Liu, C.-W., Li, X., Thompson, D., Wooding, K., Chang, T., Tang, Z., Yu, H., Thomas, P.J., and DeMartino, G.N. (2006). ATP binding and ATP hydrolysis play distinct roles in the function of 26S proteasome. Mol. Cell *24*, 39–50.

Liu, X., He, Y., Li, F., Huang, Q., Kato, T.A., Hall, R.P., and Li, C.-Y. (2015). Caspase-3 promotes genetic instability and carcinogenesis. Mol. Cell *58*, 284–296.

Liu, Y., Sun, B., Zhao, X., Gu, Q., Liu, Z.-Y., Dong, X.-Y., Che, N., and Mo, J. (2013). Basal caspase-3 activity promotes migration, invasion, and vasculogenic mimicry formation of melanoma cells. Melanoma Res. *23*, 243–253.

Lőw, P., Varga, Á., Pircs, K., Nagy, P., Szatmári, Z., Sass, M., and Juhász, G. (2013). Impaired proteasomal degradation enhances autophagy via hypoxia signaling in Drosophila. BMC Cell Biol *14*, 29.

Lu, T., Pan, Y., Kao, S.-Y., Li, C., Kohane, I., Chan, J., and Yankner, B.A. (2004). Gene regulation and DNA damage in the ageing human brain. Nature *429*, 883–891.

Lundgren, J., Masson, P., Realini, C.A., and Young, P. (2003). Use of RNA interference and complementation to study the function of the Drosophila and human 26S proteasome subunit S13. Mol. Cell. Biol. *23*, 5320–5330.

Maelfait, J., Vercammen, E., Janssens, S., Schotte, P., Haegman, M., Magez, S., and Beyaert, R. (2008). Stimulation of Toll-like receptor 3 and 4 induces interleukin-1β maturation by caspase-8. Journal of Experimental Medicine *205*, 1967–1973.

Marzec, M., Eletto, D., and Argon, Y. (2012). GRP94: An HSP90-like protein specialized for protein folding and quality control in the endoplasmic reticulum. Biochim. Biophys. Acta *1823*, 774–787.

Marzella, L., Ahlberg, J., and Glaumann, H. (1980). In vitro uptake of particles by lysosomes. Experimental Cell Research *129*, 460–466.

Massaly, N., Francès, B., and Moulédous, L. (2015). Roles of the ubiquitin proteasome system in the effects of drugs of abuse. Front. Mol. Neurosci. *7*.

Matalova, E., Lesot, H., Svandova, E., Vanden Berghe, T., Sharpe, P.T., Healy, C., Vandenabeele, P., and Tucker, A.S. (2013). Caspase-7 participates in differentiation of cells forming dental hard tissues. Dev. Growth Differ. *55*, 615–621.

Matsunaga, K., Saitoh, T., Tabata, K., Omori, H., Satoh, T., Kurotori, N., Maejima, I., Shirahama-Noda, K., Ichimura, T., Isobe, T., et al. (2009). Two Beclin 1-binding proteins, Atg14L and Rubicon, reciprocally regulate autophagy at different stages. Nat. Cell Biol. *11*, 385–396.

McIlwain, D.R., Berger, T., and Mak, T.W. (2013). Caspase Functions in Cell Death and Disease. Cold Spring Harb Perspect Biol *5*, a008656.

McStay, G.P., Salvesen, G.S., and Green, D.R. (2008). Overlapping cleavage motif selectivity of caspases: implications for analysis of apoptotic pathways. Cell Death Differ. *15*, 322–331.

Mintern, J.D., and Harris, J. (2015). Autophagy and immunity. Immunol Cell Biol *93*, 1–2.

Miura, M., Chen, X.-D., Allen, M.R., Bi, Y., Gronthos, S., Seo, B.-M., Lakhani, S., Flavell, R.A., Feng, X.-H., Robey, P.G., et al. (2004). A crucial role of caspase-3 in osteogenic differentiation of bone marrow stromal stem cells. J. Clin. Invest. *114*, 1704–1713.

Mizushima, N. (2007). Autophagy: process and function. Genes Dev. *21*, 2861–2873.

Mizushima, N., and Levine, B. (2010). Autophagy in mammalian development and differentiation. Nat Cell Biol *12*, 823–830.

Mizushima, N., Sugita, H., Yoshimori, T., and Ohsumi, Y. (1998). A new protein conjugation system in human. The counterpart of the yeast Apg12p conjugation system essential for autophagy. J. Biol. Chem. *273*, 33889–33892.

Mizushima, N., Noda, T., and Ohsumi, Y. (1999). Apg16p is required for the function of the Apg12p-Apg5p conjugate in the yeast autophagy pathway. EMBO J. *18*, 3888–3896.

Mizushima, N., Kuma, A., Kobayashi, Y., Yamamoto, A., Matsubae, M., Takao, T., Natsume, T., Ohsumi, Y., and Yoshimori, T. (2003). Mouse Apg16L, a novel WD-repeat protein, targets to the autophagic isolation membrane with the Apg12-Apg5 conjugate. J. Cell. Sci. *116*, 1679–1688.

Mogi, M., and Togari, A. (2003). Activation of caspases is required for osteoblastic differentiation. J. Biol. Chem. *278*, 47477–47482.

Mori, M., Hitora, T., Nakamura, O., Yamagami, Y., Horie, R., Nishimura, H., and Yamamoto, T. (2015). Hsp90 inhibitor induces autophagy and apoptosis in osteosarcoma cells. Int. J. Oncol. *46*, 47–54.

Murray, T.V.A., McMahon, J.M., Howley, B.A., Stanley, A., Ritter, T., Mohr, A., Zwacka, R., and Fearnhead, H.O. (2008). A non-apoptotic role for caspase-9 in muscle differentiation. J. Cell. Sci. *121*, 3786–3793.

Nagy, P., Varga, Á., Kovács, A.L., Takáts, S., and Juhász, G. (2015). How and why to study autophagy in Drosophila: it's more than just a garbage chute. Methods *75*, 151–161.

Neff, N.T., Bourret, L., Miao, P., and Dice, J.F. (1981). Degradation of proteins microinjected into IMR-90 human diploid fibroblasts. J. Cell Biol. *91*, 184–194.

Nezis, I.P., Stravopodis, D.J., Papassideri, I., Robert-Nicoud, M., and Margaritis, L.H. (2000). Stage-specific apoptotic patterns during Drosophila oogenesis. Eur. J. Cell Biol. *79*, 610–620.

Nezis, I.P., Stravopodis, D.J., Papassideri, I., Robert-Nicoud, M., and Margaritis, L.H. (2002). Dynamics of apoptosis in the ovarian follicle cells during the late stages of Drosophila oogenesis. Cell Tissue Res. *307*, 401–409.

Nezis, I.P., Lamark, T., Velentzas, A.D., Rusten, T.E., Bjørkøy, G., Johansen, T., Papassideri, I.S., Stravopodis, D.J., Margaritis, L.H., Stenmark, H., et al. (2009). Cell death during Drosophila melanogaster early oogenesis is mediated through autophagy. Autophagy *5*, 298–302.

Nezis, I.P., Shravage, B.V., Sagona, A.P., Lamark, T., Bjørkøy, G., Johansen, T., Rusten, T.E., Brech, A., Baehrecke, E.H., and Stenmark, H. (2010). Autophagic degradation of dBruce controls DNA fragmentation in nurse cells during late Drosophila melanogaster oogenesis. The Journal of Cell Biology *190*, 523–531.

Nice, D.C., Sato, T.K., Stromhaug, P.E., Emr, S.D., and Klionsky, D.J. (2002). Cooperative binding of the cytoplasm to vacuole targeting pathway proteins, Cvt13 and Cvt20, to phosphatidylinositol 3-phosphate at the pre-autophagosomal structure is required for selective autophagy. J. Biol. Chem. *277*, 30198–30207.

Nixon, R.A. (2013). The role of autophagy in neurodegenerative disease. Nat Med *19*, 983–997.

Norman, J.M., Cohen, G.M., and Bampton, E.T.W. (2010). The in vitro cleavage of the hAtg proteins by cell death proteases. Autophagy *6*, 1042–1056.

Obara, K., Sekito, T., Niimi, K., and Ohsumi, Y. (2008). The Atg18-Atg2 complex is recruited to autophagic membranes via phosphatidylinositol 3-phosphate and exerts an essential function. J. Biol. Chem. *283*, 23972–23980.

O'Donovan, N., Crown, J., Stunell, H., Hill, A.D.K., McDermott, E., O'Higgins, N., and Duffy, M.J. (2003). Caspase 3 in breast cancer. Clin. Cancer Res. *9*, 738–742.

Ohsawa, S., Hamada, S., Asou, H., Kuida, K., Uchiyama, Y., Yoshida, H., and Miura, M. (2009). Caspase-9 activation revealed by semaphorin 7A cleavage is independent of apoptosis in the aged olfactory bulb. J. Neurosci. *29*, 11385–11392.

Okuyama, R., Nguyen, B.-C., Talora, C., Ogawa, E., Tommasi di Vignano, A., Lioumi, M., Chiorino, G., Tagami, H., Woo, M., and Dotto, G.P. (2004). High commitment of embryonic keratinocytes to terminal differentiation through a Notch1-caspase 3 regulatory mechanism. Dev. Cell *6*, 551–562.

Olson, N.E., Graves, J.D., Shu, G.L., Ryan, E.J., and Clark, E.A. (2003). Caspase activity is required for stimulated B lymphocytes to enter the cell cycle. J. Immunol. *170*, 6065–6072.

Oral, O., Oz-Arslan, D., Itah, Z., Naghavi, A., Deveci, R., Karacali, S., and Gozuacik, D. (2012). Cleavage of Atg3 protein by caspase-8 regulates autophagy during receptor-activated cell death. Apoptosis *17*, 810–820.

Oura, J., Tamura, Y., Kamiguchi, K., Kutomi, G., Sahara, H., Torigoe, T., Himi, T., and Sato, N. (2011). Extracellular heat shock protein 90 plays a role in translocating chaperoned antigen from endosome to proteasome for generating antigenic peptide to be cross-presented by dendritic cells. Int. Immunol. *23*, 223–237.

Ouyang, L., Shi, Z., Zhao, S., Wang, F.-T., Zhou, T.-T., Liu, B., and Bao, J.-K. (2012). Programmed cell death pathways in cancer: a review of apoptosis, autophagy and programmed necrosis. Cell Prolif. *45*, 487–498.

Pagliarini, V., Wirawan, E., Romagnoli, A., Ciccosanti, F., Lisi, G., Lippens, S., Cecconi, F., Fimia, G.M., Vandenabeele, P., Corazzari, M., et al. (2012). Proteolysis of Ambra1 during apoptosis has a role in the inhibition of the autophagic pro-survival response. Cell Death Differ. *19*, 1495–1504.

Pandey, U.B., Nie, Z., Batlevi, Y., McCray, B.A., Ritson, G.P., Nedelsky, N.B., Schwartz, S.L., DiProspero, N.A., Knight, M.A., Schuldiner, O., et al. (2007). HDAC6 rescues neurodegeneration and provides an essential link between autophagy and the UPS. Nature *447*, 859–863.

Parrish, A.B., Freel, C.D., and Kornbluth, S. (2013). Cellular Mechanisms Controlling Caspase Activation and Function. Cold Spring Harb Perspect Biol *5*, a008672.

Pearl, L.H., and Prodromou, C. (2006). Structure and mechanism of the Hsp90 molecular chaperone machinery. Annu. Rev. Biochem. *75*, 271–294.

Pick, E., Kluger, Y., Giltnane, J.M., Moeder, C., Camp, R.L., Rimm, D.L., and Kluger, H.M. (2007). High HSP90 Expression Is Associated with Decreased Survival in Breast Cancer. Cancer Res *67*, 2932–2937.

Pop, C., and Salvesen, G.S. (2009). Human Caspases: Activation, Specificity, and Regulation. J. Biol. Chem. *284*, 21777–21781.

Pozuelo-Rubio, M. (2011). 14-3-3ζ binds class III phosphatidylinositol-3-kinase and inhibits autophagy. Autophagy *7*, 240–242.

Prodromou, C. (2012). The “active life” of Hsp90 complexes. Biochim. Biophys. Acta *1823*, 614–623.

Ranford, J.C., Coates, A.R., and Henderson, B. (2000). Chaperonins are cell-signalling proteins: the unfolding biology of molecular chaperones. Expert Rev Mol Med *2*, 1–17.

Ravikumar, B., Moreau, K., Jahreiss, L., Puri, C., and Rubinsztein, D.C. (2010). Plasma membrane contributes to the formation of pre-autophagosomal structures. Nat. Cell Biol. *12*, 747–757.

Rebecca, V.W., and Amaravadi, R.K. (2016). Emerging strategies to effectively target autophagy in cancer. Oncogene *35*, 1–11.

Rich, T., Allen, R.L., and Wyllie, A.H. (2000). Defying death after DNA damage. Nature *407*, 777–783.

Richter, K., Haslbeck, M., and Buchner, J. (2010). The Heat Shock Response: Life on the Verge of Death. Molecular Cell *40*, 253–266.

Riedl, S.J., Fuentes-Prior, P., Renatus, M., Kairies, N., Krapp, S., Huber, R., Salvesen, G.S., and Bode, W. (2001). Structural basis for the activation of human procaspase-7. Proc. Natl. Acad. Sci. U.S.A. *98*, 14790–14795.

Ritossa, F. (1996). Discovery of the heat shock response. Cell Stress Chaperones *1*, 97–98.

Rusten, T.E., Lindmo, K., Juhász, G., Sass, M., Seglen, P.O., Brech, A., and Stenmark, H. (2004). Programmed autophagy in the Drosophila fat body is induced by ecdysone through regulation of the PI3K pathway. Dev. Cell *7*, 179–192.

Sadowski, M., and Sarcevic, B. (2010). Mechanisms of mono- and poly-ubiquitination: Ubiquitination specificity depends on compatibility between the E2 catalytic core and amino acid residues proximal to the lysine. Cell Division *5*, 19.

Saelens, X., Festjens, N., Vande Walle, L., van Gurp, M., van Loo, G., and Vandenabeele, P. (2004). Toxic proteins released from mitochondria in cell death. Oncogene *23*, 2861–2874.

Samali, A., Cai, J., Zhivotovsky, B., Jones, D.P., and Orrenius, S. (1999). Presence of a pre-apoptotic complex of pro-caspase-3, Hsp60 and Hsp10 in the mitochondrial fraction of jurkat cells. EMBO J *18*, 2040–2048.

Schoenmann, Z., Assa-Kunik, E., Tiomny, S., Minis, A., Haklai-Topper, L., Arama, E., and Yaron, A. (2010). Axonal degeneration is regulated by the apoptotic machinery or a NAD+-sensitive pathway in insects and mammals. J. Neurosci. *30*, 6375–6386.

Scott, R.C., Schuldiner, O., and Neufeld, T.P. (2004). Role and Regulation of Starvation-Induced Autophagy in the Drosophila Fat Body. Developmental Cell *7*, 167–178.

Selimovic, D., Porzig, B.B.O.W., El-Khattouti, A., Badura, H.E., Ahmad, M., Ghanjati, F., Santourlidis, S., Haikel, Y., and Hassan, M. (2013). Bortezomib/proteasome inhibitor triggers both apoptosis and autophagy-dependent pathways in melanoma cells. Cell. Signal. *25*, 308–318.

Shalini, S., Dorstyn, L., Dawar, S., and Kumar, S. (2015). Old, new and emerging functions of caspases. Cell Death Differ *22*, 526–539.

Shi, Y. (2002). Mechanisms of Caspase Activation and Inhibition during Apoptosis. Molecular Cell *9*, 459–470.

Siegelin, M.D., Dohi, T., Raskett, C.M., Orlowski, G.M., Powers, C.M., Gilbert, C.A., Ross, A.H., Plescia, J., and Altieri, D.C. (2011). Exploiting the mitochondrial unfolded protein response for cancer therapy in mice and human cells. J Clin Invest *121*, 1349–1360.

Simon, D.J., Weimer, R.M., McLaughlin, T., Kallop, D., Stanger, K., Yang, J., O'Leary, D.D.M., Hannoush, R.N., and Tessier-Lavigne, M. (2012). A caspase cascade regulating developmental axon degeneration. J. Neurosci. *32*, 17540–17553.

Sirois, I., Groleau, J., Pallet, N., Brassard, N., Hamelin, K., Londono, I., Pshezhetsky, A.V., Bendayan, M., and Hébert, M.-J. (2012). Caspase activation regulates the extracellular export of autophagic vacuoles. Autophagy *8*, 927–937.

Slee, E.A., Adrain, C., and Martin, S.J. (2001). Executioner caspase-3, -6, and -7 perform distinct, non-redundant roles during the demolition phase of apoptosis. J. Biol. Chem. *276*, 7320–7326.

Sordet, O., Rébé, C., Plenchette, S., Zermati, Y., Hermine, O., Vainchenker, W., Garrido, C., Solary, E., and Dubrez-Daloz, L. (2002). Specific involvement of caspases in the differentiation of monocytes into macrophages. Blood *100*, 4446–4453.

Spradling, A.C. (1993). Germline cysts: Communes that work. Cell *72*, 649–651.

Stoven, S., Silverman, N., Junell, A., Hedengren-Olcott, M., Erturk, D., Engstrom, Y., Maniatis, T., and Hultmark, D. (2003). Caspase-mediated processing of the Drosophila NF-kappaB factor Relish. Proc. Natl. Acad. Sci. U.S.A. *100*, 5991–5996.

Sun, Q., Fan, W., Chen, K., Ding, X., Chen, S., and Zhong, Q. (2008). Identification of Barkor as a mammalian autophagy-specific factor for Beclin 1 and class III phosphatidylinositol 3-kinase. Proc. Natl. Acad. Sci. U.S.A. *105*, 19211–19216.

Sun, Q., Westphal, W., Wong, K.N., Tan, I., and Zhong, Q. (2010). Rubicon controls endosome maturation as a Rab7 effector. Proc. Natl. Acad. Sci. U.S.A. *107*, 19338–19343.

Sun, Q., Zhang, J., Fan, W., Wong, K.N., Ding, X., Chen, S., and Zhong, Q. (2011). The RUN domain of rubicon is important for hVps34 binding, lipid kinase inhibition, and autophagy suppression. J. Biol. Chem. *286*, 185–191.

Suzuki, S., and be, K. (1985). Topological structural analysis of digitized binary images by border following. Computer Vision, Graphics, and Image Processing *30*, 32–46.

Suzuki, K., Kirisako, T., Kamada, Y., Mizushima, N., Noda, T., and Ohsumi, Y. (2001a). The pre-autophagosomal structure organized by concerted functions of APG genes is essential for autophagosome formation. EMBO J. *20*, 5971–5981.

Suzuki, Y., Nakabayashi, Y., and Takahashi, R. (2001b). Ubiquitin-protein ligase activity of X-linked inhibitor of apoptosis protein promotes proteasomal degradation of caspase-3 and enhances its anti-apoptotic effect in Fas-induced cell death. PNAS *98*, 8662–8667.

Svandova, E., Lesot, H., Vanden Berghe, T., Tucker, A.S., Sharpe, P.T., Vandenabeele, P., and Matalova, E. (2014). Non-apoptotic functions of caspase-7 during osteogenesis. Cell Death Dis *5*, e1366.

Taherbhoy, A.M., Tait, S.W., Kaiser, S.E., Williams, A.H., Deng, A., Nourse, A., Hammel, M., Kurinov, I., Rock, C.O., Green, D.R., et al. (2011). Atg8 transfer from Atg7 to Atg3: a distinctive E1-E2 architecture and mechanism in the autophagy pathway. Mol Cell *44*, 451–461.

Taipale, M., Jarosz, D.F., and Lindquist, S. (2010). HSP90 at the hub of protein homeostasis: emerging mechanistic insights. Nat. Rev. Mol. Cell Biol. *11*, 515–528.

Takeshige, K., Baba, M., Tsuboi, S., Noda, T., and Ohsumi, Y. (1992). Autophagy in yeast demonstrated with proteinase-deficient mutants and conditions for its induction. J. Cell Biol. *119*, 301–311.

Talanian, R.V., Quinlan, C., Trautz, S., Hackett, M.C., Mankovich, J.A., Banach, D., Ghayur, T., Brady, K.D., and Wong, W.W. (1997). Substrate Specificities of Caspase Family Proteases. J. Biol. Chem. *272*, 9677–9682.

Tanida, I., Minematsu-Ikeguchi, N., Ueno, T., and Kominami, E. (2005). Lysosomal turnover, but not a cellular level, of endogenous LC3 is a marker for autophagy. Autophagy *1*, 84–91.

Tanji, T., and Ip, Y.T. (2005). Regulators of the Toll and Imd pathways in the Drosophila innate immune response. Trends Immunol. *26*, 193–198.

Thukral, L., Sengupta, D., Ramkumar, A., Murthy, D., Agrawal, N., and Gokhale, R.S. (2015). The Molecular Mechanism Underlying Recruitment and Insertion of Lipid-Anchored LC3 Protein into Membranes. Biophys J *109*, 2067–2078.

Thumm, M., Egner, R., Koch, B., Schlumpberger, M., Straub, M., Veenhuis, M., and Wolf, D.H. (1994). Isolation of autophagocytosis mutants of Saccharomyces cerevisiae. FEBS Lett. *349*, 275–280.

Tiwari, M., Lopez-Cruzan, M., Morgan, W.W., and Herman, B. (2011). Loss of caspase-2-dependent apoptosis induces autophagy after mitochondrial oxidative stress in primary cultures of young adult cortical neurons. J. Biol. Chem. *286*, 8493–8506.

Tiwari, M., Sharma, L.K., Vanegas, D., Callaway, D.A., Bai, Y., Lechleiter, J.D., and Herman, B. (2014). A nonapoptotic role for CASP2/caspase 2: modulation of autophagy. Autophagy *10*, 1054–1070.

Tsukada, M., and Ohsumi, Y. (1993). Isolation and characterization of autophagy-defective mutants of Saccharomyces cerevisiae. FEBS Lett. *333*, 169–174.

Tsvetkov, A.S., Mitra, S., and Finkbeiner, S. (2009). Protein turnover differences between neurons and other cells. Autophagy *5*, 1037–1038.

Vaux, D.L., and Silke, J. (2005). IAPs – the ubiquitin connection. Cell Death Differ *12*, 1205–1207.

Vila, M., and Przedborski, S. (2003). Targeting programmed cell death in neurodegenerative diseases. Nat Rev Neurosci *4*, 365–375.

Vogl, D.T., Stadtmauer, E.A., Tan, K.-S., Heitjan, D.F., Davis, L.E., Pontiggia, L., Rangwala, R., Piao, S., Chang, Y.C., Scott, E.C., et al. (2014). Combined autophagy and proteasome inhibition: a phase 1 trial of hydroxychloroquine and bortezomib in patients with relapsed/refractory myeloma. Autophagy *10*, 1380–1390.

Wachmann, K., Pop, C., van Raam, B.J., Drag, M., Mace, P.D., Snipas, S.J., Zmasek, C., Schwarzenbacher, R., Salvesen, G.S., and Riedl, S.J. (2010). Activation and specificity of human caspase-10. Biochemistry *49*, 8307–8315.

Wang, C., Liu, Z., and Huang, X. (2012). Rab32 is important for autophagy and lipid storage in Drosophila. PLoS ONE *7*, e32086.

Wells, B.S., Yoshida, E., and Johnston, L.A. (2006). Compensatory proliferation in Drosophila imaginal discs requires Dronc-dependent p53 activity. Curr. Biol. *16*, 1606–1615.

Whitesell, L., and Lindquist, S.L. (2005). HSP90 and the chaperoning of cancer. Nat. Rev. Cancer *5*, 761–772.

Wirawan, E., Vande Walle, L., Kersse, K., Cornelis, S., Claerhout, S., Vanoverberghe, I., Roelandt, R., De Rycke, R., Verspurten, J., Declercq, W., et al. (2010). Caspase-mediated cleavage of Beclin-1 inactivates Beclin-1-induced autophagy and enhances apoptosis by promoting the release of proapoptotic factors from mitochondria. Cell Death Dis *1*, e18.

Woenckhaus, C., Giebel, J., Failing, K., Fenic, I., Dittberner, T., and Poetsch, M. (2003). Expression of AP-2alpha, c-kit, and cleaved caspase-6 and -3 in naevi and malignant melanomas of the skin. A possible role for caspases in melanoma progression? J. Pathol. *201*, 278–287.

Won, J., Kim, D.Y., La, M., Kim, D., Meadows, G.G., and Joe, C.O. (2003). Cleavage of 14-3-3 protein by caspase-3 facilitates bad interaction with Bcl-x(L) during apoptosis. J. Biol. Chem. *278*, 19347–19351.

Woo, M., Hakem, R., Furlonger, C., Hakem, A., Duncan, G.S., Sasaki, T., Bouchard, D., Lu, L., Wu, G.E., Paige, C.J., et al. (2003). Caspase-3 regulates cell cycle in B cells: a consequence of substrate specificity. Nat. Immunol. *4*, 1016–1022.

Wu, H., Wang, M.C., and Bohmann, D. (2009). JNK protects Drosophila from oxidative stress by trancriptionally activating autophagy. Mech Dev *126*, 624–637.

Xanthoudakis, S., Roy, S., Rasper, D., Hennessey, T., Aubin, Y., Cassady, R., Tawa, P., Ruel, R., Rosen, A., and Nicholson, D.W. (1999). Hsp60 accelerates the maturation of pro-caspase-3 by upstream activator proteases during apoptosis. EMBO J *18*, 2049–2056.

Xie, Z., Nair, U., and Klionsky, D.J. (2008). Atg8 controls phagophore expansion during autophagosome formation. Mol. Biol. Cell *19*, 3290–3298.

Xu, C., Liu, J., Hsu, L.-C., Luo, Y., Xiang, R., and Chuang, T.-H. (2011). Functional interaction of Hsp90 and Beclin 1 modulates Toll-like receptor-mediated autophagy. FASEB J fj.10-167676.

Xu, D., Wang, Y., Willecke, R., Chen, Z., Ding, T., and Bergmann, A. (2006). The effector caspases drICE and dcp-1 have partially overlapping functions in the apoptotic pathway in Drosophila. Cell Death Differ. *13*, 1697–1706.

Yamano, T., Mizukami, S., Murata, S., Chiba, T., Tanaka, K., and Udono, H. (2008). Hsp90-mediated Assembly of the 26 S Proteasome Is Involved in Major Histocompatibility Complex Class I Antigen Processing. J. Biol. Chem. *283*, 28060–28065.

Yan, X.X., Najbauer, J., Woo, C.C., Dashtipour, K., Ribak, C.E., and Leon, M. (2001). Expression of active caspase-3 in mitotic and postmitotic cells of the rat forebrain. J. Comp. Neurol. *433*, 4–22.

Yang, Z., and Klionsky, D.J. (2010). Eaten alive: a history of macroautophagy. Nat Cell Biol *12*, 814–822.

Yang, Z., Huang, J., Geng, J., Nair, U., and Klionsky, D.J. (2006). Atg22 recycles amino acids to link the degradative and recycling functions of autophagy. Mol. Biol. Cell *17*, 5094–5104.

Yeh, Y.-Y., Wrasman, K., and Herman, P.K. (2010). Autophosphorylation within the Atg1 activation loop is required for both kinase activity and the induction of autophagy in Saccharomyces cerevisiae. Genetics *185*, 871–882.

Yorimitsu, T., and Klionsky, D.J. (2005). Autophagy: molecular machinery for self-eating. Cell Death Differ. *12 Suppl 2*, 1542–1552.

You, M., Savaraj, N., Kuo, M.T., Wangpaichitr, M., Varona-Santos, J., Wu, C., Nguyen, D.M., and Feun, L. (2013). TRAIL induces autophagic protein cleavage through caspase activation in melanoma cell lines under arginine deprivation. Mol. Cell. Biochem. *374*, 181–190.

Young, J.C., Moarefi, I., and Hartl, F.U. (2001). Hsp90: a specialized but essential protein-folding tool. J. Cell Biol. *154*, 267–273.

Yu, Z.-Q., Ni, T., Hong, B., Wang, H.-Y., Jiang, F.-J., Zou, S., Chen, Y., Zheng, X.-L., Klionsky, D.J., Liang, Y., et al. (2012). Dual roles of Atg8-PE deconjugation by Atg4 in autophagy. Autophagy *8*, 883–892.

Yue, L., Karr, T.L., Nathan, D.F., Swift, H., Srinivasan, S., and Lindquist, S. (1999). Genetic analysis of viable Hsp90 alleles reveals a critical role in Drosophila spermatogenesis. Genetics *151*, 1065–1079.

Zermati, Y., Garrido, C., Amsellem, S., Fishelson, S., Bouscary, D., Valensi, F., Varet, B., Solary, E., and Hermine, O. (2001). Caspase activation is required for terminal erythroid differentiation. J. Exp. Med. *193*, 247–254.

Zhang, J. (2013). Autophagy and Mitophagy in Cellular Damage Control. Redox Biol *1*, 19–23.

Zheng, T.S., Hunot, S., Kuida, K., Momoi, T., Srinivasan, A., Nicholson, D.W., Lazebnik, Y., and Flavell, R.A. (2000). Deficiency in caspase-9 or caspase-3 induces compensatory caspase activation. Nat. Med. *6*, 1241–1247.

Zhou, J., Tan, S.-H., Nicolas, V., Bauvy, C., Yang, N.-D., Zhang, J., Xue, Y., Codogno, P., and Shen, H.-M. (2013). Activation of lysosomal function in the course of autophagy via mTORC1 suppression and autophagosome-lysosome fusion. Cell Res *23*, 508–523.